Monitoring and Detection of Cracks in Steel Girders of Bridges Using a Distributed Binary Crack Sensor

by

Farnaz Raeisi Mehdiabadi

A Thesis submitted to the Faculty of Graduate Studies of

The University of Manitoba

in partial fulfilment of the requirements of the degree of

DOCTOR OF PHILOSOPHY

Department of Civil Engineering
University of Manitoba
Winnipeg, MB, Canada

ABSTRACT

Bridges are key elements in transportation system. One of the critical deficiencies in aging bridges is formation and propagation of small cracks under cyclic loading. Cracks may form in steel girders due to defects in welding or material in the fabrication time. Over time, cracks may grow into the web of steel girders, propagate spontaneously and finally may result in the failure of the girder. Therefore, to prevent the unpredictable loss of service and associated expenses, it is critical to detect cracks before they reach a length that compromises the safety of the structure. Distributed sensors are required if there are many possible points of crack formation. Available distributed crack monitoring techniques are excessively costly to be applied to typical short and medium span bridges. In this work, an innovative distributed binary crack sensor has been developed. The sensor can be installed on the entire length of steel girders of bridges at a fraction of the cost and is capable of detecting cracks with opening of 0.2 mm or less. The crack sensor is composed of a thin wire-(0.09 mm diameter) and an adhesive. An experimental apparatus has been designed to simulate the crack opening on the web of steel girders and materials have been tested on the apparatus. A Finite Element Model of the sensor has been simulated in ABAQUS to study the effect of different parameters such as bonding properties between wire and epoxy as well as position of the wire in the epoxy on the detected crack opening. The crack sensor has been tested on small-scale girder in the lab in ambient temperature. It also has been tested on the girder in an environmental chamber for two extreme temperatures of -30ºC and +40ºC. The study shows that temperature has minimal effect on the performance of the crack sensor. A Finite Element Model of two typical steel girders from two medium span bridges predicts that a binary cracks sensor 15 cm to 25 cm above the tension flange will detect crack that have grown to a length of 35-40 cm at the threshold of 0.2 mm

detection. The FEM analysis also predicts that 35-40 cm long cracks do not compromises the safety of the structure.

The distributed binary crack sensor has been field tested for more than a year on a real-scale girder of a bridge in Canada to study the installation procedure and effect of environmental condition on the sensor.

ACKNOWLEDGMENT

Writing this thesis puts an end to another chapter in my life, a chapter I've always dreamed for. Achieving this goal was not possible without the supports of my advisors, my family and friends.

I would like to express my sincere gratitude to my advisor Prof. Aftab Mufti for the continuous support during my research, for his patience and immense knowledge. His invaluable insights helped me during the time of research and writing of this thesis. I could not have imagined having a better advisor for my Ph.D study.

I would also like to express my special appreciation and thanks to my co-advisor Professor Douglas J. Thomson for the consistent encouragement and invaluable insights I received for all my works during these years. I appreciate all your contributions of time, ideas and supports. You have been a tremendous mentor for me.

Besides my advisors, I would like to thank the rest of my thesis committee: Prof. Dagmar Svecova, Prof. Baidar Bakht, and Prof. Dean McNeill, for their insightful comments. I would like to thank the staff and manager of the McQuade Structures Laboratory for helping me with my experiments.

Last but not the least, I would like to thank my family specially my parents for supporting me throughout writing this thesis, my beloved husband – Houshang- words can not express how grateful I am for all your supports and my lovely little daughter –Hanna May- for bringing me joy and happiness during all the hard works.

FARNAZ RAEISI

DEDICATION

I would like to dedicate this thesis to:

My parents for their unconditional supports,

My beloved husband- Houshang- for all the supports and sacrifices,

My lovely Hanna May who brings joy to our life

And

My professors at BIHE who have sacrificed their lives for the education of Baha'i youth in Iran

CONTRIBUTION OF AUTHORS

This thesis is comprised of three journal papers. Two of them have been published and one has been submitted. All the papers are multi-authored. F. Raeisi is the first author on all papers. Contributions of other authors for these papers are as follow:

Chapter 3: Farnaz Raeisi, A. Mufti, G. Mustapha and D. J. Thomson "Crack detection in steel girders of bridges using a broken wire electronic binary sensor" Journal of Civil Structural Health Monitoring, vol.7, pp. 233-243, 2017.

The idea has been developed by Dr. Mufti and Dr. Thomson. I have carried out the required background studies and experiments. G. Mustapha helped with the idea from the industrial point of view. I have prepared the first draft of the paper and it has been edited by Dr. Thomson and Dr. Mufti. I am the corresponding author of this paper and have prepared responses to comments.

Chapter 4: Farnaz Raeisi, A. Mufti and D. J. Thomson, "A Finite Element Model and Experimental Investigation of the Influence of Pre-Straining of Wire on the Sensitivity of Binary Crack Sensors", Journal of Civil Structural Health Monitoring (2018). https://doi.org/10.1007/s13349-018-0290-7

In this chapter of the thesis, I have carried out the required background studies, Finite Element Analysis, fabrication of samples and experiments. Dr. Mufti and Dr. Thomson provided valuable advices on different issues during the work and have provided insights on experimental and analytical results. I prepared the manuscript, which was edited by Dr. Thomson and Dr. Mufti. I am the corresponding author of this paper and have prepared responses to comments.

Chapter 5: Farnaz Raeisi, Aftab Mufti and Douglas J. Thomson, "Placement of Binary Crack Sensor on Simply Supported I-Shaped Steel Girders", Submitted to the Journal of Smart Material and Structures, August 2018

In this work, I have done the stress intensity factor calculations, background studies, FEM analysis. Dr. Mufti and Dr. Thomson have provided input and insight on my analysis. I prepared the manuscript, which was then edited by Dr. Thomson and Dr. Mufti. I am the corresponding author of this paper and have prepared responses to comments.

A part of this chapter is excerpted form conference paper; **Farnaz Raeisi, Aftab Mufti, Mustapha Gamal and Douglas J. Thomson, "Binary Crack Sensor for Steel Girder Bridges: Installation Procedure in Field", submitted to the 10th international conference on short and medium span bridges, Quebec, August 2018**

In this work, I have done the analysis and was a team member in installation of binary crack sensor on the bridge. I have prepared the first draft of the paper which was edited by Dr. Thomson and Dr.Mufti. Mr. Mustapha –the industry partner- provided the resources for installation part and has been monitoring the data since installation time. I am the corresponding author of this paper and have prepared responses to comments.

TABLE OF CONTENTS

ABSTRACT ..... **I**

ACKNOWLEDGMENT ..... **III**

DEDICATION ..... **IV**

CONTRIBUTION OF AUTHORS ..... **V**

TABLE OF CONTENTS ..... **VII**

LIST OF TABLES ..... **I**

LIST OF FIGURES ..... **III**

LIST OF COPYRIGHTED MATERIAL FOR WHICH PERMISSION WAS OBTAINED ..... **XI**

LIST OF MATERIALS FOR WHICH PERMISSION FROM CO-AUTHORS WERE OBTAINED ..... **XII**

ABBREVIATIONS ..... **XIII**

CHAPTER 1: INTRODUCTION **1**

1.1. GENERAL BACKGROUND 1

1.2. PROBLEM DEFINITION 3

1.3. METHODOLOGY AND APPROACH 3

1.4. SCOPE OF RESEARCH 4

1.5. OBJECTIVE & SIGNIFICANCE 5

1.6. CONTRIBUTIONS 6

CHAPTER 2: LITERATURE REVIEW GENERAL **8**

2.1 INTRODUCTION 8

2.2 CRACK DETECTION METHODS 10

2.2.1 Periodic Inspection Using Non-Destructive Test Methods 11

2.2.2 Continues Monitoring 15

2.3 SUMMARY 19

CHAPTER 3: CRACK DETECTION IN STEEL GIRDERS OF BRIDGES USING A BROKEN WIRE ELECTRONIC BINARY SENSOR 20

3.1 ABSTRACT 20

3.2 INTRODUCTION 21

3.3 METHODOLOGY AND PROCEDURE 25

3.3.1 Wire and Adhesive Selection 25

3.3.2 Testing the bond between wire and adhesive 26

3.3.3 Experimental Apparatus 28

3.3.4 Test on Steel Beam in Lab 30

3.3.5 Preparation, application and instrumentation 30

3.3.6 Test in Environmental Chamber 33

3.4. RESULTS AND DISCUSSION 33

3.4.1 Test on experimental apparatus 33

3.4.2 Test on steel beam in the lab 37

3.4.3 Bonding Properties test 39

3.5. CONCLUSION& FUTURE WORKS 40

CHAPTER 4: A FINITE ELEMENT AND EXPERIMENTAL INVESTIGATION OF THE INFLUENCE OF PRE-STRAINING OF WIRE ON THE SENSITIVITY OF BINARY CRACK SENSOR 42

4.1 ABSTRACT 42

4.2 INTRODUCTION 43
4.3 METHODOLOGY AND PROCEDURE 47
4.3.1 Experimental procedure 47
4.3.2 Tensile properties of wire 48
4.3.3 Pre-straining wire 49
4.3.4 Tensile properties of epoxy 50
4.3.5 Bonding between wire and epoxy 51
4.4 RESULTS & DISCUSSION 54
4.4.1 Experimental apparatus 54
4.4.2 Tensile properties of wire 55
4.4.3 Tensile properties of Epoxy 56
4.4.4 Bonding Properties 57
4.5 FINITE ELEMENT SIMULATION 61
4.5.1 Introduction 61
4.5.2 Simulation 63
4.5.3 Discretization 63
4.5.4 Load and Boundary Condition 64
4.5.5 Constraints 66
4.5.6 Numerical analysis 67
4.5.7 Post processing 67
4.5.8 Effect of pre-straining 68
4.5.9 Effect of bonding properties 70
4.5.10 Wire radius versus crack opening 70

4.5.11 Effect of position of wire in the epoxy 72

4.6 CONCLUSION& FUTURE WORKS 73

CHAPTER 5: PLACEMENT OF BINARY CRACK SENSOR ON SIMPLY SUPPORTED I-SHAPED STEEL GIRDERS 76

5.1. ABSTRACT 76

5.2 INTRODUCTION 77

5.3 CALCULATION OF THE MAXIMUM STABLE LENGTH OF A CRACK 80

5.4. FINITE ELEMENT SIMULATION 88

5.4.1 Introduction 88

5.4.2 Simulation 88

5.5. RESULTS & DISCUSSION 90

5.5.1. Stress Intensity Factor Estimation 90

5.5.2. Optimum Position for Distributed Crack Sensors 92

5.5.3. Feasibility Study of Using an Array of Strain Gauges for Crack Detection 95

5.5.4. Optimum Position for Placing Fibre Optic Sensors on Girder A, B 97

5.6. INSTALLATION ON LARGE-SCALE GIRDER OF A BRIDGE 99

5.7. CONCLUSION 100

CHAPTER 6: CONCLUSION & FUTURE WORKS 102

REFERENCES 105

APPENDIX A: SENSING CIRCUIT 113

APPENDIX B: EXPERIMENTAL RESULTS USING LOCTITE QUICKTITE & M-BOND ADHESIVES 115

APPENDIX C: FINITE ELEMENT SIMULATION TO STUDY EFFECT OF CHANGES IN MECHANICAL PROPERTIES OF THE ADHESIVE ON THE DETECTED CRACK OPENING 117

APPENDIX D: SENSITIVITY ANALYSIS OF BINARY SENSOR 118

APPENDIX E: PLACEMENT OF SENSOR ON GIRDERS WITH CRACK EXTENDED PARTIALLY INTO THE BOTTOM FLANGE 120

APPENDIX F: COST ESTIMATION FOR THREE METHODS OF DISTRIBUTED MONITORING 122

LIST OF TABLES

TABLE 3. 1 TEST RESULTS OF BINARY SENSOR ON EXPERIMENTAL APPARATUS 36

TABLE 3. 2. TEST RESULTS OF BINARY SENSOR ON STEEL GIRDER AT AMBIENT TEMPERATURE IN THE LAB 38

TABLE 3. 3 TEST RESULTS OF BINARY SENSOR ON STEEL GIRDER IN ENVIRONMENTAL CHAMBER 39

TABLE 3. 4 TEST RESULTS OF MICROBOND TEST. IT SHOWS THE BONDING BETWEEN WIRE AND ADHESIVE IS SUFFICIENT AND WIRE IS THE WEAKEST ELEMENT 40

TABLE 4. 1. TEST RESULTS OF MW79-C GAUGE 39 MAGNET WIRE IN COMBINATION WITH LOCTITE E-20NS EPOXY AS THE BINARY SENSOR ON THE EXPERIMENTAL APPARATUS. USING NOT PRE-STRAINED WIRE WILL RESULT IN INCONSISTENT CRACK OPENINGS AND THE AVERAGE IS MORE THAN THE DESIRED CRACK OPENING OF 0.2 MM. BY PRE-STRAINING THE WIRE RESULTS ARE MORE CONSISTENT AND IN THE RANGE OF THE DESIRED CRACK OPENING OF 0.2 MM. 55

TABLE 4. 2. MECHANICAL PROPERTIES OF WIRE MW-79C GAUGE 39 56

TABLE 4. 3. MECHANICAL PROPERTIES OF LOCTITE EPOXY E-20NS 57

TABLE 4. 4. DISPLACEMENT CALCULATION BETWEEN THE WIRE AND BEADS OF EPOXY 60

TABLE 4. 5. INTERFACIAL BONDING STRESS AND STIFFNESS BETWEEN WIRE MW79-C AND EPOXY E-20NS 62

TABLE 4. 6. CRACK OPENING WIDTH BASED ON DIFFERENT THICKNESS OF EPOXY AND DIFFERENT POSITIONS OF WIRE IN THE EPOXY 73

TABLE 5. 1. STRESS INTENSITY FACTOR (SIF) FOR GIRDERS A AND B FOR DIFFERENT LENGTH OF THE CRACK 87

TABLE 5. 2. NUMBERS IN THE TABLE ARE THE MAXIMUM DISTANCE (CM) BETWEEN STRAIN GAUGES TO DETECT A 10ME SHIFT IN THE MEASURED STRAINS. (GIRDER A) 97

TABLE 5. 3. NUMBERS IN THE TABLE ARE THE MAXIMUM DISTANCE (CM) BETWEEN STRAIN GAUGES TO DETECT A 10ME SHIFT IN THE MEASURED STRAINS. (GIRDER B)..... 97

TABLE 5. 4. COMPARISON BETWEEN THREE TYPES OF CRACK MONITORING USING DISTRIBUTED STRAIN GAUGES, FIBER OPTIC SENSOR AND BINARY CRACK SENSOR..... 98

TABLE C. 1. EFFECT OF CHANGE IN MECHANICAL PROPERTIES OF EPOXY ON THE DETECTED CRACK OPENING..... 117

LIST OF FIGURES

FIGURE 1. 1. A) DISTRIBUTED BINARY CRACK SENSOR WILL BE INSTALLED ON THE ENTIRE LENGTH OF STEEL GIRDERS AT SPECIFIED POSITIONS. B) AS SOON AS STRAINS FROM CRACK TRANSFERS TO THE EPOXY, EPOXY BREAKS C) OVER TIME CRACK WIDEN AND WILL RESULT IN INCREASE IN THE STRAINS OF WIRE AND FINALLY WILL CAUSE THE WIRE TO BREAK [17, 24] 4

FIGURE 2. 1. FOUR STAGES OF CRACK FORMATION AND PROPAGATION IN A STEEL GIRDER OF A BRIDGE 9

FIGURE 2. 2. ULTRASONIC TESTING A) TRANSDUCER POSITION AFFECTS THE DETECTION OF THE CRACK, B) TYPICAL UT READING FOR AN UN-CRACKED PLATE, C) TYPICAL UT READING FOR A CRACKED PLATE 13

FIGURE 2. 3. A) AS SOON AS A CRACK FORMS IN A GIRDER, WAVES WILL BE EMITTED TO THE SURFACE AND THE TRANSDUCERS WILL RECEIVE THE EMITTED SIGNALS. B) THE DAQ PROCESSES THE SIGNALS AND PLOTS THE EVENTS [40] 15

FIGURE 3. 1. A) BINARY SENSOR IS INSTALLED ON THE ENTIRE LENGTH OF THE STEEL GIRDER B) AS LONG AS THE CRACK WIDTH IS LESS THAN 0.2MM, CRACK PROPAGATES THROUGH THE EPOXY BUT WIRE IS STILL CONNECTED C) OVER TIME CRACK WIDEN AND CAUSES THE WIRE TO BREAK, THE RESISTANCE OF COPPER WIRE WILL TEND TO UNLIMITED AND ELECTRICAL CURRENCY IN THE CIRCUIT WILL TEND TO ZERO 25

FIGURE 3. 2. A) DIFFERENT DIMENSIONS OF MICROBEADS OF EPOXY ON COPPER WIRE, A MARKER WAS USED TO MARK THE ENDS OF THE BEADS (BLACK MARKS ON THE BEADS). B) THE LOAD FRAME (INSTRON 3366) WAS USED FOR PULL OUT TEST, THE FREE END OF WIRE WAS HELD IN

THE UPPER GRIP AND THE OTHER END WITH EPOXY WAS RESTRAINED USING THE KNIFE EDGE C) THE KNIFE EDGE RESTRAINS THE BEAD OF EPOXY TO TEST THE PULL OUT OF THE WIRE. 27

FIGURE 3. 3. A) LAYOUT OF THE TEST SETUP CONSISTING OF TWO STEEL PLATES, MICROMETER AND DISPLACEMENT GAUGE. THE BINARY SENSOR INSTALLED ON IT, B) BY TURNING THE MICROMETER PLATE A MOVES FROM PLATE B AND THE GAP BETWEEN TWO PLATES GETS WIDER. THE DISPLACEMENT GAUGE RECORDS THE GAP OPENING BETWEEN TWO PLATES, C) THE ENDS OF THE BINARY SENSOR ARE CONNECTED IN SERIES WITH A RESISTOR TO AN ELECTRICAL SOURCE WITH THE DAQ, MEASURING THE VOLTAGE ACROSS THE RESISTOR. AS SOON AS THE WIRE BREAKS, THE CONTINUITY OF THE WIRE WILL BE SEVERED, CHANGING THE RESISTANCE FROM A SHORT (Ω=0) TO AN OPEN (Ω=∞) [58] 29

FIGURE 3. 4. BINARY SENSOR, CONNECTION WIRE, DAQ AND RESISTOR MAKE AN ELECTRICAL CIRCUIT ON THE WEB OF A STEEL GIRDER 31

FIGURE 3. 5. A) 3-METER SPAN SIMPLY SUPPORTED STEEL BEAM WITH A PRE-EXISTING CRACK AT MID-SPAN. B) CROSS-SECTION OF THE BEAM, THE HATCHED AREA IS THE CRACKED PART. THE ENTIRE BOTTOM FLANGE HAS CUT AND CONTINUED 38.5MM INTO THE WEB TOWARDS TOP FLANGE C) THE BEAM AND ITS SUPPORTS UNDER LOAD FRAME D) A DISPLACEMENT GAUGE WAS MOUNTED TO RECORD THE CRACK OPENING 33

FIGURE 3. 6. A)EXPERIMENTAL APPARATUS- BINARY SENSOR, DISPLACEMENT GAUGE(PI-5-200, TOKYO SOKKI KENKYUJO) AND MICROMETER ON STEEL PLATES, B) AS SOON AS THE OPENING BETWEEN TWO STEEL PLATES REACHES TO 0.2MM THE BINARY SENSOR BREAKS [57] 34

FIGURE 3. 7. BINARY SENSOR BREAKS AT 0.12 MM CRACK OPENING AND THERE IS A SUDDEN CHANGE IN RESISTANCE OF WIRE 36

FIGURE 3. 8. BINARY SENSOR BREAKS AT 0.14MM CRACK OPENING AND THERE IS A SUDDEN CHANGE IN RESISTANCE OF WIRE 38

FIGURE 4. 1. A) THE BINARY SENSOR IS INSTALLED ON THE ENTIRE LENGTH OF THE STEEL GIRDER. THE EPOXY ADHERES THE WIRE TO THE STEEL GIRDER. WHEN CRACK FORMS IN STEEL GIRDER, THE STRAINS WILL BE TRANSFERRED FROM STEEL GIRDER TO THE EPOXY B) AS LONG AS THE CRACK WIDTH IS LESS THAN 0.2MM, CRACK PROPAGATES THROUGH THE EPOXY BUT WIRE IS STILL CONNECTED C) OVER TIME, UNDER TENSILE STRESSES, CRACK WIDEN TO 0.2MM WIDTH AND CAUSES THE WIRE TO BREAK. AS THE WIRE BREAKS, THE RESISTANCE OF WIRE WILL TEND TO UNLIMITED AND ELECTRICAL CURRENCY IN THE CIRCUIT WILL TEND TO ZERO [17, 24] 45

FIGURE 4. 2. SCHEMATIC OF THE APPARATUS FOR TESTING DIFFERENT COMBINATION OF WIRE AND ADHESIVE. TWO STEEL PLATES ARE CONNECTED TO EACH OTHER AT ONE END WITH A FLEXURAL HINGE AND THE GAP BETWEEN TWO PLATES SIMULATES THE CRACK ON A STEEL GIRDER. TURNING THE MICROMETER WILL CAUSE PLATE A MOVES FROM PLATE B AND WIDEN THE CRACK. THE DISPLACEMENT GAUGE RECORDS THE GAP OPENING BETWEEN TWO PLATES. THE ENDS OF THE BINARY SENSOR ARE CONNECTED IN SERIES WITH A RESISTOR TO AN ELECTRICAL SOURCE WITH THE DAQ, MEASURING THE VOLTAGE ACROSS THE RESISTOR. AS SOON AS THE WIRE BREAKS, THE CONTINUITY OF THE WIRE WILL BE SEVERED, CHANGING THE RESISTANCE FROM A SHORT ($\Omega=0$) TO AN OPEN ($\Omega=\infty$) [17] 48

FIGURE 4. 3 TEST TO MEASURE TENSILE PROPERTIES OF INSULATED COPPER WIRE. THE WIRE WAS GLUED TO TWO PIECES OF CARDBOARDS AND CARDBOARDS WERE MOUNTED ON THE LOAD FRAME (INSTRON3366) 49

FIGURE 4. 4. TENSILE TEST OF LOCTITE EPOXY E-20NS; A) DIMENSIONS OF COUPON BASED ON ASTM D638, THE THICKNESS IS EQUAL TO 4MM. B) AFTER 24HR OF CURING, COUPONS OF

EPOXY WERE READY FOR TESTING, C) THE COUPON OF EPOXY WAS MOUNTED INTO THE GRIPS OF THE LOAD FRAME FOR TENSILE TEST 50

FIGURE 4. 5. A) BEADS OF EPOXY ON THE WIRE. PREPARING BEADS IS A RANDOM PROCESS AND HENCE THERE IS VARIATION IN THE SIZE OF BEADS. B) POSITION AND DEFORMATION OF BEADS OF EPOXY AFTER MICROBOND TEST, IN SOME CASES (BEAD #2) THE SLIPPAGE BETWEEN WIRE AND THE BEAD IS VISIBLE 53

FIGURE 4. 6. A) FORCE-DISPLACEMENT DIAGRAM OF MICROBOND TEST BETWEEN A BEAD OF EPOXY AND WIRE (GAUGE 39 AND GAUGE 30). IN CASE OF GAUGE 39, SINCE THE EMBEDDED LENGTH OF WIRE IN EPOXY IS GREATER THAN 0.6MM, THE WIRE FRACTURES BEFORE DEBONDING. THEREFORE, GAUGE 30 WAS USED FOR THE MICROBOND TEST. B) FORCE VERSUS TOTAL DISPLACEMENT BETWEEN A BEAD OF EPOXY AND WIRE GAUGE 30. AT INITIAL STEPS OF APPLYING LOAD, THE BOND BETWEEN WIRE AND EPOXY IS STRONG AND THERE IS A SMALL DISPLACEMENT AT THE INTERFACE OF WIRE AND EPOXY (PART A). BY INCREASING THE LOAD, USING THE LOAD FRAME, THE INTERFACE BONDING STARTS TO WEAKEN (PART B) UNTIL IT REACHES POINT C AT WHICH THE INTERFACIAL BOND BREAKS COMPLETELY AND THE BEAD STARTS SLIDING ON THE WIRE (PART D). 58

FIGURE 4. 7. A) FORCE-DISPLACEMENT DIAGRAM OF TENSILE TEST OF WIRE AND MICROBOND TEST. B) AS THE WIRE PULLS OUT OF EPOXY, A PART OF ITS DISPLACEMENT IS DUE TO ITS ELASTIC AND PLASTIC DEFORMATION. IN ORDER TO CALCULATE THE DISPLACEMENT BETWEEN WIRE AND THE BEAD OF EPOXY, THE WIRE DEFORMATION SHOULD BE DEDUCTED FROM THE TOTAL DISPLACEMENT. C) THE NET DISPLACEMENT BETWEEN WIRE AND EPOXY VERSUS THE APPLIED FORCE 60

FIGURE 4. 8. FINITE ELEMENT SIMULATION OF THE SENSOR ON STEEL APPARATUS A) STEEL PLATES APPARATUS WERE SIMULATED IN ABAQUS USING A 4-NODE CONVENTIONAL SHELL ELEMENTS, B) AN S4 SHELL ELEMENT AND THE INTEGRATION POINT ON IT. 5 SECTION POINTS ARE CONSIDERED THROUGH THE THICKNESS [66], C) THE EPOXY AND THE WIRE WERE SIMULATED USING AN 8-NODE 3-D CONTINUUM SOLID ELEMENTS, D) THE BOUNDARY CONDITION OF THE SIMULATION 65

FIGURE 4. 9. RESULTS OF EXPERIMENTS AND FINITE ELEMENT ANALYSIS OF THE BINARY SENSOR ON THE APPARATUS. A)WIRE IS NOT PRE-STRAINED, EXPERIMENTAL RESULTS ARE IN A WIDE RANGE AND MORE THAN THE DESIRED CRACK OPENING OF 0.2 MM BUT NUMERICAL RESULTS ARE IN AN ACCEPTABLE RANGE, B) WIRE IS PRE-STRAINED BY 5%, RESULTS ARE MORE UNIFORM AND LESS THAN 0.2MM. USING THE INTERFACIAL STIFFNESS OF 75MPA/MM RESULTS IN A CRACK OPENING OUT OF HIGHER BAND OF EXPERIMENT C) WIRE IS PRE-STRAINED BY 10%. RESULTS ARE UNIFORM AND LESS THAN 0.2 MM. 69

FIGURE 4. 10. DIAMETER OF WIRE AT DISTANCES FROM THE CRACK CENTRE. BY INCREASING THE CRACK OPENING, THE CHANGE IN THE DIAMETER INCREASES. THE ENTIRE PROCESS OF DIAMETER CHANGE (NECKING OF THE WIRE) STARTS AT 0.4MM DISTANCE FROM THE CENTRE OF THE CRACK FOR ALL CRACK OPENINGS..... 71

FIGURE 4. 11. POSITIONING OF THE WIRE IN EPOXY ON STEEL PLATES. THE WIRE WILL BE POSITIONED AT DIFFERENT DEPTH OF THE EPOXY TO STUDY THE EFFECT OF WIRE PLACEMENT ON DETECTED CRACK OPENING OF BINARY SENSOR 72

FIGURE 5. 1. A) THE BINARY CRACK SENSOR WILL BE INSTALLED ON THE ENTIRE LENGTH OF A STEEL GIRDER AT A SPECIFIED POSITION. IT IS COMPRISED OF WIRE WHICH IS ADHERES TO THE STEEL GIRDER USING AN ADHESIVE. BY FORMATION OF A CRACK IN THE STEEL GIRDER, STRAINS WILL

BE TRANSFERRED FROM STEEL GIRDER TO THE EPOXY B) CRACK PROPAGATES THROUGH THE EPOXY WHEN CRACK OPENING ON THE GIRDER IS LESS THAN 0.2 MM BUT WIRE REMAINS CONNECTED C) OVER TIME, UNDER TENSILE STRESSES, CRACK OPENING INCREASES AND CAUSES THE WIRE TO BREAK. AS SOON AS THE WIRE BREAKS, THE RESISTANCE OF WIRE WILL TEND TO UNLIMITED AND ELECTRICAL CURRENCY IN THE CIRCUIT WILL TEND TO ZERO [17] 79

FIGURE 5. 2. THREE BASIC MODES OF DISPLACEMENT BETWEEN TWO SURFACES OF CRACK; A) MODE I, OPENING, B) MODE II, SHEAR AND C) MODE III, TEARING..... 82

FIGURE 5. 3. PARAMETERS OF CALCULATING THE STRESS INTENSITY FACTOR OF A CENTER-CRACKED TENSION PLATE; SIF DEPENDS ON FAR-FIELD STRESS, LENGTH AND GEOMETRY OF THE CRACK 83

FIGURE 5. 4. A) GEOMETRY AND POSITION OF STRAIN GAUGES ON BOTH GIRDERS A AND B, B) CROSS SECTION OF GIRDER A, C) CROSS SECTION OF GIRDER B 85

FIGURE 5. 5. DISTRIBUTION FACTOR OF A PASSING TRUCK OVER GIRDERS OF A BRIDGE. A) BY PASSING A TRUCK OVER AN 8-SPAN BRIDGE-AT THE SHOWN POSITION-, APPROXIMATELY 35% OF LOAD WILL BE CARRIED BY GIRDER A, B) BY PASSING THE SAME TRUCK OVER A 4-SPAN BRIDGE AT THE SHOWN POSITION, GIRDER B WILL CARRY APPROXIMATELY 38% OF THE TOTAL LOAD. 85

FIGURE 5. 6. A) FINITE ELEMENT MODEL OF THE SIMPLY SUPPORTED STEEL GIRDER UNDER SERVICE LOADS. B) CONVENTIONAL SHELL ELEMENTS, C) FIVE INTEGRATION SECTION POINTS THROUGH THE THICKNESS, D) 30CM CRACK ON THE WEB OF THE STEEL GIRDER..... 89

FIGURE 5. 7. STRESS INTENSITY FACTOR CALCULATION A) FOR GIRDER A AND B) FOR GIRDER B. IN BOTH CASES AT SMALLER CRACK LENGTHS THE FEM RESULTS AND THE MANUAL CALCULATIONS ARE IN GOOD AGREEMENT C) COMPARING CALCULATED SIF AND THE CRITICAL

VALUE FOR GIRDER A, D) COMPARING CALCULATED SIF AND THE CRITICAL VALUE FOR GIRDER B 91

FIGURE 5. 8. A) CRACK OPENING VS DISTANCE FROM BOTTOM FLANGE (GIRDER A) FOR CRACKS WITH DIFFERENT LENGTHS VARYING FROM 20 CM TO 80 CM. BY POSITIONING THE BINARY SENSOR AT 15CM TO 25CM ABOVE THE BOTTOM FLANGE, ANY CRACK LONGER THAN 40CM CAN BE DETECTED. B) CRACK OPENING VS DISTANCE FROM BOTTOM FLANGE (GIRDER B) FOR CRACKS WITH DIFFERENT LENGTHS VARYING FROM 20 CM TO 60 CM. BY POSITIONING THE BINARY SENSOR AT 15CM TO 22 CM ABOVE THE BOTTOM FLANGE, ANY CRACK LONGER THAN 40CM CAN BE DETECTED. 94

FIGURE 5. 9. MEASURED STRAIN AT 250 MM ABOVE THE BOTTOM FLANGE FOR GIRDERS A. THE MEASURED STRAIN AT MID-SPAN UNDER LIVE LOAD IS APPROXIMATELY 58ME. AS SOON AS A CRACK FORMS IN THE GIRDER, THERE WILL BE SUDDEN DROP IN THE MEASURED STRAIN. IN ORDER TO DETECT THE 10ME SHIFT IN THE STRAIN, STRAIN GAUGES SHOULD BE PLACED AT MAXIMUM 101 CM FROM EACH OTHER TO DETECT CRACKS LONGER THAN 40 CM. THEREFORE, APPROXIMATELY 30 STRAIN GAUGES FOR GIRDER A ARE REQUIRED. 96

FIGURE 5. 10. INSTALLATION OF BINARY CRACK SENSOR ON A 30-METER SPAN STEEL GIRDER OF A BRIDGE IN 7 SEGMENTS. 99

FIGURE 5. 11. INSTALLATION PROCEDURE OF THE BINARY SENSOR ON GIRDER A. 100

FIGURE A. 1. SENSING CIRCUIT OF THE BINARY CRACK SENSOR 113

FIGURE A. 2. TYPICAL OUTPUT OF THE BINARY CRACK SENSOR 114

FIGURE B. 1. LOCTITE QUICKTITE WAS USED TO INSTALL THE WIRE ON THE STEEL PLATES. MICRO CRACKS ON THE SURFACE OF THE ADHESIVE AFTER CURING CAUSED INCONSISTENCY IN THE DETECTED CRACK OPENINGS. 115

FIGURE B. 2. TYPICAL DETECTED CRACK OPENING. ALTHOUGH THE DETECTED CRACK OPENING WAS LESS THAN THE DESIRED OPENING, MICRO CRACKS ON THE SURFACE OF THE ADHESIVE RESULTED IN INCONSISTENT RESULTS. 115

FIGURE B. 3. TYPICAL FORCE-DISPLACEMENT DIAGRAM OF BINARY SENSOR USING M-BOND EPOXY. 116

FIGURE B. 4. M-BOND WAS USED TO INSTALL THE WIRE ON THE STEEL PLATES. THE INITIAL DEBONDING BETWEEN WIRE AND ADHESIVE RESULTED IN WIDER EFFECTIVE CRACK OPENING. IN ORDER FOR WIRE TO REACH THE FINAL STRAIN, WIDER CRACK OPENING WAS REQUIRED. 116

FIGURE D. 1. CUMULATIVE PROBABILITY OF THE DETECTED CRACK OPENING AT EACH POSITION OF THE CRACK. BY PLACING THE SENSOR AT 15 CM TO 25 CM ABOVE THE TENSION FLANGE IN GIRDER A, CRACKS WITH MINIMUM 40 CM LENGTH CAN BE DETECTED 119

FIGURE E. 1. CRACK OPENING VS DISTANCE FROM BOTTOM FLANGE FOR DIFFERENT CRACK LENGTH ON GIRDER A. CRACK STARTS AT DEFICIENCIES ON THE WEB OF THE GIRDER AND PROPAGATES INTO THE WEB. CRACKS WILL BE ARRESTED IN THE BOTTOM FLANGE. 121

LIST OF COPYRIGHTED MATERIAL FOR WHICH PERMISSION WAS OBTAINED

- Farnaz Raeisi, A. Mufti, G. Mustapha and D. J. Thomson "Crack detection in steel girders of bridges using a broken wire electronic binary sensor" Journal of Civil Structural Health Monitoring, vol.7, pp. 233-243, 2017.
- Farnaz Raeisi, A. Mufti and D. J. Thomson, "A Finite Element Model and Experimental Investigation of the Influence of Pre-Straining of Wire on the Sensitivity of Binary Crack Sensors", Journal of Civil Structural Health Monitoring (2018). https://doi.org/10.1007/s13349-018-0290-7

LIST OF MATERIALS FOR WHICH PERMISSION FROM CO-AUTHORS WERE OBTAINED

- Farnaz Raeisi, A. Mufti, G. Mustapha and D. J. Thomson "Crack detection in steel girders of bridges using a broken wire electronic binary sensor" Journal of Civil Structural Health Monitoring, vol.7, pp. 233-243, 2017.
- Farnaz Raeisi, A. Mufti and D. J. Thomson, "A Finite Element Model and Experimental Investigation of the Influence of Pre-Straining of Wire on the Sensitivity of Binary Crack Sensors", Journal of Civil Structural Health Monitoring (2018). https://doi.org/10.1007/s13349-018-0290-7
- Farnaz Raeisi, Aftab Mufti and Douglas J. Thomson, "Placement of Binary Crack Sensor on Simply Supported I-Shaped Steel Girders", Submitted to the Journal of Smart Material and Structure, Aug. 2018
- Farnaz Raeisi, Aftab Mufti, Mustapha Gamal and Douglas J. Thomson, "Binary Crack Sensor for Steel Girder Bridges: Installation Procedure in Field", Presented at the 10th International conference on short and medium span bridges, Quebec, August 2018

ABBREVIATIONS

AASHTO	American Association of State Highway and Transportation Officials
ASTM	American Society for Testing and Materials
CIF	Constraint Induced Fracture
DAQ	Data Acquisition System
FHWA	Federal Highway Administration
NDT	Non-Destructive Tests
NDE	Non-Destructive Evaluation
SHM	Structural Health Monitoring
SIF	Stress Intensity Factor
UT	Ultrasound Test

CHAPTER 1: INTRODUCTION

1.1. GENERAL BACKGROUND

In a transportation system, bridges are counted as a key element. Among various categories of superstructures, steel girder bridges are the most numerous one (around 40% of bridges) [1–3]. During 1950's and 70's there was a period of major bridge construction in North America and many other parts of the world [3]. Studies have concluded that many of those bridges are reaching the end of their designed service life [4, 5]. One of the critical deficiencies which may occur in aging steel bridges is crack formation and propagation over time [6]. Cracks may form as a result of cyclic loading over time. Welding defects, discontinuities in material or geometry, defects introduced in manufacture or construction may lead to fatigue development during the service life of a girder [6, 7]. Detecting cracks in steel girders before they reach to an unsafe stage is critical to prevent the unpredictable loss of service and associated expenses. The most common method for bridge condition assessment is to perform visual inspections. Variations in inspector's skill, the accessibility to required parts of the structure and the significant time between inspections are significant limitations to the value of visual inspection for crack detection [8]. In addition to these practical limitations, the small size of fatigue cracks make the detection process challenging using

visual inspections [9]. To augment visual inspection, several other non-destructive evaluation (NDE) methods have been developed to assess the integrity of bridge girders. Acoustic emission, eddy current and ultrasound testing are some examples of NDE techniques [10]. However, NDE techniques are expensive and are performed at discrete time intervals. Therefore, small cracks might form at time interval between two sequential inspection and grow to lengths that will compromise the structure. Two examples of this issue are the fracture in a girder of I-95 Highway Bridge over the Brandywine River and in a girder of the Diefenbaker Bridge over North Saskatchewan River in Prince Albert, Canada [11, 12]. It is desirable to have methods that can provide continuous information on the integrity of the bridge [13]. Continuous Structural Health Monitoring is one means of providing more quantitative and timely estimates of structural integrity[14]. In general, continuous monitoring techniques can be divided into two categories; discrete monitoring (including strain gauges, short gauge or long gauge sensors) and distributed monitoring (which includes installation of a smart film or fibre optic sensors) [15–23]. Using discrete monitoring sensors, the local behaviour of structures can be monitored. However, in long and deep girders of bridges, cracks may occurs in locations far from the sensor and would be challenging to detect [15]. In order to be able to detect cracks at any location of the girder, an impractical number of sensors might be needed to ensure crack detection. Distributed monitoring techniques are more comprehensive since the sensor is installed on the entire length of the girder [15]. Few distributed monitoring methods are available such as installation of smart film or fibre optic sensors. Zhang et al have demonstrated the use of a smart film for detecting cracks on concrete structures, but has not studied its application in steel girders[22, 23]. Also, existing fiber optic sensors and installation job are very costly. The cost of the sensing systems exceeds $1000/m. At this cost level the technology is only practical for a very few structures. Due the numerous

bridges and other structures that would benefit from continuous distributed monitoring, and also considering the fact that existing methods developed to inspect bridges are usually expensive and impractical to be used, there is a need for an accurate and cost-effective sensor system.

The objective of this research is to develop and test a distributed binary crack sensor which can be installed easily and at a fraction of the cost on the entire length of steel girders and is capable of detecting cracks with opening of less than 0.2mm which is comparable with what fibre optic sensors can detect [16].

1.2. PROBLEM DEFINITION

Available continuous distributed monitoring sensors which can detect the presence of cracks on steel girders of bridges are costly which makes them impractical to be used for most of the bridges. Due to numerous bridges which are aging and required to be monitored, there is a need to develop a sensor which can be installed easily in a fraction of the cost on steel girders of bridges.

1.3. METHODOLOGY AND APPROACH

The binary crack sensor is a distributed sensor composed of a thin wire which can be installed on the entire length of a steel girder using a carefully designed adhesive. The sensor is designed so that when a crack of less than 0.2 mm forms the local increase in strain will be coupled to the wire causing it to break. The break can be easily detected using standard electronics. The design of the adhesive and wire system is very challenging to meet this goal. To develop this sensor, different materials have been tested. The adhesive was selected from two different categories; cyanoacrylate and epoxy. To test the material, a small-scale experimental apparatus was designed. Combinations of wire and adhesive were tested on the apparatus and combinations with best results were tested on a large-scale steel girder in the lab. The sensor was tested at room temperature, -30ºC and +40ºC. Mechanical properties and bonding properties between the wire and adhesive have been

tested to be used in finite element simulation. Finite Element Model of the sensor has been simulated in program ABAQUS to be used to guide the design and testing for future applications.

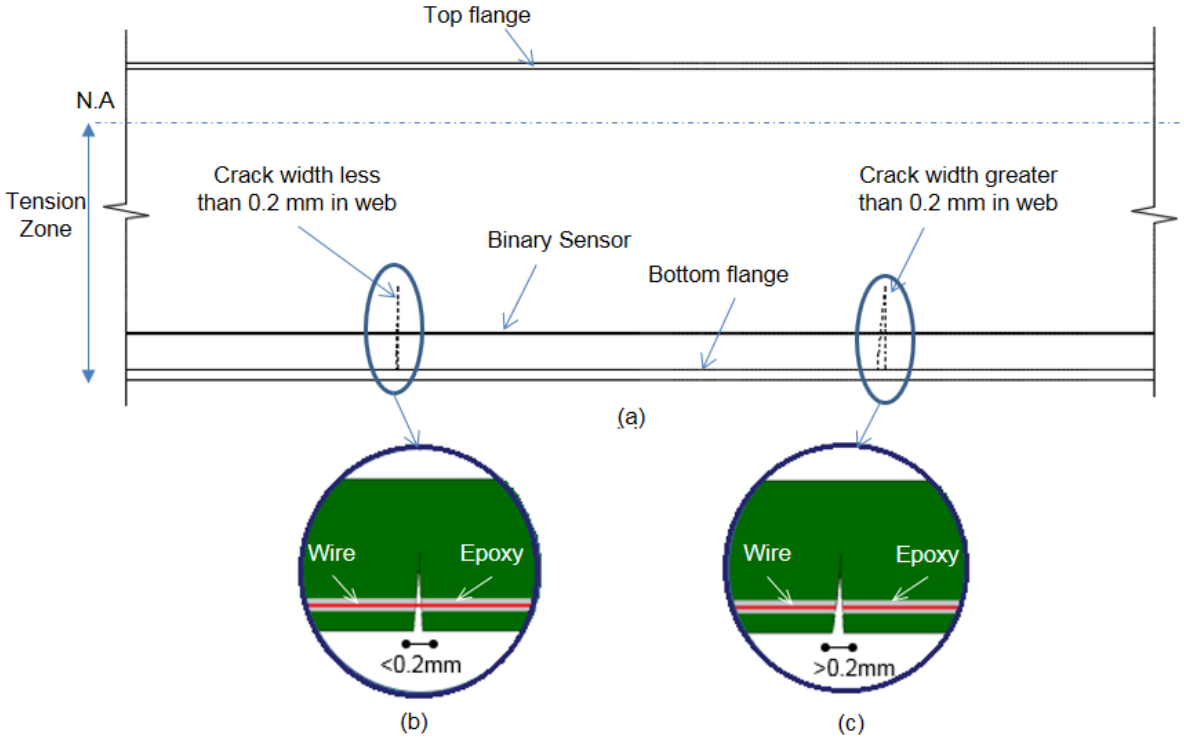

Figure 1. 1. a) Distributed binary crack sensor will be installed on the entire length of steel girders at specified positions. b) As soon as strains from crack transfers to the epoxy, epoxy breaks c) over time crack widen and will result in increase in the strains of wire and finally will cause the wire to break [17, 24]

1.4. SCOPE OF RESEARCH

The overall purpose of this research is to develop a distributed binary crack sensor to detect cracks in steel girders of bridges. The binary crack sensor has the capability to detect 0.2 mm crack openings and it has been tested at ambient temperature, -30ºC and +40ºC.

1.5. OBJECTIVE & SIGNIFICANCE

The main objective of this project is to design a distributed binary crack sensor that can be easily deployed on large structures at low cost. This sensor will be installed on I-shape steel girders of bridges to detect cracks with opening of less than 0.2 mm.

In this context, the following specific objective are identified:

- To design, build and test a wire and adhesive system that forms a binary sensor capable of detecting crack openings less than 0.2 mm in steel girders of bridges. The tests related to this aspect are described in Chapter 3.
- To measure the mechanical properties and bonding properties between materials so that an FEM of the binary sensor can be created to simulate the operation of the binary sensor and to allow future optimization of the sensor The tests related to this aspect are described in Chapter 4.
- To test the binary crack sensor application on a small scale steel girder in lab at ambient temperature and two extreme temperature (-30ºC and +40ºC).The tests related to this aspect are described in Chapter 3.
- To field test the application of the binary crack sensor on a girder of a bridge in Canada to investigate the installation procedure and the effect of environmental conditions on the application of the binary crack sensor
- To use Finite Element Analysis to for determining the pre-straining limit of the wire for effective crack detection. This aspect of the work is discussed in Chapter 4.
- To use Finite Element Analysis to determine the optimum placement of distributed sensors, including the binary sensor, for the detection of cracks in typical steel I- shaped girders. This aspect of the work is discussed in Chapter 5.

- To estimate the stress intensity factor (SIF) in typical I-shaped steel girders and to estimate the crack opening along the crack for different lengths to confirm that the sensor threshold of 0.2 mm is suitable. This aspect of the work is discussed in Chapter 5.

This sensor can also be used in structures other than bridges, such as residential buildings, community structures, transportation infrastructure, mining, oil and gas structures and many other infrastructures.

The sensitivity of the sensor system to temperature has been also investigated so that it can be used in the Northern parts of Canada.

1.6. CONTRIBUTIONS

The following part describes contributions of this work;

- An innovative distributed binary sensor has been developed for detecting crack openings less than 0.2mm on steel girders of bridges. The sensor can be installed at a fraction of the cost and has been tested for extreme temperatures on a small scale steel girder in an environmental chamber. The sensor has also been field tested on a bridge in Canada over a year to investigate the installation procedure as well as the effect of environmental conditions on the sensor.
- An FEM of the binary sensor has been simulated in ABAQUS to study the effect of different parameters on the application of the sensor and to be used in future for other applications. In order to create the Finite Element Model, the mechanical properties of materials were determined and the bond between wire and adhesive was determined using a micro-bond experiment.
- The use of the binary sensor has been simulated using a Finite Element Model of I-shaped girders from two typical medium span steel girder bridges. An ABAQUS simulation was

used to estimate the crack opening for different crack lengths to estimate the optimal placement of distributed sensors. The critical length of the crack was estimated for the typical steel girders using the SIF concept.

CHAPTER 2: LITERATURE REVIEW GENERAL

2.1 INTRODUCTION

Highway bridges are regarded as one of the most critical elements in transportation infrastructures [25]. One of the most common structural types of bridges is the slab-on-girder configuration [2]. The majority of superstructure of this type of highway bridges includes steel girders most of which were built more than 50 years ago (between 1950 to 1970) and are reaching the end of their design service life [3–5]. Federal Highway Association of USA reports that by the end of 2016, approximately 253,000 bridges are classified as steel girder bridges. This number is approximately 40% of the total number of bridges in US. The inspections show that almost 13% of the steel girder bridges (32,000 bridge) are structurally deficient [26]. Generally, steel plate girders are made of two steel flanges which are welded to the web to form an I-shape cross section. For a bridge to function completely, other elements such as bracings, stiffeners, cover plates, etc- are connected to the girders using welding connections or bolts. Over time, cyclic truck traffic may cause cracks mainly at weld locations; these cracks develop due to inherent defects in the welds and are referred to as constraint induced fractures (CIFs). Some cracks may also form due to out of plane displacement of a small portion of the web (distortion-induced). Cracks may also form as a result

of welding defects at welding intersections (Constraint Induced Fractures). The Constraint Induced Fractures (CIF) generally occurs at the junction of the gusset plates and webs. A small defect in the welding of the intersection results in high stress concentration that leads to crack formation and propagation. Crack on the Diefenbaker Bridge over North Saskatchewan River in Prince Albert, Saskatchewan, Canada in 2011 and on the Hoan Bridge on I-794 in Milwaukee, Wisconsin, USA in December 2000 are examples of CIF [12]. Crack may also occur due to material defects, defects introduced in manufacture or construction at the position of those details with low fatigue resistance such as web gusset plates [6, 7, 9, 27]. Over time, the initial discontinuity may grow in size and propagate in a certain direction. For example, in a study on the Quinnipiac River Bridge, Fisher et al. [28] have suggested different stages of crack initiation and propagation on the web of the steel girder. At the first stage, the crack initiates due to the initial fabrication condition. Then in the second phase, the crack penetrates into the web of the girder under the cyclic loads. In stage 3, crack propagates spontaneously in the web towards the tension flange and if not arrested it continues to the tension flange from one end and propagates in the web from other end of the crack (stage 4).

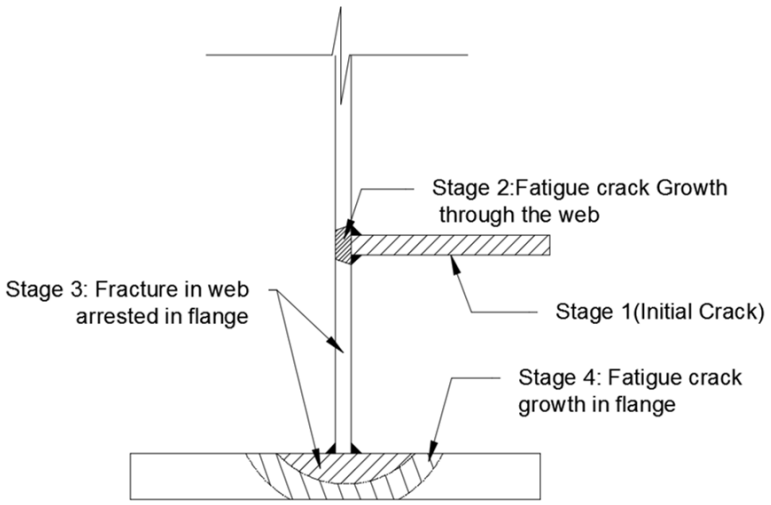

Figure 2. 1. Four stages of crack formation and propagation in a steel girder of a bridge

Figure 2. 1 shows the suggested stages of crack formation and propagation in a typical girder of a bridge [28]. In steel girder of bridges, transverse cracks -which forms perpendicular to the longitudinal axis of the girder- are the critical ones. Transverse cracks will propagate into the web of the girder and will cause the loss of cross section and therefore will reduce the structural capacity. If not detected, the crack may reach an unstable length and propagate spontaneously. At this stage, the girder is not able to carry the applied load. Therefore, it is critical to detect cracks before they reach the critical length [7, 11, 12, 29].

2.2 CRACK DETECTION METHODS

The need for monitoring the condition of bridges became evident after 1960's as the result of catastrophically failure of few steel bridges- Kings Bridge in Melbourne, Australia (1962) and Silver Bridge, at West Virginia,USA (1967)-[9, 30]. Rules and guidelines were organized for inspection of bridges after December 1967 when 2235-foot Silver Bridge, at West Virginia, collapsed into the Ohio River, resulted in the death of 46 civilians [31].

For many years the visual inspection was the only method for evaluating the condition of bridges. In recent decades, other Non-Destructive Evaluation (NDE) methods are also being applied to augment the visual inspection. When a crack forms in a girder, it affects the local strain field around the crack and wave propagation properties. In addition, the crack formation and propagation may generate acoustic waves. The NDE methods, uses these parameters to detect and characterize the cracks (strain gauges, fiber optic sensors, acoustic emission method, …) [29].

In this work, NDE methods are divided into two major categories:

1. Periodic monitoring
2. Continuous monitoring

2.2.1 Periodic Inspection Using Non-Destructive Test Methods

Visual Inspection

Visual inspection has been one of the most common types of NDE methods in last decades which provides a general overview of the current state of the bridge [8, 32]. Since conducting the visual inspection does not require any specific testing equipment, It makes it more economical compare to other methods of inspection [30]. However, the visual inspection is suffering from some limitations which in some cases may result in inconsistent evaluations. Potential limitations of visual inspection can be categorized as timing, interpretability and accessibility [8].

- Timing: According to FHWA the bridge inspection period should not exceed 24 months [33] and for specific bridges, the visual inspection will be done at time intervals less than 2 years [8]. However, in the time interval between two sequential inspections, cracks may form and propagate [29]. For example, in 2003 a fractured occurred in one of the girders of I-95 Highway Bridge over the Brandywine River just a few months after the last full inspection [11]. Crack in a girder of the Diefenbaker Bridge over North Saskatchewan River in Prince Albert, Canada is another example of this issue. Although the bridge had been inspected regularly and at no time during the visual inspections cracks were noted in the girders, a major crack through the flange in one of the girders was observed by a canoeist [12].
- Interpretability: Since the results of visual inspection are subject to the inspector's interpretations, at some cases the condition assessment of the bridge might be inadequate. Therefore, in order to get more accurate assessments, having a trained engineer who knows about the elements of a structure to find most possible places of forming a crack in the structure will be required [8, 30].

- Accessibility: One major difficulty in conducting the visual inspection is the accessibility to the point of inspection such as top surface of the top flange. The method is also not reliable since some small fatigue cracks may be inconspicuous or covered by paint which makes it hard for the inspector to detect it [8, 9, 30].

In order to detect small cracks, other NDE methods should be applied to enhance the visual inspection [34].

Ultrasonic Testing (UT)

One of the common NDT techniques for inspecting steel bridges is the pulse-echo ultrasonic method [10]. This method is based on generating and sending sound waves above the audible range to the test specimen. The wave characteristics and signals change as the crack propagates and reflect from different surfaces and in-homogeneities of the test object. By receiving and processing signals from the material, any defect in the object can be determined [10, 35–37]. The test setup which is being used for pulse-echo method is composed of a transducer which emits the ultrasonic pulse, a data acquisition system (DAQ) which collects the reflected pulses and a spatial control system which records the coordinate of the transducer at each time [36]. The transducer moves on the surface of the objective plate and sends and receives the pulsed waves. The reflected pulse comes from either an imperfection within the object or the edge of the object. The time difference between the moment of sending out of the wave and receiving time of the wave are used to determine the thickness of the plate. Any peak in the measured wave indicates the existence of an imperfection in the plate [35, 37]. Figure 2.2 (b) and (c) shows a typical reading of a pulse-echo scan. When the transducer is positioned at a plate with no imperfections, the sound will be sent to the specimen and will be reflected from the edge of the specimen (Figure 2.2 a,b). By moving the

transducer to the crack location, the reflections from any discontinuity and also from the edge of the crack will be plotted on the monitoring device (Figure 2.2 c).

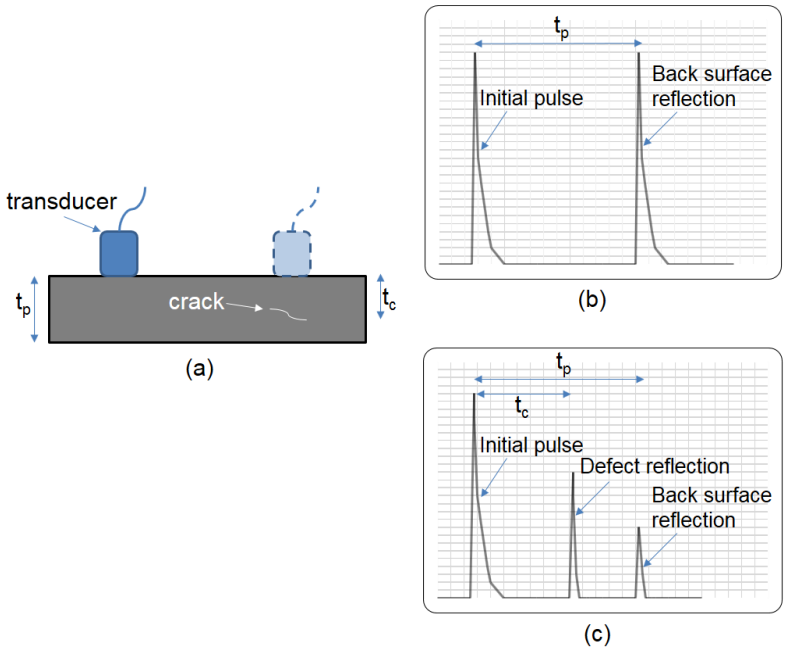

Figure 2. 2. Ultrasonic testing a) transducer position affects the detection of the crack, b) typical UT reading for an un-cracked plate, c) typical UT reading for a cracked plate

Although The Ultrasound method has been used to detect cracks in steel girder bridges for decades, the available limitations make it difficult to be used for most of the bridges [9, 30, 35, 38]:

- The ultrasound method is time consuming
- The testing area should be clean of paint and any debris
- The inspector should be knowledgeable in the use of the method
- The results may vary according to inspector's interpretations
- Due to available noises, only sever cracks and damages can be identified.
- Crack growth monitoring is not possible using this method

To overcome the above limitations of this method, it is required to be applied in combination with other NDT methods.

Acoustic Emission (AE)

The word "acoustic" refers to hearing. For a long time, there have been sounds which were emitted before collapsing of any structure. The concept of acoustic emission (AE) dates back to 1939, when the watchman of a suspension bridge reported hearing fracturing sounds coming from the cables on silent nights. After that event, research on this phenomenon began and in the early 1950's Kaiser published a paper entitled" Results and Conclusions of Sound in Metallic Materials under Tensile Stress". During 1950's and 1960's the AE method became a known and used in the non-destructive evaluation of civil infrastructure [34, 39].

The Acoustic emission utilizes high frequency sound waves to detect crack propagation. As soon as crack propagates on the structure, it releases energy which travels in the form of high-frequency stress waves. By separating the background noise from the available signals the condition of the structure can be determined [9, 34].

In order to monitor the crack propagation on a steel girder, AE transducers are installed at known positions where cracks are thought to be propagating. The transducers receive the released waves and convert them into a voltage.

The voltage is digitized by a DAQ often using some form of amplifier. The digitized signals are processed and plotted as the acoustic emission output versus time graphs, as shown in Figure 2.3. By using the AE method, the crack initiation time, fatigue crack growth and the fracture time can be estimated. Although the AE systems are one of the most well developed NDE monitoring techniques that can be used in places which are difficult to access using other techniques, the available background noise and the fact that the transducers should be installed at short distances from each other to cover the entire girder, makes it costly and impractical to be used for detecting small cracks on most bridges [38].

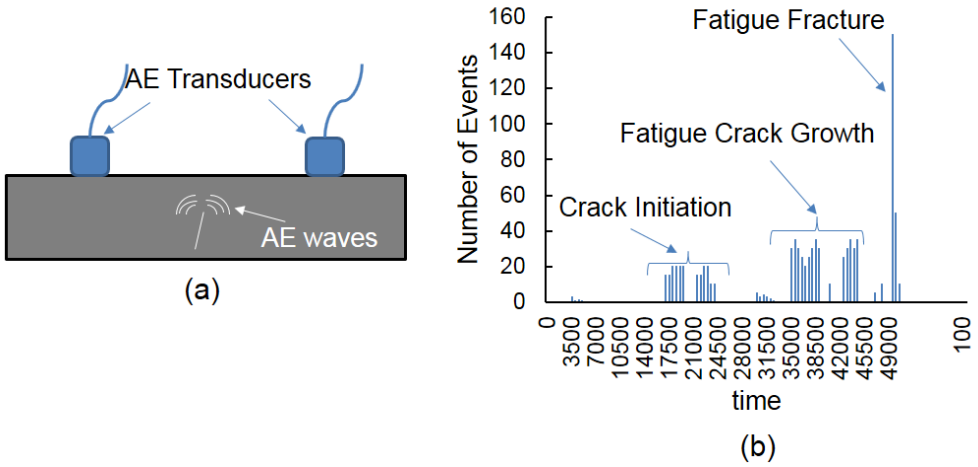

Figure 2. 3. a) As soon as a crack forms in a girder, waves will be emitted to the surface and the transducers will receive the emitted signals. b) The DAQ processes the signals and plots the events [40]

2.2.2 Continues Monitoring

Vibration based damage detection

Utilization of vibration-based damage detection method was first started in the aerospace and offshore oil industries. In the last few decades, the application of vibration-based damage detection methods in structural and bridge engineering have been explored by many researchers. The basic concept used in this technique is the correlation between the dynamic responses (such as mode shape and natural frequency) of a damaged system with those of the undamaged ones. As soon as a damage occurs in a bridge, there will be changes in the stiffness, boundary conditions or damping properties. The changes can be monitored by a variety of available sensors, being accelerometers, strain gauges, etc. The measured data (which is initially in time domain) then can be converted to frequency domain or modal domain for analysis. Although the conversion between time and frequency or modal domains may result in losing some data, but the majority of research has been

focusing on the modal domain analysis due to simplicity in interpretation of natural frequencies and mode shapes. However, research has been carried out to discover advanced techniques in using the gathered data of the dynamic responses in any of the domains. Some of the techniques can be categorized as Natural Frequency Based methods, Mode Shape Based methods, Mode Shape Curvature Based methods, Time Series methods and etc. [20, 41, 42]

Among these methods, the natural frequency based method and the mode shape based method have been one of the most commonly explored methods for damage detection in bridges. Many researchers have studied these methods on either laboratory models or real condition bridges such as Farrar et al. on the I-40 Bridge over the Rio Grande in New Mexico [43], Schallhorn et al. on US 30 near Ames in Iowa [42] and De Roeck et al. on the Z24 Bridge in Switzerland [20]. The result of the research proves that there are some advantages in using the vibration-based damage detection methods compare to other SHM techniques. Advantages may include the flexibility in placing the sensors around the crack and the ability of the method to detect the presence of crack, to locate the position of the crack, to quantify the severity of the crack and to predict the remaining life of the bridge [42].

Although there are advantages in using the vibration-based damage detection method to monitor the condition of a bridge, the uncertainty in measurements makes it impractical for detecting small cracks in steel girders of bridges. Studies prove that measurements are sensitive to temperature, loading condition, noise and other unknown parameters which will effect the reliability of the technique [42].

Strain-based sensing using strain gauges

Structural condition assessment using strain gauges are one of the most common strategies used on steel girder bridges. In general there are two approaches available for crack detection in steel

girders using the strain gauges; direct sensing and indirect sensing. In the first approach (direct sensing), strain gauges are directly in contact with the surface containing the crack. The formation of a crack changes the strain field around the crack. The perturbation in the strain can be used to detect the presence of the crack. For example, when a transvers crack forms in a girder (perpendicular to the flange), the longitudinal strains around the crack will be perturbed; strains at the crack tips will increase and at other locations will decrease. Therefore, by measuring a shift in the strain, the presence of a crack can be identified. Although this method has the advantage of simple interpretation of measurements to detect the presence of a crack, however it requires a large number of sensors which will result in complex wiring and large number of data acquisition channels and will cause an increase in the overall cost of monitoring.

The second approach-indirect sensing method- is based on strain measurements at positions far from the surface containing the crack. In this method, the strain gauges will be mounted on the flanges of the girder.

Since in this method, the strain gauges are not in contact with the surface containing the crack, algorithms are required to predict the damage in the girder. The three most common algorithm in this method are based on three sets of data:

- Live load distribution in girders
- Pick strains and live load stresses
- Neutral axis location

Any changes in the measured data, may reflect a damage in the girder [44]. In this method, sophisticated algorithms are required to analyse the data from the sensors and the algorithms should consider the effects of noise, loading condition and other uncertainties. However, the

advantage of using this method of monitoring is the small number of strain gauges for monitoring the strains.

In general, in the strain-based monitoring technique the effect of temperature variation of the strain gauges as well as the mounting variations should be considered in the results [15, 29, 44, 45].

Fiber Optic Sensors

Since 1990's, the fiber optic sensors are being used for structural health monitoring purposes. In a simple explanation, a fibre optic sensor is made of two major parts of core and cladding with two different refractive indexes. The light travels in the core with a diameter of 5μm. The cladding (with a diameter of 125μm) is supporting the core and reducing the loss of light which is travelling within the core. In general, finer optic sensors will be categorized as extrinsic and intrinsic. Available fiber optic sensors are under intrinsic category and can be sub-categorized as short gauge (2 mm to 50 mm length), long gauges having a length of more than 50 mm and distributed sensors. All three gauge lengths are being used for monitoring of structures. According to Glisic and Inaudi [15], the short gauge fiber optic sensors gives information on the local behaviour of the structure but might miss damages which may occur in un-instrumented parts of the structure which are not instrumented. The long gauge monitoring sensors will cover most of the regions of the structure and can give enough information about the behaviour of the structure. However, the ability to identify the damage in locations far from the sensor might be challenging due to environmental and loading conditions. Therefore, distributed fibre optic sensors are more practical to be used for detecting damages in steel girders of bridges.

There are two main principles in using the distributed fibre optic sensors; Rayleigh scattering and Brillouin scattering. The Brillouin scattering is less sensitive to optical losses and can be used for monitoring bridges with long spans. Distributed fiber optic sensors based on Brillouin scattering

is one common way of crack detection in steel girder of bridges [16, 46, 47]. In this method the fiber optic sensor will be installed at specified positions on the girder and can provide information along the entire length of the girder. The crack can be detected as an unusual high strain in the monitoring process but detecting the crack width is challenging due to accuracy of the system. Although the sensors are designed to detect crack width of greater than 0.5mm, in a study, Mufti, Thomson et al. [16] has been able to detect the crack width of 0.2mm using the Brillouin based fiber optic sensor [16].

2.3 SUMMARY

In General, the monitoring techniques for detecting cracks in steel girder of bridges can be categorized as periodic inspection using NDT and continuous monitoring using SHM techniques. Depending on the condition of the bridge, the NDT methods will be conducted at 1-year or 2-year intervals. Therefore, small cracks may form and propagate in the time interval between two inspection and be missed in the inspection time. Continuous monitoring techniques are the solution to this issue. Available monitoring techniques such as vibration-based or strain-based damage detection methods are one way of detecting cracks in steel girders of bridges. However, both techniques are affected by environmental and loading conditions. Using the FOS is one common technique in detecting the cracks. However, the high cost of installation and DAQ systems makes it impractical to be used for most of the bridges.

Considering the limitations of existing monitoring systems and the fact that the number of infrastructures in need of monitoring is getting higher, there is a need for an accurate and cost-effective sensor system. In this research a distributed binary crack sensor has been developed and demonstrated. The binary crack sensor can be installed at a fraction of the cost on the entire length of steel girders and is capable of detecting cracks with less than 0.2 mm opening.

CHAPTER 3: CRACK DETECTION IN STEEL GIRDERS OF BRIDGES USING A BROKEN WIRE ELECTRONIC BINARY SENSOR

3.1 ABSTRACT

North American infrastructure, including steel bridges, are aging and reaching the end of their service lives. Over time, environmental stresses and cyclic truck traffic over bridges may lead to crack formation and crack propagation in the steel girders used in bridges. Cracks in steel girders decreases the load bearing capacity of the superstructure and may lead to failure of the structure. Existing methods of crack detection can not be practically deployed over larger structures. There is a need for a low cost distributed crack sensing system. Given the critical nature of bridges a continuous monitoring system would be preferred. Available continuous monitoring systems, such as Fiber Optic Sensors (FOS) are expensive which makes them unfeasible to be used for most of the bridges. In this paper, a new low cost and accurate Binary sensor for detecting cracks in steel girders is discussed. The Binary sensor is comprised of wire bonded onto the girder using an adhesive. When the girder cracks, the crack is coupled to the wire, via the adhesive, causing it to also crack. The sensing system detects the open circuit in the wire created by the crack. A critical

figure of merit for this system is the minimum crack width required to cause the wire to break. In the present work, cracks of less than 0.2mm width can be reliably detected on steel girders.

KEYWORDS: Structural Health Monitoring, Binary sensor, Crack detection, Steel girders

3.2 INTRODUCTION

North American infrastructure includes many bridges, which are reaching the end of their designed service life. As an example, in Canada more than 40% of bridges were built over 50 years ago [5]. Steel material is one of the common types of bridge constructions. FHWA categorizes approximately 30 percent of bridges as steel bridges [48]. Over time, environmental stresses and cyclic truck traffic over bridges may lead to crack formation and crack propagation in the steel girders [6]. Therefore, the detection of cracks in steel girders is important for public safety and to prevent the unpredictable loss of service and associated expenses. To address this need a number of methods for crack detection are employed and a number are in various stages of research and development.

The most common method of assessing the condition of a bridge is to perform visual inspections. However, visual inspection suffer from limitations due to variations in inspector's skill, the accessibility to required parts of the structure and the significant time between inspections [8]. These practical limitations and also the potentially small size of fatigue cracks make it challenging to detect fatigue cracks in a timely manner using visual inspections [9]. To augment visual inspection, several other non-destructive evaluation (NDE) methods have been developed to assess the integrity of bridge girders such as acoustic emission, eddy current and ultrasound testing [10]. Visual and NDE inspection techniques are performed at discrete time intervals. Between these inspections there is a risk that a crack may form and grow to an unsafe state. For example in 2003, just a few months after the last full inspection of the I-95 Highway Bridge over the Brandywine

River, a fracture occurred in one of its girders [11]. Another example is the Diefenbaker Bridge over North Saskatchewan River in Prince Albert, Canada. Although the bridge had been inspected regularly and at no time in visual inspections cracks were noted in the girders, a canoeist observed a major crack through the flange in one of the girders [12]. In order to detect cracks at initial stages before they grow to an unsafe state, several continuous in-situ monitoring approaches have been developed.

The techniques of Structural Health Monitoring (SHM) have also been used to perform continuous real-time crack detection. There are two general categories of sensors for crack monitoring; discrete (such as strain gauges, short gauge or long gauge sensors) and distributed (such as fiber optic sensors) [15].

Discrete monitoring:

In discrete or point monitoring systems the sensors are installed at predetermined points in the structure where crack formation is believed to be most probable [49]. Although these types of sensors will give valuable data about behavior of the structure, they rely on a priori predictions of where cracks will form [15]. If the structure has structural characteristics or defects that are not accounted for in the predictions, then cracks may form at positions not monitored by the sensors. Once cracks have formed they can be monitored using crack propagation gauges. However, these are only useful for known cracks [50]. There are experimental large array sensor systems currently under development that may dramatically reduce the cost of such sensors, but these are still in the early laboratory demonstration phase [45].

Detecting the movement of neutral axis of the girder can also be used for detecting cracks in steel girders. When cracks form in a girder there will be a significant shift in the neutral axis near the position of the crack. However, the uncertainties due to loading patterns, boundary condition and

environmental affects lead to the need for closely spaced strain gauges [18]. In order to achieve reliable crack detection, pairs of strain gauges would need to be placed at spacing on the order of the depth of the girder from each other, which will make it impractical for most bridges [14,15].

Distributed monitoring:

Vibration based damage detection method has been investigated as a means to detect damage such as cracks in structures such as girders[20]. Farrar et al. has used vibration based methods to detect cracks in the girder of I-40 bridge over the Rio Grande [17,16]. In their experiments on a decommissioned bridge, the monitored resonant frequencies changed by less than 0.8% until the simulated crack extended completely through the flange of the girder [21]. However, bridges are subjected to different operational and environmental conditions such as changing temperature and boundary conditions, which can dominate the subtle structural changes induced by cracks [18,19]. It is unclear if vibration based damage detection will be capable of detecting cracks before they compromise the structural integrity or the load rating [53].

Zhang et al have demonstrated the use of a smart film for detecting cracks. However, this method is only applicable for concrete structures and has not been studied for application to crack detection in steel girders [22, 23]. In addition the dimensions of the film demonstrated to date make it impractical to be used for the large steel girders [49].

A distributed SHM system that has seen field application in crack monitoring of larger steel girders has been fiber optic sensors [54]. However, fiber optic sensor hardware and installation procedure can be very costly and may exceed $300,000 per girder, which makes this technology only justified in very limited cases. The high cost of available fiber optic sensors prevents owners and infrastructure managers from using them regularly.

Considering all the available monitoring systems, there is a need for a low cost easily installed distributed crack sensor. In this paper, a low-cost binary sensor will be demonstrated that is able to detect cracks of less than 0.2 mm width in steel girders, which is equal or less than what fiber optic sensors can detect [16]. The binary sensor is a composite system which is comprised of wire that is bonded to the steel girder using an adhesive. When a crack forms in the steel girder, the adhesive transfers the strain from the steel girder to the wire. When the crack opens to a sufficient width the breaking strain of the wire is exceeded and the wire will break. The breaking of the wire will cause a sudden change in the resistance of the wire that can be easily detected. The adhesive-wire combination is designed to transfer the strain to the wire, without the wire to adhesive bond being compromised.

The sensor works by attaching both ends of the wire to a data acquisition system (DAQ) that measures resistance. The unbroken sensor has a resistance equal to resistance of the copper wire. In the sensor demonstrated in this work, when a crack of less than 0.2 mm forms in steel girder it will propagate through the adhesive and will cause the adhesive to break. Over time the crack will widen and the strains from steel beam and adhesive will be transferred to the wire and there will be a local increase in the strain of the wire. When the strain exceeds the breaking strain, the wire will break (Figure 3. 1). This can be detected by measuring the electrical continuity of the wire. As soon as wire breaks, the circuit will change from closed form ($R \rightarrow const.$) to an open ($R \rightarrow \infty$) and there will be a sudden change in the resistance of circuit as the cross-sectional area of the wire will become 0. The electrical resistance of copper wire can be written as:

$$R = \rho \frac{l}{A}$$

Where ρ is resistivity, R is the resistance, l is the length and A is the cross sectional area of the wire. As soon as wire breaks, the cross sectional area of the wire will change to zero ($A \rightarrow 0$) which leads to an increase in resistance of wire ($R \rightarrow \infty$).

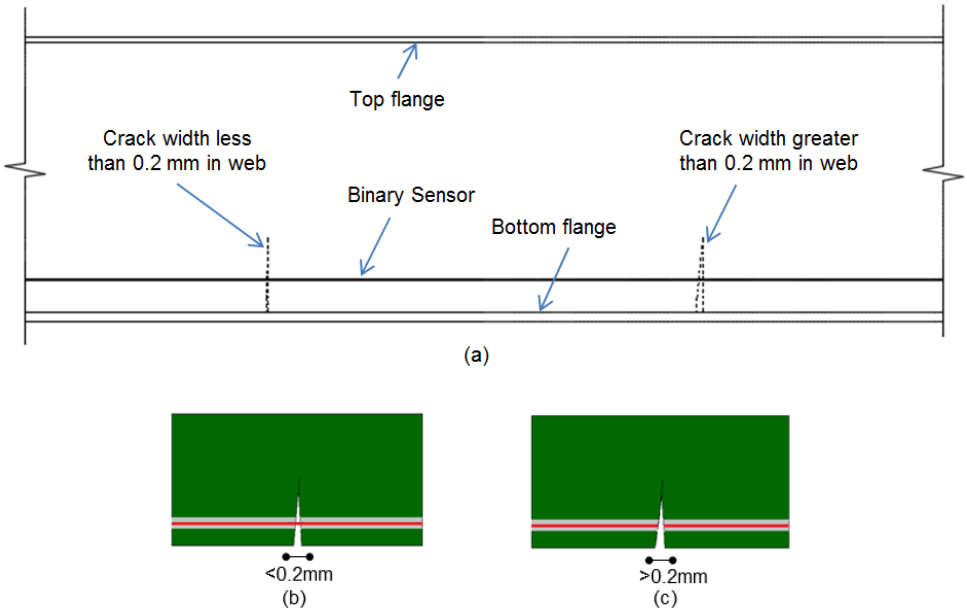

Figure 3. 1. a) Binary sensor is installed on the entire length of the steel girder b) as long as the crack width is less than 0.2mm, crack propagates through the epoxy but wire is still connected c) over time crack widen and causes the wire to break, the resistance of copper wire will tend to unlimited and electrical currency in the circuit will tend to zero

3.3 METHODOLOGY AND PROCEDURE

3.3.1 Wire and Adhesive Selection

One of the most challenging parts in developing the binary sensor is to design the adhesive and wire system. In selecting materials for wire and adhesive, several points should be considered. The breaking strain of the wire should be less than that required to cause the wire to break due to a crack opening of up to 0.2 mm. In addition, the adhesive is required to transfer the strain from the crack on the steel beam to the wire so that the wire breaks at less than the required crack width. If

the adhesive is excessively elastic, the strain will be transferred to a long length of the wire and the wire will not break at less than the required crack opening of 0.2 mm. The bond between wire and adhesive must be strong enough to transfer enough strain to break the wire before debonding. With a carefully designed wire and adhesive, the strain will be coupled from the crack to the wire, and the wire will break at less than the desired crack width of 0.2 mm. In this work, it was found that insulated copper wire and epoxy adhesive can meet the requirements for the binary sensor.

Copper wire is available with insulating coatings in diameters from 0.01 mm to 1 mm. In general, smaller diameter wires break at smaller crack widths and therefore the wire size is chosen to be the smallest diameter which is manually manageable [22]. Gauge 39 wire (diameter of 0.09 mm) has been selected. The main criteria for selecting the adhesive is that should effectively couple the strain from the steel girder to the copper wire, without debonding from the wire. Loctite E-20NS is a two part epoxy that has good elastic properties with good shear bond to both steel and various polymers. In addition, E-20NS also has a relatively high (>80ºC) glass transition temperature, which means it will not become plastic at low temperatures. Other adhesives were tested; this work will focus on the results with E-20NS.

3.3.2 Testing the bond between wire and adhesive

As mentioned in part 3.3.1, the bond between adhesive and wire should be adequate to couple the strain from the adhesive to the wire. If the bond is insufficient, when the initial crack opens it may cause the wire to debond from the adhesive. When the wire debonds from the adhesive, the strain will be distributed over a greater length requiring a wider crack to break the wire as compared to a bonded assembly. If the bonding is sufficiently poor, the binary sensor will not reach the desired goal of breaking at a crack opening of less than 0.2 mm. In this work, microbond tests were used to characterize the wire to adhesive bond properties. Microbond testing is a type of pullout test for

small diameter fibers. In this method, the fibre is pulled out of a small bead of epoxy being restrained by a knife-edge [55].

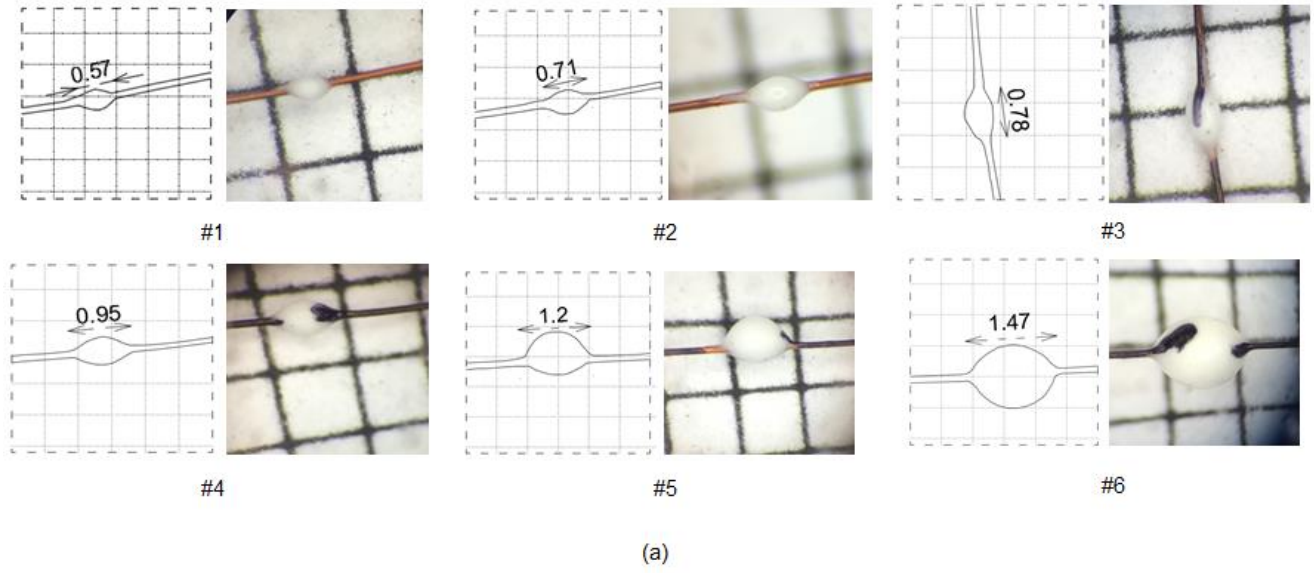

(a)

(b)

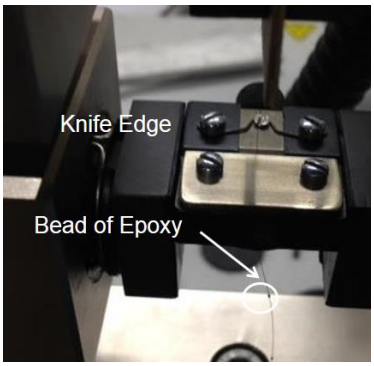

(c)

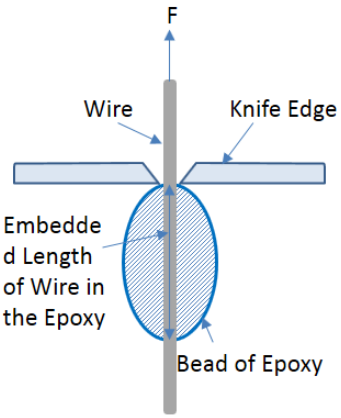

(d)

Figure 3. 2. a) Different dimensions of microbeads of epoxy on copper wire, a marker was used to mark the ends of the beads (black marks on the beads). b) The load frame (INSTRON 3366) was used for pull out test, the free end of wire was held in the upper grip and the other end with epoxy was restrained using the knife edge c) The knife edge restrains the bead of epoxy to test the pull out of the wire, d) Schematic of the knife edge and embedded wire in the bead of epoxy

The diameter of copper wire used for the binary sensor is about 0.09 mm, which requires a bead of less than 0.5 mm diameter to be attached to the wire for the micro bond test [56]. Different

dimensions of beads of epoxy were prepared by scraping small amounts of epoxy onto the wire using a wooden applicator under a microscope. Surface tension pulled the epoxy into roughly spherical beads. The dimensions of the beads were measured from images taken with a microscope (see Figure 3. 2a). After at least 24 hours of curing, the fibre and bead were tested using a small load frame (Instron Model number 3366). As shown in Figure 3. 2, the free end of wire was mounted in the upper grip of the machine and the other end with a bead of epoxy was restrained using a knife edge [25]. The test was executed at a speed rate of 0.1mm/min, which is typical for microbond testing [56].

3.3.3 Experimental Apparatus

An experimental apparatus has been designed to simulate the crack opening on the web of a steel girder and combinations of wire and adhesive have been tested using this test setup. The schematic of the test setup is shown in Figure 3. 3 [57].

The experimental apparatus includes two hinged steel plates, a displacement gauge (PI-5-200, Tokyo Sokki Kenkyujo) to measure the crack opening and a micrometer to controllably open the simulated crack. The steel plates are connected to each other at one end with a flexural hinge and are free to slide on a low friction surface. Turning the micrometer applies force to the edge of the steel plate and will cause plate A to split from plate B. This simulates a crack opening on a steel plate. Over time and by continuing to turn the micrometer, the gap between two steel plates will widen as shown in Figure 3. 3. The turning of the micrometer represents an increase of load, which happens in the real structure, and causes the crack width to expand. To measure the gap between two plates a displacement gauge (PI-gauge with a resolution of ±0.01 mm) is used. Both ends of the binary sensor and displacement gauge are connected to a Data Acquisition system (DAQ) which records the resistance of the wire and gap opening between two steel plates at 1000

samples/s. In order to observe the crack width at which the wire fractures, the electrical resistance of the wire is measured. The ends of the binary sensor are connected in series with a resistor to an electrical source with the DAQ measuring the voltage across the resistor. As soon as the wire breaks, the continuity of the wire will be severed, changing the resistance from a short (Ω=0) to an open (Ω=∞).

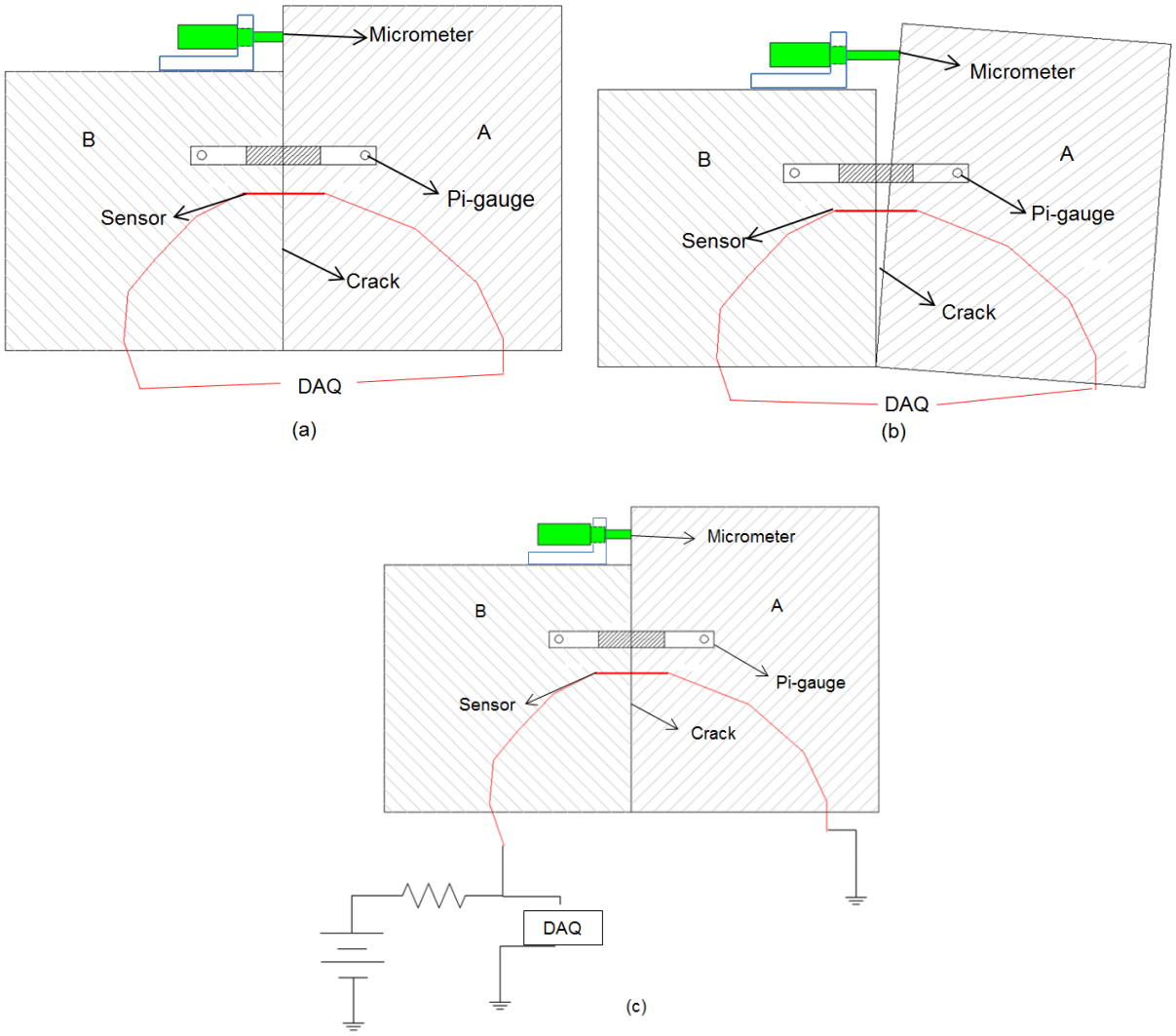

Figure 3. 3. a) Layout of the test setup consisting of two steel plates, micrometer and displacement gauge. The binary sensor installed on it, b) by turning the micrometer plate A moves from plate B and the gap between two plates gets wider. The displacement gauge records the gap opening between two plates, c) The ends of the binary sensor are connected in series with a resistor to an

electrical source with the DAQ, measuring the voltage across the resistor. As soon as the wire breaks, the continuity of the wire will be severed, changing the resistance from a short ($\Omega=0$) to an open ($\Omega=\infty$) [58]

3.3.4 Test on Steel Beam in Lab

After completing tests on the simulated crack apparatus the two best combinations were selected for laboratory testing on a steel girder. In this case, best refers to combinations that have acceptable bonding and reproducible properties. The steel girder provides testing conditions closer to those that are expected in the field.

3.3.5 Preparation, application and instrumentation

A W250x67 section steel beam was simply supported over a 3.0 meter span (Figure 3. 5a, b); to simulate hinge supports, both ends of the steel beam were restrained against horizontal and vertical displacements but the rotation was allowed. A crack was created at mid-span for testing the binary sensor. The crack was formed by cutting the beam through the bottom flange and into the web about 40 mm above the bottom flange. The cut was filled by re-welding. An actuator applied approximately 60 KN load to the top flange of the beam at mid span, which induced a new crack in the weld.

Prior to installation of the Binary sensor, paint and any other coating were removed from the surface of the steel. The Binary sensor was connected directly to the steel. This provides the best possible bond between epoxy and the steel beam and strain transfer from the steel to the epoxy and then to the wire. A belt sander was used to remove the paint and then sandpaper was used manually to level the surface. The last step of preparation was cleaning the surface with isopropyl alcohol to remove any dirt or contamination.

After cleaning the surface, the sensor was positioned on the web. The sensor positioned to be 21 mm above the bottom flange which is almost half of the length of the crack. This is also the position of the displacement sensor on the opposite side of the girder. The copper wire was held temporary on this position with electrical tape. A form was used to control the geometry of the epoxy. A 2mm-thick foam tape was used to build this formwork. The first piece of tape was positioned approximately 1 mm above and the second piece of tape 1 mm below the wire. This formed a gap into which the epoxy was injected. The epoxy was injected using a gun (Product Number LCT98472) with a mixing nozzle. A uniform depth of epoxy was created by using a blade to skim the top of the formwork and remove excess epoxy. After one day of curing, the formwork was removed.

The sensor is an electrical closed circuit which will change to an open circuit as soon as the opening crack causes the wire to break. The change from short circuit to open circuit was detected using a power supply and a series resistor while measuring the voltage drop across the sensor (Figure 3. 4). When the sensor was a short circuit, very little voltage was observed across the sensor. When the wire breaks and becomes an open circuit, the voltage of the supply is observed across the sensor. The change is very dramatic and easily observed. With the completed electrical circuit, the sensor was ready for testing.

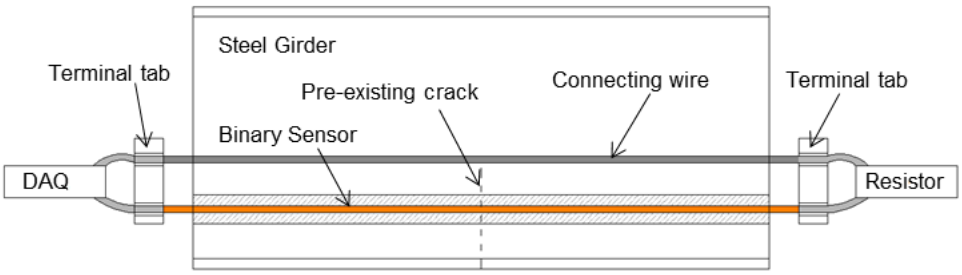

Figure 3. 4. Binary sensor, connection wire, DAQ and resistor make an electrical circuit on the web of a steel girder

A 1000 KN capacity actuator was used to apply increasing load on the beam (Figure 3. 5). The loading rate was 1mm/min. By gradually increasing the load, the pre-existing crack opened and widened until the sensor broke. This was detected by monitoring as outlined above. In order to measure the crack opening an electrical displacement gauge (PI-5-200, Tokyo Sokki Kenkyujo), was installed on the opposite side of the steel beam (Figure 3. 5 d). In addition to displacement gauge and the binary sensor, four strain- gauges were mounted to record strains at specific locations of the beam in order to compare the results with finite element analysis. The deflection of the beam at mid-span was recorded with an LVDT (SLS-190 Penny&Gills)

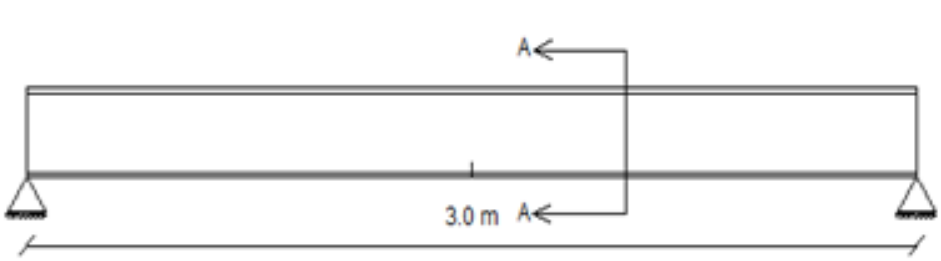

(a)

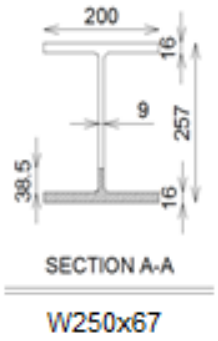

(b)

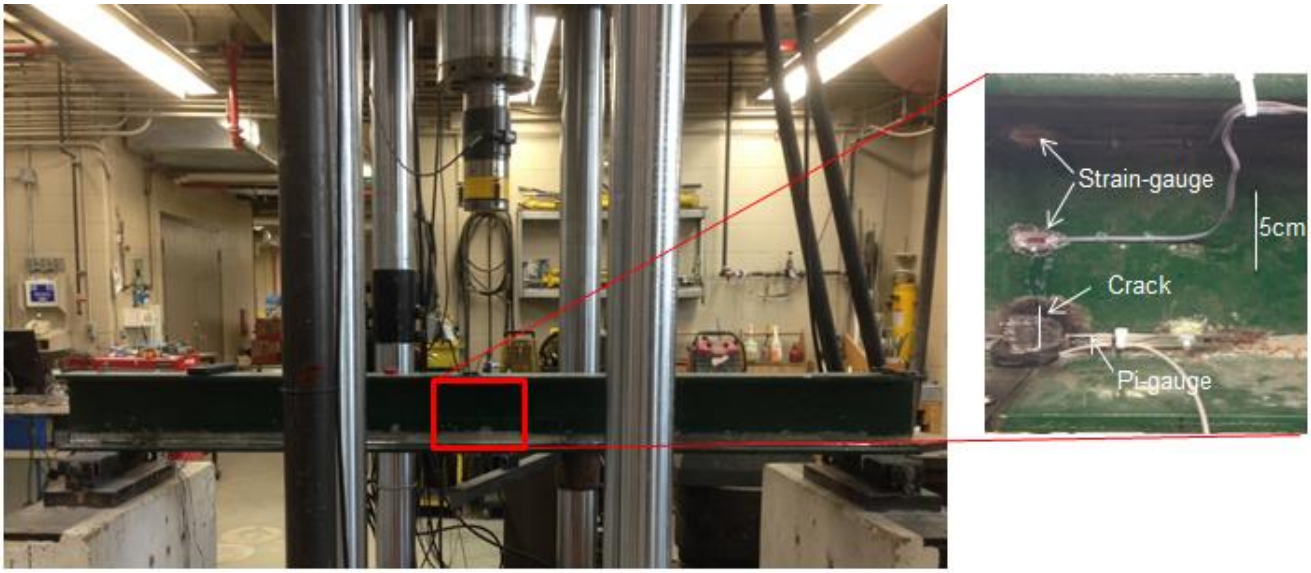

(c) (d)

Figure 3. 5. a) 3-meter span simply supported steel beam with a pre-existing crack at mid-span. b) Cross-section of the beam, the hatched area is the cracked part. The entire bottom flange has cut and continued 38.5mm into the web towards top flange c) the Beam and its supports under load frame d) a displacement gauge was mounted to record the crack opening

3.3.6 Test in Environmental Chamber

The binary sensor is designed to be installed on girders of bridges. Since bridges are facing different temperature conditions, it is required to test the application of binary sensor at both low and high temperatures. In order to do so, the same 3.0 meter span, simply supported steel girder with a pre-existing crack at mid-span was moved to an environmental chamber. The chamber can be cooled down to -30ºC and heat up to +40ºC. A temperature sensor was installed on the girder to measure and record temperature of surface of the girder.

The binary sensor was installed on the girder at +22 ºC -which is the ambient temperature-. After 24 hours of curing, the chamber was turned on to heat the chamber to +40ºC and to cool the chamber down to -30ºC (although the room temperature was showing -30ºC, the temperature at surface of the girder was -15ºC). It took 4 hours to reach -30ºC and two hours to reach +40ºC. The test temperatures were alternated between +40ºC and -30 ºC.

3.4. RESULTS AND DISCUSSION

3.4.1 Test on experimental apparatus

As mentioned earlier in part 3.3.1, copper wire gauge 39 (D=0.09 mm) was used due to its availability and ease of handling. In addition to the epoxy, two adhesives from cyanoacrylate category; Loctite Quicktite and M-Bond 200/VPG were also tested. These results are not presented in detail in this work. Six tests of each adhesive were done. Before application of the adhesive on the steel plates, sandpaper was used to remove the paint from the surface. Then alcohol was used

to clean the surface contamination. Figure 3. 6 shows the sensor on the experimental setup. By turning the micrometer and increasing the gap between two steel plates to less than 0.2mm, the binary sensor breaks. The broken sensor is shown in Figure 3. 6.

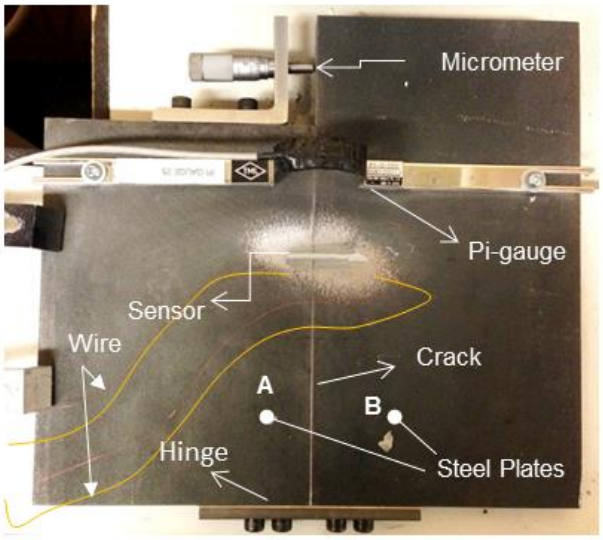

(a)

(b)

Figure 3. 6. a)Experimental apparatus- Binary sensor, displacement gauge(PI-5-200, Tokyo Sokki Kenkyujo) and micrometer on steel plates, b) as soon as the opening between two steel plates reaches to 0.2mm the binary sensor breaks [57]

The first adhesive tested was Loctite QuickTite which is a gel adhesive and sets in 2 minutes. The crack width at which the binary sensor could detect was about 0.15 mm which is less than the

desired crack width; but after curing there were few cracks forming on the surface of the adhesive which made the results unpredictable and therefore not considered any further [58].

The other cyanoacrylate which was tested was M-Bond 200. This adhesive is commonly used for installing strain gauges on steel beams. Using this adhesive, the binary sensor broke at much more than 0.2 mm. There was extensive debonding between wire and adhesive, which caused the wire to break at wider than the acceptable crack opening.

From epoxy category, Epoxy Steel (Lepage part number 1418151) was tested. Epoxy steel is a two part adhesive. Portions of resin and hardener are mixed together to make the adhesive. It takes 5 minutes to set and a further 24 hours to reach full strength. Test results for this combination of copper wire and epoxy are discussed in another paper [57]. Although the test results of epoxy steel and copper wire were often favorable, the results are extremely dependant on using accurate portions of resin and hardener and maintaining a consistent mixing procedure. Increasing resin content may lead to a more plastic adhesive, which leads to the wire breaking at unacceptably wide crack openings. In order to get repeatable and consistent results a more accurate way of mixing parts is required.

One method of ensuring a consistent mix and complete mixing is to use a mixing tube. Loctite Epoxy E-20NS is a two part epoxy which comes with a cartridge and a mixing tube. The package of epoxy is designed in a way that the resin to hardener ratio is more consistently dispensed at a two to one (2:1) ratio. Using the mixing tube resulted in a well-mixed epoxy which gave consistent results.

Combination of copper wire and Loctite E-20NS was tested on the experimental apparatus. By turning the micrometer the epoxy breaks in a brittle manner and by increasing the distance between the steel plates the strains will transfer to the wire and cause the wire to break. As mentioned in

part 3.3, as soon as the wire breaks, there will be a sudden change in the resistance of the wire (Figure 3. 7).

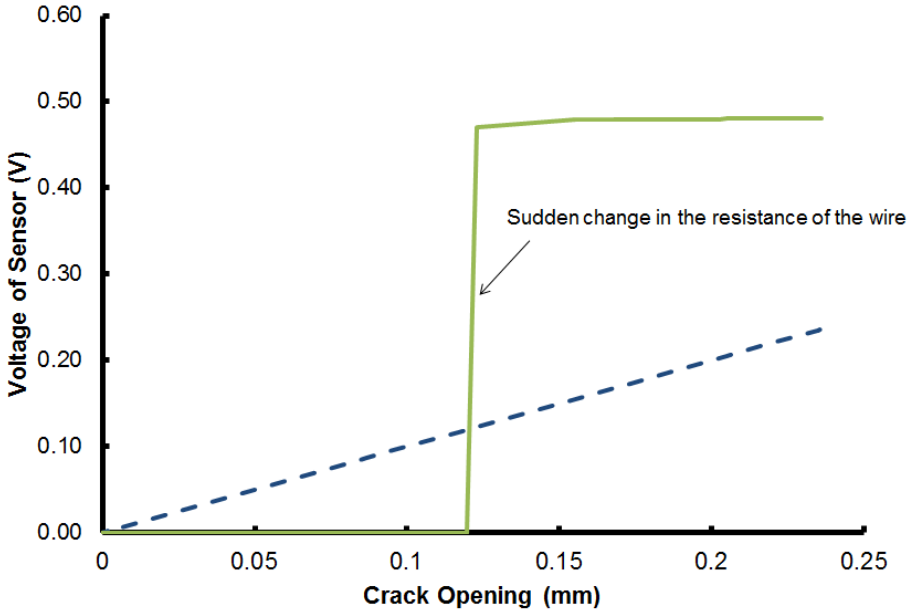

Figure 3. 7. Binary sensor breaks at 0.12 mm crack opening and there is a sudden change in resistance of wire

Results of 13 experiments are shown in Table 3. 1. As it is shown, the binary sensor can detect cracks of width 0.09 to 0.16 mm width on this experimental apparatus. In all of the cases the wire broke at less than 0.2 mm. The mean breaking crack width was 0.13 mm and the standard variation was 0.03 mm.

Test Number	1	2	3	4	5	6	7	8	9	10	11	12	13
Crack width opening(mm)	0.15	0.16	0.14	0.14	0.16	0.16	0.09	0.09	0.11	0.12	0.13	0.12	0.16

Table 3. 1 Test results of Binary sensor on experimental apparatus

3.4.2 Test on steel beam in the lab

Ambient temperature

As discussed in part 3.4.1, the best combinations of wire and adhesive which could detect crack openings of less than 0.2 mm were copper wire gauge 39 with Loctite Epoxy E-20NS or Epoxy Steel (Lepage Company). Two sets of experiments were designed to test these combinations on the steel beam; the first one was copper wire with Epoxy Steel- test number S1 to S6-, the second one was the same copper wire with Loctite Epoxy E-20NS- test number L1 to L6.

After installation of the sensor as discussed in part 3.3.4, the beam was tested under load. By increasing the load, the pre-cracked beam deflected and the crack increased in width. While the crack opening was still less than 0.1 mm, the epoxy fractured. As the load increased, the crack opening increased transferring the strain to the copper wire and causing the wire to break resulting in a sudden change resistance (Figure 3. 8).

The result of test number S1 to S6 are shown in Table 3.2. The test results vary from 0.16±0.01to 0.41±0.01. The larger variation observed in this test compared to the steel plate test is attributed to variation in the mixture ratio of hardener and resin. As discussed before, equal parts of epoxy should be mixed accurately together to yield an adhesive with consistent properties. When mixing the two parts for a sensor on a beam, which is larger than the laboratory test set up, it was found that this mixing ratio and consistent mixing was very difficult to achieve. Therefore, this adhesive was not considered further.

Using the of Loctite Epoxy E-20NS, was a solution to resolve the mixing problem. This epoxy application system includes a mixing tube which mixes two portions of resin with one portion of hardener and then applies it on the surface.

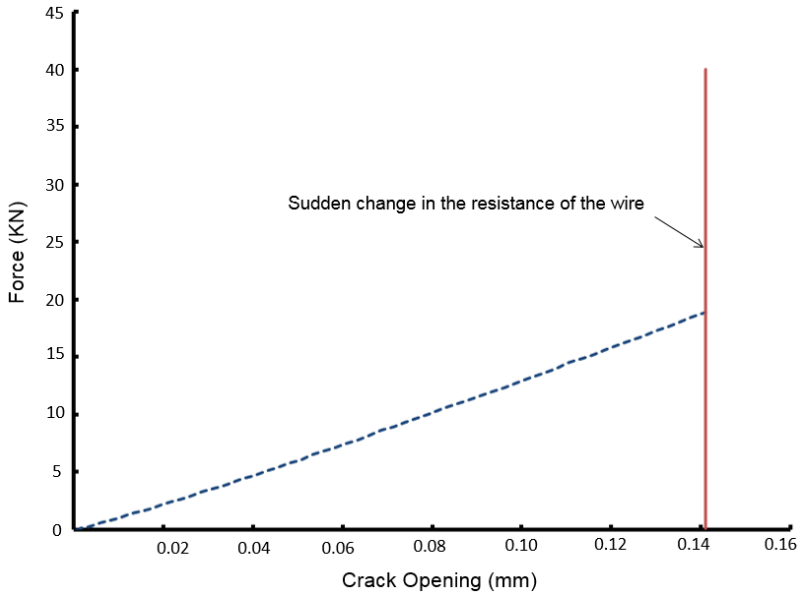

Figure 3. 8. Binary sensor breaks at 0.14mm crack opening and there is a sudden change in resistance of wire

Test Number		Crack width opening(mm)
S	S1	0.24±0.01
	S2	0.41±0.01
	S3	0.16±0.01
	S4	0.24±0.01
	S5	0.16±0.01
	S6	0.19±0.01
L	L1	0.13±0.01
	L2	0.13±0.01
	L3	0.13±0.01
	L4	0.19±0.01
	L5	0.14±0.01
	L6	0.14±0.01

Table 3. 2. Test results of Binary sensor on steel girder at ambient temperature in the lab

Table 3 shows the result of test number L1 to L6 which varies from 0.13±0.01 to 0.19±0.01. As it is shown in Table 3. 2 and Figure 3. 8, the results of Loctite Epoxy E-20NS are consistent and less than 0.2 mm. The system is functional, however further optimization is in process.

Environmental chamber test

Six sets of experiments were executed. Each set was consisting of two tests (one at -30 ºC and another one at +40ºC). Results for these sets are shown in Table 3.3. As it is shown the binary sensor can detects crack openings in range of 0.1 mm to 0.26 mm at -30 ºC (the mean breaking crack width was 0.16 mm and the standard variation was 0.06 mm) and between 0.1 mm to 0.17 mm at +40 ºC (the mean breaking crack width was 0.14 mm and the standard variation was 0.02 mm). Results from this experiment demonstrate that changes in temperature have minimal effect on the behaviour of the binary sensor. In ambient temperatures, as well as the two extremes, stresses were transferred to the copper wire causing it to break at less than 0.2 mm, on average. This is expected as the epoxy's glass transition temperature is 87 ºC, which is well above the testing temperatures.

Test Number	1	2	3	4	5	6
Crack opening at -30 ºC	0.26	0.1	0.14	0.11	0.24	0.14
Crack opening at +40 ºC	0.1	0.13	0.17	0.16	0.13	0.16

Table 3. 3 Test results of Binary sensor on steel girder in environmental chamber

3.4.3 Bonding Properties test

As discussed in part 3.3.2, the microbond test was executed to measure the bonding properties between the wire and adhesive and verify that the wire is the weakest mechanical element of the

system. The wire with a small bead (less than 0.5 mm in diameter) of epoxy was mounted on the load frame and the load was applied at a rate of 0.5 mm/min. In all six samples, the wire broke before the bond to the wire failed. This demonstrates that the bonding between wire and adhesive is sufficient to ensure the wire is the weakest mechanical element.

The results are shown in Table 3.4.

Sample	1	2	3	4	5	6
L_{bond} (mm)	0.57	0.71	0.78	0.95	1.2	1.47
Comments	Wire broke	Wire broke	Wire broke	Wire broke	Wire broke	Wire broke

Table 3. 4 Test results of microbond test. It shows the bonding between wire and adhesive is sufficient and wire is the weakest element

3.5. CONCLUSION& FUTURE WORKS

Available crack monitoring methods, for steel girders are either not sufficient or not economical for large scale monitoring. For example, using fibre optic sensors for monitoring cracks in steel girder requires very involved installation procedures and expert interpretation of the results to determine if a crack is forming. In this paper, a new binary sensor was demonstrated that is economical and has the potential to easily be installed over large structures. The binary sensor is a composite structure which consists of copper wire and epoxy adhesive. When a crack of greater than 0.2 mm forms in a steel girder, the binary sensor breaks and produces an easy to interpret signal. In this paper the approach to choosing materials for a binary sensor was described. Results from experimental tests demonstrate that the binary sensor can detect cracks of less than 0.2mm at ambient temperature. The binary sensor was tested at two extreme temperatures -30 ºC and +40 ºC and the behavior of the sensor was not significantly changed. The sensor is practical but further development is required.

Future work will include installation on a girder in the field to test the installation procedure and also to expose the sensor to different condition such as vibration and freeze thaw cycles.

A Finite Element Model of the binary sensor should be developed to predict the optimal placement of the sensors for crack detection and to predict what the optimum properties of the wire and adhesive should be for the binary sensor.

CHAPTER 4: A FINITE ELEMENT AND EXPERIMENTAL INVESTIGATION OF THE INFLUENCE OF PRE-STRAINING OF WIRE ON THE SENSITIVITY OF BINARY CRACK SENSOR

4.1 ABSTRACT

Steel girder bridges make up a significant percentage of all bridges. Many of the steel girder bridges are aging and approaching their designed service lives. Crack formation and its propagation over time is one of the main deficiencies of aging steel girders and may results in unusable or unsafe service conditions. Existing distributed crack detection methods such as fiber optics sensors are costly to deploy and maintain. A new cost effective binary sensor has been developed, has the potential to be installed on steel girder bridges at a fraction of the cost and is sensitive enough to detect the presence of a crack opening with a width of 0.2mm. The crack sensor is a closed electrical circuit, comprised of copper wire and epoxy. When a crack forms in the steel girder, the strain will be transferred to the wire through the adhesive. As the crack on the girder widens over time, strains in the wire increases until it reaches its ultimate tensile strain. The wire then fractures and creates an open circuit. This can be detected by monitoring the electrical continuity of the sensor. One of the main challenges in developing the binary sensor is to select appropriate materials for both wire and adhesive. The final tensile strain as well as the bonding

stiffness between the wire and the epoxy have important impacts on the performance of the sensor. In this work, pre-straining the sensor wire was found to be effective in minimizing the width of the detected crack opening. The average was reduced from 0.36mm to 0.13mm and the standard deviation reduced from 0.16 to 0.03. In addition, microbond test was carried on to estimate the interfacial bonding stiffness between wire and epoxy. The interfacial stress was found to be approximately 2.0MPa. These parameters were used in a Finite Element Model of the sensor to predict the behaviour of the binary sensor and consequently to optimize the installation position of the sensor on a girder of a bridge.

KEYWORDS: Binary sensor, Crack detection, Steel bridges, Finite Element Analysis, Interfacial bonding stiffness

Acknowledgments

The authors wish to express their gratitude and appreciation for the supports received from the following organizations: Natural Science and Engineering Research Council of Canada, Canada Foundation for Innovation, Research Manitoba, Canadian Microelectronic Corporation, Structural Monitoring Technologies

4.2 INTRODUCTION

Bridges are key elements of the transportation system. In North America and many other parts of the world there was a major period of bridge building more than 50 years ago (between 1950 and 1970) and the superstructure of the majority of them were made of steel (around 40% of bridges)[3]. Studies show that many bridges are reaching the end of their designed service life [4, 5]. One of the main deficiencies which may occur in aging steel bridges is crack formation and propagation over time [6]. Cracks may form as a result of welding defects, material defects, defects introduced in manufacture or construction and from fatigue development during the service life

[6, 7]. Detecting cracks in steel girders before they reach an unsafe stage or have significantly reduced the load carrying capacity is critical [7, 11, 12] . To ensure that structures will have sufficient structural capacity to maintain continuous operation as well as safety to the public, new approaches will need to be employed to augment visual inspection [6, 48]. Non-destructive evaluation (NDE) methods can be used to detect and evaluate cracks on steel girder of bridges. Methods such as acoustic emission, eddy current and ultrasound testing [10, 13]. However, NDE methods are expensive and often time consuming and access to the point of evaluation is not always possible and it is desirable to have methods that can provide continuous information on the integrity of the bridge [13]. Structural Health Monitoring is a means of providing more quantitative and timely information on structural integrity[14]. In general, Structural Health Monitoring system can be divided into two categories; discrete monitoring such as using strain gauges, short gauge or long gauge sensors and distributed monitoring such as installing the smart film or fibre optic sensors [13, 16–23]. Discrete monitoring sensors give information on the local behaviour of structures. However, for large structures cracks may occurs in locations far from the sensor and would be challenging to detect [15]. This problem could be addressed by having enough sensors to detect cracks at any location in the structure, but this may require an impractical number of sensors. Distributed monitoring techniques are more comprehensive since the sensor is installed on the entire length of the girder [15]. However, distributed monitoring with existing approaches such as fiber optics are expensive to install and operate [59]. One recently demonstrated low cost distributed monitoring approach is the binary sensor, which is an insulated wire bonded to the steel girder. The binary sensor is installed on entire length of the girder with an emphasis on parts of the structure where cracks are expected to form such as the web height where high tensile stresses exists or at tensile flange (Figure 4. 1). The binary sensor detects cracks before they open up to 0.2

mm width [17]. When a large enough crack opens under the sensor, the wire will break and this can be detected by monitoring the resistance of the wire.

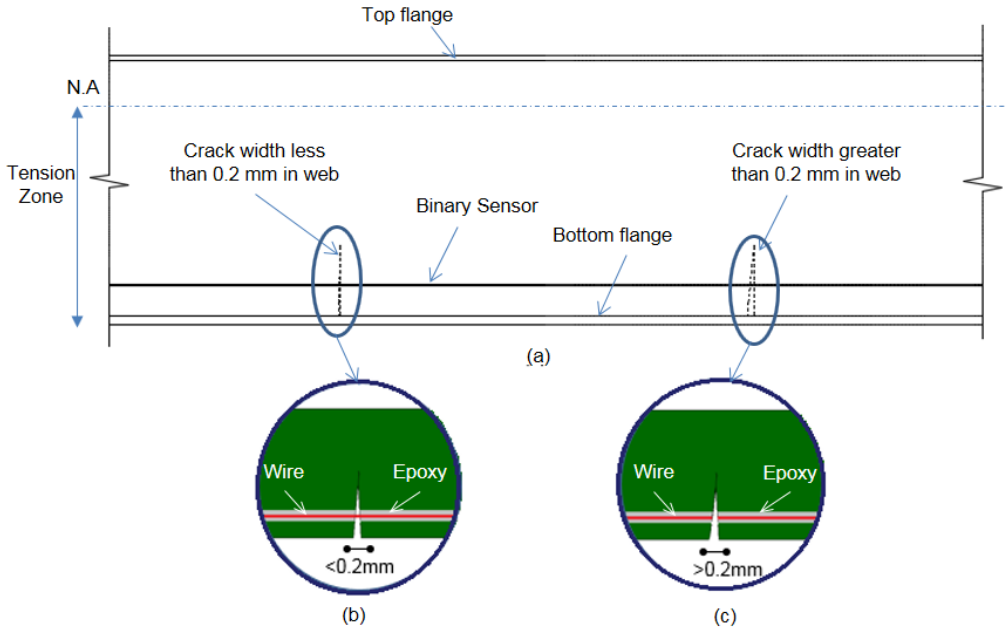

Figure 4. 1. a) The Binary sensor is installed on the entire length of the steel girder. The epoxy adheres the wire to the steel girder. When crack forms in steel girder, the strains will be transferred from steel girder to the epoxy b) as long as the crack width is less than 0.2mm, crack propagates through the epoxy but wire is still connected c) over time, under tensile stresses, crack widen to 0.2mm width and causes the wire to break. As the wire breaks, the resistance of wire will tend to unlimited and electrical currency in the circuit will tend to zero [17, 24]

The Binary sensor is a designed composite system which is consists of insulated copper wire and an adhesive. The insulated copper wire adheres to the steel girder using a precisely selected epoxy. One of the main critical parts in designing the binary sensor is selecting the material for wire and epoxy. Extensive testing has been carried out to find materials with bonding strong enough to transfer the strain from the crack on the steel girder to the wire and cause the wire to break. The tests was done on an experimental apparatus designed to simulate the crack opening (Figure 4. 2).

After testing materials on the apparatus, the best candidates were tested on a cracked steel girder in the lab in ambient temperature as well as two extreme temperatures (-30ºC and +40ºC). The experimental process of selecting the material was explained in a previous work [17]. The previous trial and error experimental approach has yielded a practical combination of wire and adhesive, but having an accurate numerical model would predict the behaviour of the binary sensor under many more experimental conditions than is practically possible. For example, it could predict the behaviour under different levels of pre-strain in the copper wire and for different positions of the wire within the adhesive. This finite Element Model (FEM) of the sensor and experimental apparatus could also help to accelerate the process of selecting new materials for binary sensor as well as to determine the optimum position of the sensor on steel girder.

In this work, a finite element model of the binary sensor and the experimental determination of the required material properties was carried out. ABAQUS was selected as the finite element program to simulate the binary sensor. The main material properties that needed to be determined were the mechanical properties of the wire and epoxy and the bonding properties between wire and epoxy, since the bond is the main means by which strain is coupled to the wire [17]. The bond between the wire and adhesive needs to be strong enough to transfer the strain from crack opening on steel girder to the wire. Otherwise, if the bond between wire and adhesive is not sufficient, the sensor will not fracture at crack openings less than 0.2mm of width. Another critical specification is the tensile properties of the wire. Since the binary sensor will be installed on the places with high tensile stress (web height where tensile stress is maximum or at tensile flange), it will behave in tensile mode. Therefore, the ultimate tensile strain of the wire will affect the results and are required to be measured for calculations. In the current work, copper wire with varying ultimate tensile strain has been obtained by using pre-straining. In addition, the tensile strength of both wire

and epoxy as well as the bonding properties between the wire and the epoxy have been experimentally determined. Using the experimentally determined properties, simulation of the binary sensor was carried out in ABAQUS and compared to the experimental ones.

4.3 METHODOLOGY AND PROCEDURE

4.3.1 Experimental procedure

The binary sensor is comprised of thin insulated wire and adhesive. Mechanical properties of both wire and adhesive are important factors in developing the binary sensor. Therefore, wire and adhesive are being tested initially on an experimental apparatus and the combination which breaks at the desired crack opening of 0.2 mm, will be considered for further testing. The apparatus and testing procedure is described in a previous work [17]. The apparatus is made of two steel plates connected to each other using a flexural hinge at one end. Plates are free to slide at one edge. A displacement gauge (PI-5-200, Tokyo Sokki Kenkyujo) is installed on the apparatus to measure the opening between two plates (Figure 4. 2) [17].

In this work, insulated copper wire MW79-C gauge 39 with an insulation layer of polyurethane was selected. The wire was bonded on the apparatus using Loctite E-20NS epoxy. By turning the micrometer the gap between two plates widened and caused an increase in tensile strain of the wire and consequently resulted in fracture of the wire. The wire may fracture at different crack openings due to its ultimate tensile strain. Therefore measuring and controlling the final strain of the wire is critical. In next two parts, experimental method of measuring and controlling the tensile strain of the wire has been explained. Another key factors in controlling the detected crack opening is behaviour of epoxy under tensile stresses as well as the bonding properties between wire and epoxy. These parameters are also being discussed in following parts.

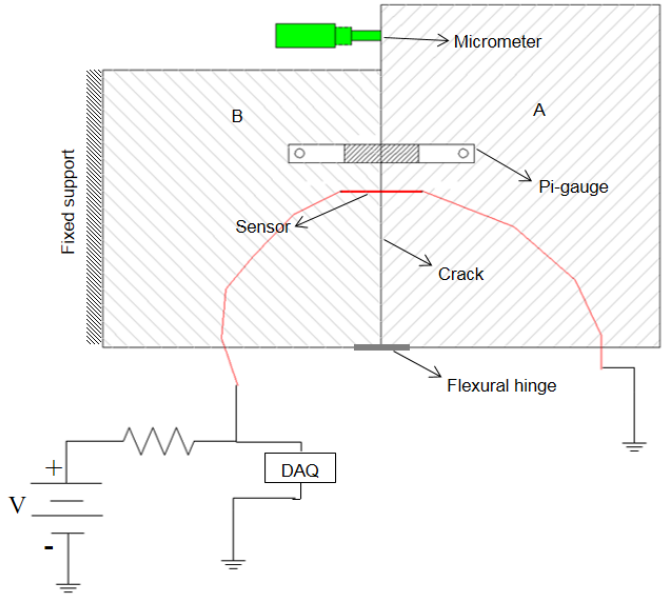

Figure 4. 2. Schematic of the apparatus for testing different combination of wire and adhesive. Two steel plates are connected to each other at one end with a flexural hinge and the gap between two plates simulates the crack on a steel girder. Turning the micrometer will cause plate A moves from plate B and widen the crack. The displacement gauge records the gap opening between two plates. The ends of the binary sensor are connected in series with a resistor to an electrical source with the DAQ, measuring the voltage across the resistor. As soon as the wire breaks, the continuity of the wire will be severed, changing the resistance from a short ($\Omega=0$) to an open ($\Omega=\infty$) [17]

4.3.2 Tensile properties of wire

The wire that will be used for binary sensor can be selected from a wide range of available magnet wires. One of the main important characteristics of the selected wire is the ultimate tensile strain of the wire. In this work, insulated copper wire MW79-C, gauge 39 (0.09 mm diameter) was used for testing.

Tensile properties of the wire was measured according to ASTM C1557. In order to measure the force and displacement of the wire, a small load frame (INSTRON 3366) was used. In this method, the wire was cut into small pieces (25 mm gauge length) and was mounted on mounting tabs (in

this case, thin cardboards) which were made to hold the ends of wire firm and non-slipping in the grips. The wires were bonded to the cardboards using an epoxy and the cardboards were mounted on the grips of the load frame (Figure 4. 3). Test was conducted at a constant speed rate of 0.5 mm/min [60]. Six samples were tested and force- displacement diagrams were plotted. Results are discussed in future parts.

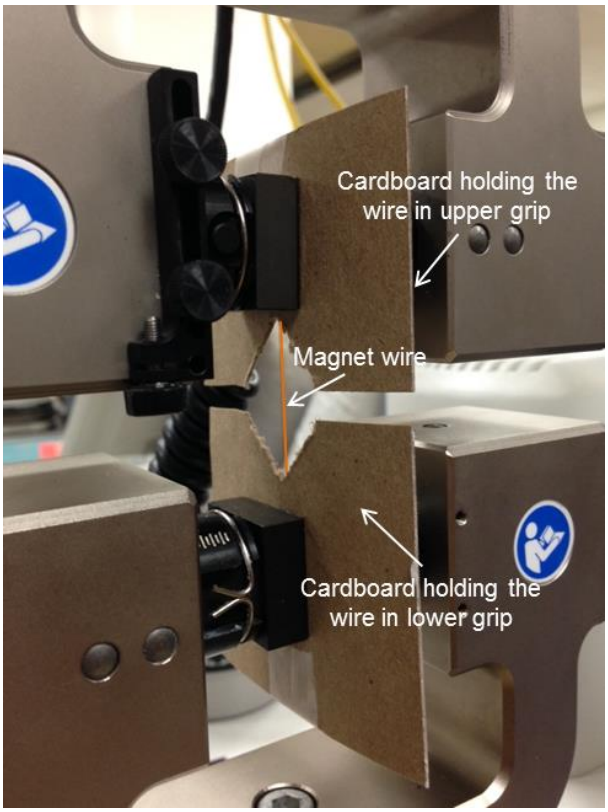

Figure 4. 3 Test to measure tensile properties of insulated copper wire. The wire was glued to two pieces of cardboards and cardboards were mounted on the load frame (INSTRON3366)

4.3.3 Pre-straining wire

Pre-straining was used to control the final tensile strain of the wire. It was thought that by pre-straining it would be possible to reduce the crack opening required to cause the wire to break. The wire (gauge 39, MW79-C) was pre-strained by 5% and 10%. The pre-straining was done by using

the load frame (INSTRON3366). Specific lengths of wire were cut for pre-straining and testing on the experimental apparatus. Two ends of wire were mounted on the grips of the load frame and the wire was stretched to reach the desired strain. Afterwards, the pre-strained wire was used for testing on the experimental apparatus. Results of pre-straining and crack width detection are discussed in part 4.4.

4.3.4 Tensile properties of epoxy

The final strength of epoxy was measured according to ASTM D638. Coupons of epoxy were made in accordance with the dimensions of type I (Figure 4. 4). In order to prepare the coupon, a formwork was made out of polyethylene plastic material.

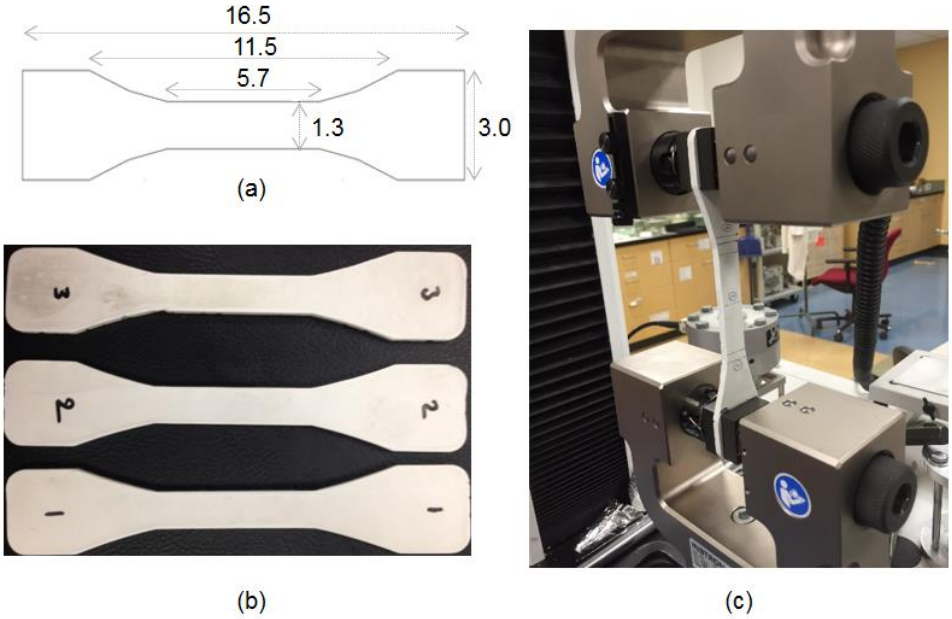

Figure 4. 4. Tensile test of Loctite Epoxy E-20NS; a) Dimensions of coupon based on ASTM D638, the thickness is equal to 4mm. b) After 24hr of curing, coupons of epoxy were ready for testing, c) The coupon of epoxy was mounted into the grips of the load frame for tensile test

The Loctite epoxy E-20NS is a two part epoxy. The epoxy applicator includes a mixing tube which mixes two portions of resin and one portion of hardener. Then, the epoxy was poured into the

formwork. In order to prevent the adhesion of the epoxy to the formwork, the inside surface of the formwork was cleaned and covered with a releasing agent (oil-WD40). A plastic knife was used to remove the extra epoxy from the surface and make the surface smooth and level. This procedure was done on the vibrating table to reduce the amount of air bubbles in the coupon. After 24 hours of curing, coupons were taken out of formwork and were sanded to make a uniform cross section. Thickness and width of coupons were measured at specific sections as mentioned in ASTM D638. Then, both ends of coupon were mounted into the grips of a Load frame (INSTRON 3366). Test was done at constant speed rate of 5mm/min[61].

4.3.5 Bonding between wire and epoxy

One of the main characteristics of the binary sensor which will affect the detected crack opening, is the bonding between wire and adhesive. If the bonding between wire and adhesive is not sufficient, it will cause the wire to de-bond from the adhesive at small forces. This will result in distribution of the induced strains over a greater length of wire and will cause the wire to break at wider crack opening than 0.2 mm.

In order to measure the bonding between wire and adhesive, the microbond test was conducted [55]. In this method, small droplets of epoxy were formed on the wire using a thin pointed stick. Surface tension of the wire created a spherical shape of epoxy. This procedure was done under microscope to make the beads as small as possible [17].

The diameter of wire which was selected for the binary sensor is about 0.09 mm. According to Sockalingam and Nilakantan [56] as well as previous experimental results [17], the maximum embedded length of wire in the bead of epoxy should be less than 0.6 mm to prevent the wire breakage:

$$\mathbf{l_e} < \frac{\boldsymbol{\sigma_f D_f}}{\mathbf{4\tau_{ult}}} \quad (1)$$

Where, l_e is the embedded length of wire in epoxy, D_f is diameter of wire, σ_f is tensile strength of wire:

$$\boldsymbol{\sigma_f} = \frac{\boldsymbol{P}}{\boldsymbol{\pi} \times \frac{\boldsymbol{D_f}^2}{\boldsymbol{4}}} \quad (2)$$

And τ_{ult} is the interfacial shear stress between wire and adhesive:

$$\boldsymbol{\tau_{ult}} = \frac{\boldsymbol{P}}{\boldsymbol{\pi} \times \boldsymbol{D_f} \times \boldsymbol{l_e}} \quad (3)$$

In order to calculate the tensile strength of wire, the applied load (P) was measured during the tensile experiment as discussed in part 4.3.2. The maximum applied load before the wire (gauge 39) breaks is equal to 1.6 N. Using equations (1) to (3) the required embedded length to avoid breaking the wire before pulling it out of epoxy will be calculated as follow:

$$\sigma_f = \frac{1.6}{\pi \times \frac{0.09^2}{4}} = 251 MPa \quad (4)$$

$$\tau_{ult} > \frac{1.6}{\pi \times 0.09 \times 0.6} = 9.4\ MPa \rightarrow l_e < 0.6 \text{ mm} \quad (5)$$

Even after many trials, due to the small size of the wire, it was not possible to form beads smaller than 0.6 mm. For beads that were formed on the 39 gauge wire, the wire always failed before any slippage between wire and the bead of epoxy was observed. Therefore, in order to estimate the bond strength, a larger diameter wire was used. A larger diameter of wire was only used for the bond strength test (gauge 30, D=0.26 mm). According to the measurements in this work (Table 4. 2), the maximum tensile stress of MW79-C wire is approximately 251 MPa. Considering the results of gauge 39 (equation 5), the interfacial shear stress between MW79-C wire and adhesive

is more than 9.4 MPa, therefore the maximum embedded length of wire in the adhesive will be calculated as:

$$l_e < \frac{251 \times 0.26}{4 \times 9.4} = 1.7\ mm \qquad (6)$$

Magnet wire MW79-C gauge 30 was selected for the microbond test. The beads of epoxy were applied on the surface of the wire and cured for 24 hours. The dimensions of the beads of epoxy were measured using a microscope. Photomicrographs of the beads before the test are shown in Figure 4. 5(a). The microbond test was conducted using a small load frame (Instron Model number 3366). The end of the wire without an epoxy bead was held in the grip of the load frame and the other end was restrained by placing the bead against a knife edge (such as LSXF4-5 One dimensional rotary adjustable slit), that was held by the lower grip [55].

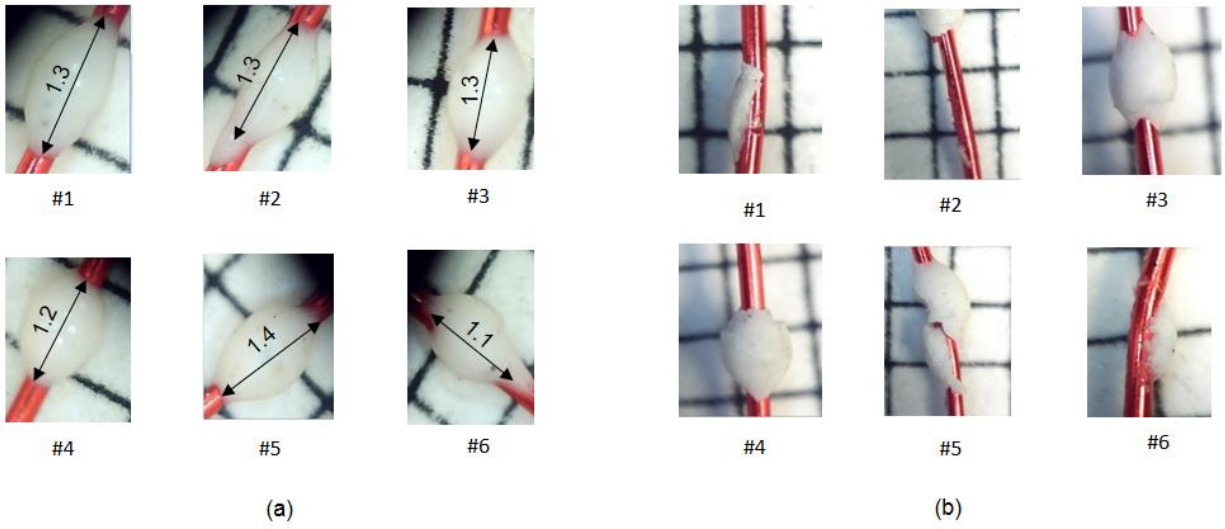

Figure 4. 5. a) Beads of epoxy on the wire. Preparing beads is a random process and hence there is variation in the size of beads. b) Position and deformation of beads of epoxy after microbond test, in some cases (bead #2) the slippage between wire and the bead is visible

The knife edge is composed of two single bevel edge blades that can be adjusted down to zero clearance. The bead is restrained by the flat edge and the clearance is adjusted to be just slightly

greater than the diameter of the wire. The test was executed at 0.1 mm/min speed rate, which is a typical rate for microbond test [56]. Photomicrographs of the beads after completion of the microbond tests are shown in Figure 4. 5(b). In some examples, the slippage of the bead on the wire is visible (bead #2).

4.4 RESULTS & DISCUSSION

4.4.1 Experimental apparatus

Combinations of wire and adhesive were tested on the experimental apparatus. As it is shown in Table 4. 1, the average crack opening at which the wire fractured was 0.34 mm; which is more than the desired crack opening (0.2 mm). Also, the detected crack openings were not consistent and they varied in a wide range- between 0.13mm to 0.6 mm- with a standard deviation of 0.16 mm. The variation in the detected crack opening might be because of existing kinks on the surface of the wire which may lead to different initial lengths of the wire and finally result in different breaking lengths. Pre-straining the wire found to be a solution to this problem. By pre-straining the wire the kinks will be removed from surface of the wire and consequently will lead to more uniform results as well as lesser detected crack opening.

The ultimate tensile strain of MW79-C wire which was used in this work is 23% (The method of testing and results is discussed in another parts of this paper). In order to get uniform results, the wire was pre-strained by 5% and 10% and the ultimate tensile strain was reduced to 18% and 13%. After pre-straining the wire, two sets of experiments were executed; one set using wire with 13% final strain and another using the one with 18% final strain. Results are shown in Table 4.1.

After pre-straining the wire by 5% and 10%, the average crack opening was reduced to 0.13mm with standard deviation of 0.02 mm and 0.03 mm.

Test Number	1	2	3	4	5	Mean	S.D.
Crack width opening ±0.01 (mm) not pre-strained	0.13	0.22	0.35	0.40	0.60	0.34	0.16
Crack width opening ±0.01 (mm) pre-strained by 5%	0.09	0.12	0.13	0.14	0.16	0.13	0.02
Crack width opening ±0.01 (mm) pre-strained by 10%	0.09	0.10	0.12	0.16	0.16	0.13	0.03

Table 4. 1. Test results of MW79-C gauge 39 magnet wire in combination with Loctite E-20NS epoxy as the binary sensor on the experimental apparatus. Using not pre-strained wire will result in inconsistent crack openings and the average is more than the desired crack opening of 0.2 mm. By pre-straining the wire results are more consistent and in the range of the desired crack opening of 0.2 mm.

The average crack opening of 0.13 mm proves the fact that stretching the wire will reduce the ultimate tensile strain and consequently the crack opening at which wire fractures. On the other hand stretching the wire to pre-strain, removed kinks from the surface of the wire and resulted in more uniform results (smaller standard deviations).

4.4.2 Tensile properties of wire

The modulus of elasticity as well as ultimate tensile stress and strain was measured for wire samples. Results are shown in Table 4. 2. The ultimate tensile strain of MW79-C gauge 39 is 23%. Pre-straining the wire by 5% and 10% resulted in the reduction of the ultimate tensile to 18% and 13%. As mentioned before, it is thought that using the pre-strained wire will result in more consistent results in the experiment.

Material	Modulus of Elasticity	Yield Stress	Measured Ultimate Tensile	True-Ultimate Tensile	Tensile Strain
MW 79-C gauge 39 not pre-strained	59000±5000	213±6	240±10	304±14	23±1
MW 79-C gauge 39 pre-strained by 5%	59000±1500	213±5	250±5	303±4	18±2
MW 79-C gauge 39 pre-strained by 10%	58000±1700	227±3	251±7	291±9	13±0.3

Table 4. 2. Mechanical properties of wire MW-79C gauge 39

It should be noted that, pre-straining will not affect the long-term performance of the sensor. The S-N curve of the drawn copper wire at room temperature shows the fatigue strength of approximately 70 MPa at 10^8 cycle [62]. According to table 10.6 of CHBDC (Canadian Highway Bridge Design Code) the maximum average daily truck traffic is 4000 for class (A) highway. This results in 7,300,000 cycles in 5 years and 14,600,000 cycles in 10 years which is the maximum service life of the sensor and still less than the fatigue strength of the copper.

In addition, available load monitoring data shows a maximum of 65 micro- strain on the typical medium span bridges. This number is implies less than 20 MPa stress on the girder which is less than the fatigue strength of copper wire (70 MPa).

4.4.3 Tensile properties of Epoxy

The epoxy was also tested to estimate the modulus of elasticity as well as observing the behaviour of the epoxy under tensile loading. Three tests were conducted and the results show brittle behaviour of epoxy under tensile loading. As soon as stresses in the epoxy reach approximately

15MPa, it breaks without entering to plastic zone. The modulus of elasticity was calculated for each experiment as shown in Table 4. 3. The average modulus is 930 MPa. The measured modulus of elasticity from the experiments is in line with the manufacturers specification of a shore D hardness of 85 [63], if the relation between the modulus of elasticity and the hardness (shore D) of epoxy is used [64]. For simulation purposes E was chosen to be 930 MPa.

Test	1	2	3	Average
Modulus of Elasticity (MPa)	850	950	1000	930
Ultimate Tensile Stress(MPa)	14	13	17	15

Table 4. 3. Mechanical properties of Loctite epoxy E-20NS

4.4.4 Bonding Properties

The microbond test was carried out to measure the bonding properties between the wire and the epoxy. This property will be used later in finite element simulation. The result of this test is a force versus displacement diagram, which will be used for calculation of interfacial stress and consequently bonding properties between wire and epoxy.

As discussed in section 4.3.5, MW79-C wire gauge 30 was selected for the microbond test (Figure 4. 5). Figure 4. 6(a) shows the result of microbond test for both gauge 39 and gauge 30 wire. Using smaller diameters of wire resulted in the fracture of wire before any debonding between wire and epoxy occurs. Therefore, gauge 30 was selected for the microbond test. Figure 4. 6(b) demonstrates the typical force-displacement diagram for the microbond test between wire and beads of epoxy. This is similar to the results from previous studies [65].

As it is demonstrated in Figure 4. 6(b) at initial steps of applying load, the bond between wire and epoxy is strong and there is a small displacement at the interface of wire and epoxy (Part A). By

increasing the load, using the load frame, the interface bonding starts to weaken (part B) until it reaches point C. At this point (point C), the interfacial bond breaks completely and the bead starts sliding on the wire (part D). Displacements measured in this diagram are including wire tensile extensions as well.

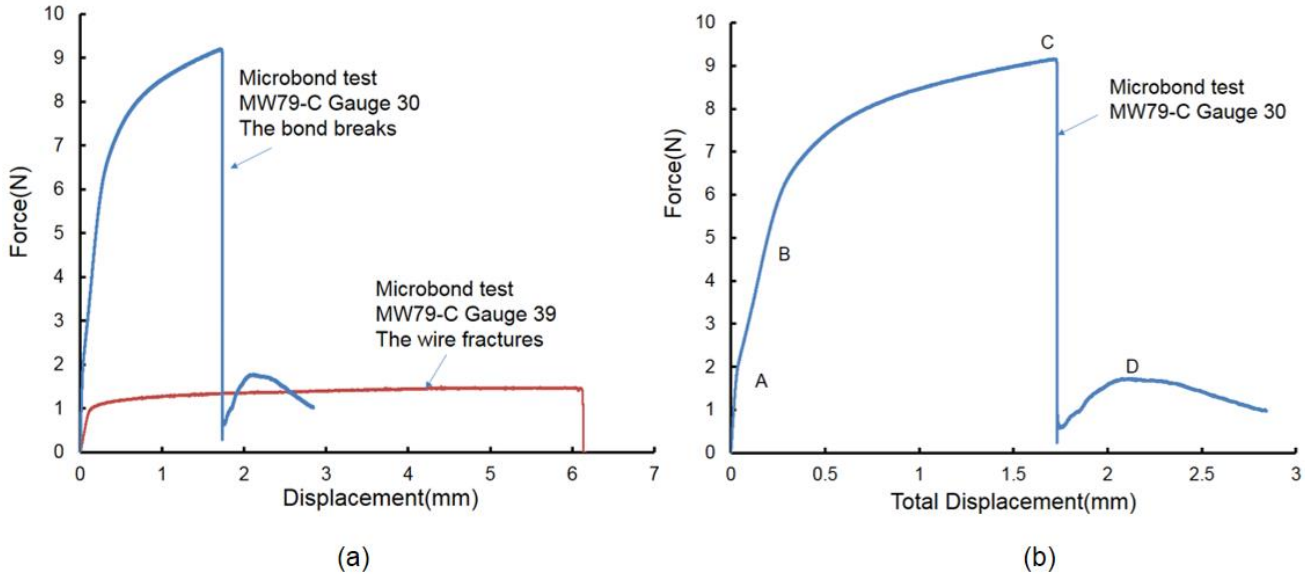

Figure 4. 6. a) Force-Displacement diagram of microbond test between a bead of epoxy and wire (gauge 39 and gauge 30). In case of gauge 39, since the embedded length of wire in epoxy is greater than 0.6mm, the wire fractures before debonding. Therefore, gauge 30 was used for the microbond test. b) Force versus total displacement between a bead of epoxy and wire gauge 30. At initial steps of applying load, the bond between wire and epoxy is strong and there is a small displacement at the interface of wire and epoxy (Part A). By increasing the load, using the load frame, the interface bonding starts to weaken (part B) until it reaches point C at which the interfacial bond breaks completely and the bead starts sliding on the wire (part D).

Since during the tests of the binary sensor -either on the apparatus or on the steel girder-, the embedded length of the wire in the epoxy is much more than the required one mentioned in part 4.3.5 and the wire always breaks at forces less than 2N, bonding properties will be calculated for the first part of diagram (Part A) which starts from 0 and increases linearly to 2N. Calculating the

stiffness properties of the bond between wire and epoxy- as will be discussed in part 4.5.5- is based on the applied force and its corresponding displacement of the bead of epoxy on the wire.

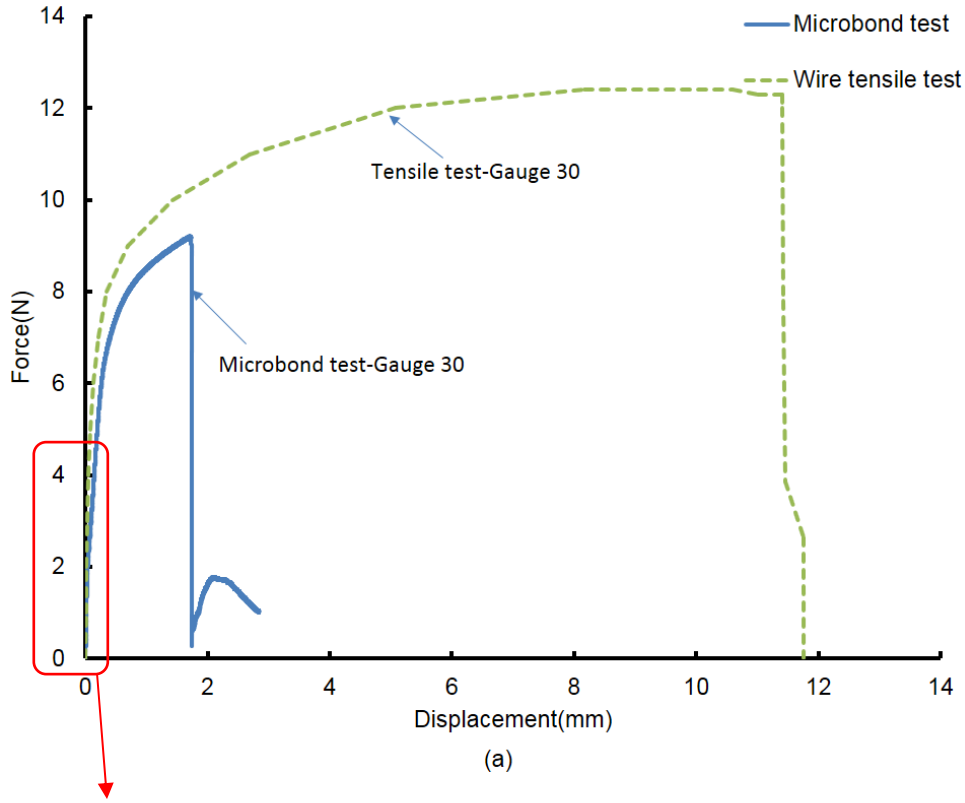

(a)

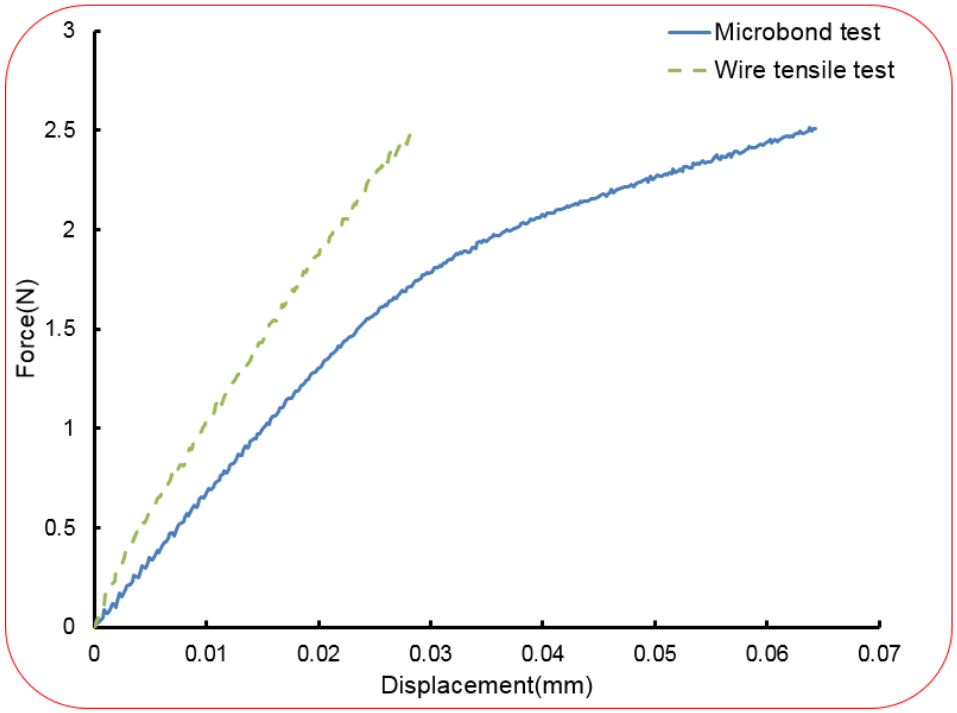

(b)

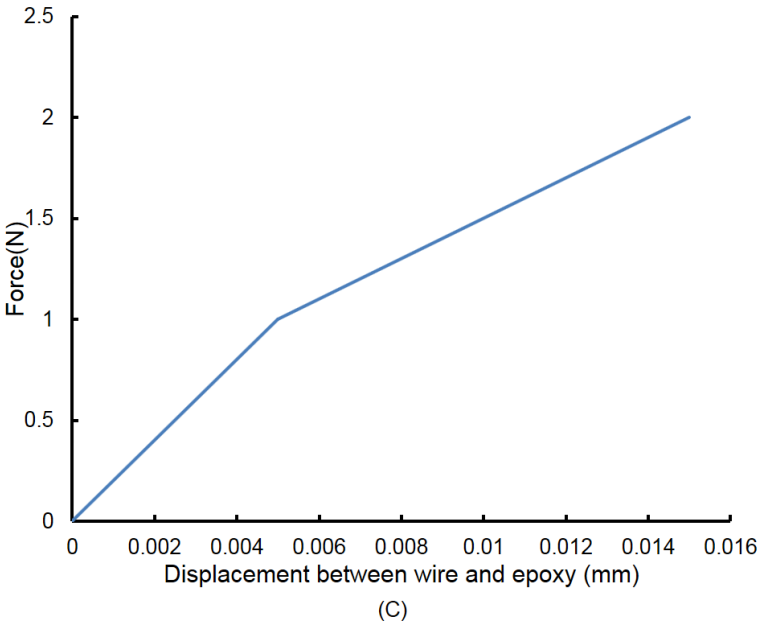

Figure 4. 7. a) Force-Displacement diagram of tensile test of wire and microbond test. b) As the wire pulls out of epoxy, a part of its displacement is due to its elastic and plastic deformation. In order to calculate the displacement between wire and the bead of epoxy, the wire deformation should be deducted from the total displacement. c) The net displacement between wire and epoxy versus the applied force

Force(N)	microbond test elongation(mm)	wire tensile test elongation(mm)	Displacement between wire and epoxy(mm) = microbond test elong. -wire tensile elong.
0	0	0	0
1	0.015	0.01	0.005
2	0.037	0.022	0.015

Table 4. 4. Displacement calculation between the wire and beads of epoxy

The displacement measured from the load frame at part A includes small movements of the bead of epoxy on wire as well as linear deformation of wire due to extension. In order to calculate the

net displacement between wire and epoxy, the elastic displacement of wire should be deducted from the total displacement (Figure 4. 7). The calculation is shown in Table 4. 4. Figure 4. 7(a) plots the force-displacement diagrams for the tensile test and microbond test for wire (gauge 30). Since part A of the behaviour of the wire and the bead is required for interfacial stiffness calculations, a close-up of the two graph is shown in Figure 4. 7(b). As it is shown in Figure 4. 7(b), at a certain force, the measured displacement of micorbond test is greater than the one from wire tensile test. This difference between two measurements is due to the small sliding between the bead of epoxy and the wire. Figure 4. 7(c) shows the net displacement between wire and epoxy versus the applied force.

Having force versus displacement diagram for the microbond test as well as the size of beads of epoxy, the interfacial stress between the wire and the epoxy can be calculated according to equation (3). The interfacial stresses between wire and adhesive for six samples are shown in Table 4. 5. (calculations for Interfacial stiffness will be discussed in part 4.5.5). Having the material properties and the bonding properties between wire and adhesive, the sensor was simulated in a Finite Element software – ABAQUS- which will be discussed in future parts.

4.5 FINITE ELEMENT SIMULATION

4.5.1 Introduction

The numerical study is initially aimed to help in finding the proper material for the binary sensor and then to find the optimal position of the Binary sensor on a steel girder for a large scale. The Finite Element Modeling (FEM) provides an effective tool to simulate laboratory conditions without the constraint of time and cost. In any commercial finite element software three steps are required to solve the engineering analysis problem; pre-processing, numerical analysis and post processing [66]. In the following parts, the simulation of the binary sensor on the apparatus will

be discussed. The Finite Element Model was simulated in ABAQUS software and results were verified with experimental results.

Sample Number	Force(N)	Displacement (mm)	Interfacial stress (MPa) (equation 3)	Interfacial Stiffness K (MPa/mm)	Average K(MPa/mm)
1	1.0	0.0036	0.94	261	225
	2.0	0.010	1.88	188	
2	1.0	0.009	0.94	104	100
	2.0	0.019	1.88	99	
3	1.0	0.007	0.94	134	130
	2.0	0.015	1.88	125	
4	1.0	0.016	1.02	64	76
	2.0	0.023	2.04	89	
5	1.0	0.0045	0.87	192	288
	2.0	0.0045	1.75	384	
6	1.0	0.005	1.11	222	235
	2.0	0.009	2.22	247	

Table 4. 5. Interfacial bonding stress and stiffness between wire MW79-C and epoxy E-20NS

4.5.2 Simulation

As mentioned before, three steps are required to complete a Finite Element Simulation: pre-processing (which includes discretization, element types, material data, load and boundary conditions), numerical analysis and post processing [67].

4.5.3 Discretization

The first part of any FEM is discretization is to divide the geometry of a physical structure into discrete elements. Each element represents a small portion of a whole structure. In this project a total of three individuals (steel plates of apparatus, epoxy and copper wire) are available to be discretized first and then be connected to each other. A total of two element types were defined in this model to simulate the sensor on the steel plates. The FEM was created in the x-y horizontal plane.

The test apparatus is made of two steel plates that can separate from each other on one edge. This is simulating the crack opening on the web of the steel girder. Two 200 mm x 200 mm rectangular plates with modulus of elasticity of 200GPa and Poisson ratio of 0.3 were simulated in ABAQUS using the 3-D four-node deformable conventional shell elements (1 mm x 1 mm dimension)(Figure 4. 8a,b). Since the thickness of the steel plates are significantly smaller than the length, shell elements are considered for this simulation. Two types of shell elements are available for simulation, conventional and continuum. For thin shell elements, conventional elements are preferred. The thickness of the conventional elements are required to define the cross section of the members and it will be specified through section properties [67]. In this simulation the thickness of plates are 20 mm. Homogeneous shell sections were selected. Five section points were assumed through the thickness of the shell (Figure 4. 8b).

Epoxy is the next part to be simulated. In this simulation, a 5 mm x 2 mm rectangular epoxy was simulated using an 8-node, 3-D solid elements (0.2 mm x 0.2 mm seed size). The meshing within the epoxy will be adjusted to the meshed embedded wire and has been done using the sweep technique with advanced front algorithm. The modulus of elasticity of epoxy as shown in Table 4.3 was considered to be 930 MPa. The last material in the simulation is a copper wire with dimensions of 5mm long and a diameter of 0.09 mm. In order to simulate the wire, an 8-node, 3-D solid elements were used (Figure 4. 8c). The element size of the wire mesh is approximately equal to 0.045 mm and the curvature control has been applied to calculate the seed distribution based on the curvature of the edge of the wire. Therefore, the wire has been simulated as a cylinder. In this simulation, the mechanical properties of the wire is the critical one, as the sensor breaks as soon as the wire reaches its ultimate tensile strain. Therefore the breaking strain and final tensile strength of the wire are required for the purpose of this simulation. As mentioned before, in order to have more uniform results the wire was pre-strained before installation. Three separate models were simulated for three different material properties of the wire (not pre-strained, pre-strained by 5% and pre-strained by 10%). The material properties of the wire are demonstrated in Table 4. 2.

4.5.4 Load and Boundary Condition

Steel plates are the base structure of this simulation which are representing the crack opening on the web of a steel girder. The other parts of the simulation (epoxy and wire) will be assembled on the steel plates. As it is shown in Figure 4. 2, there is a fixed support at the edge of plate B. By applying the force, the other plate (Plate A) moves from the fixed plate and simulates the crack opening. This happens by turning the micrometer and applying displacement to the free edge of plate A. Therefore, the edge of plate B is fixed against all translations and rotations. A displacement force was assigned to the free edge of plate A.

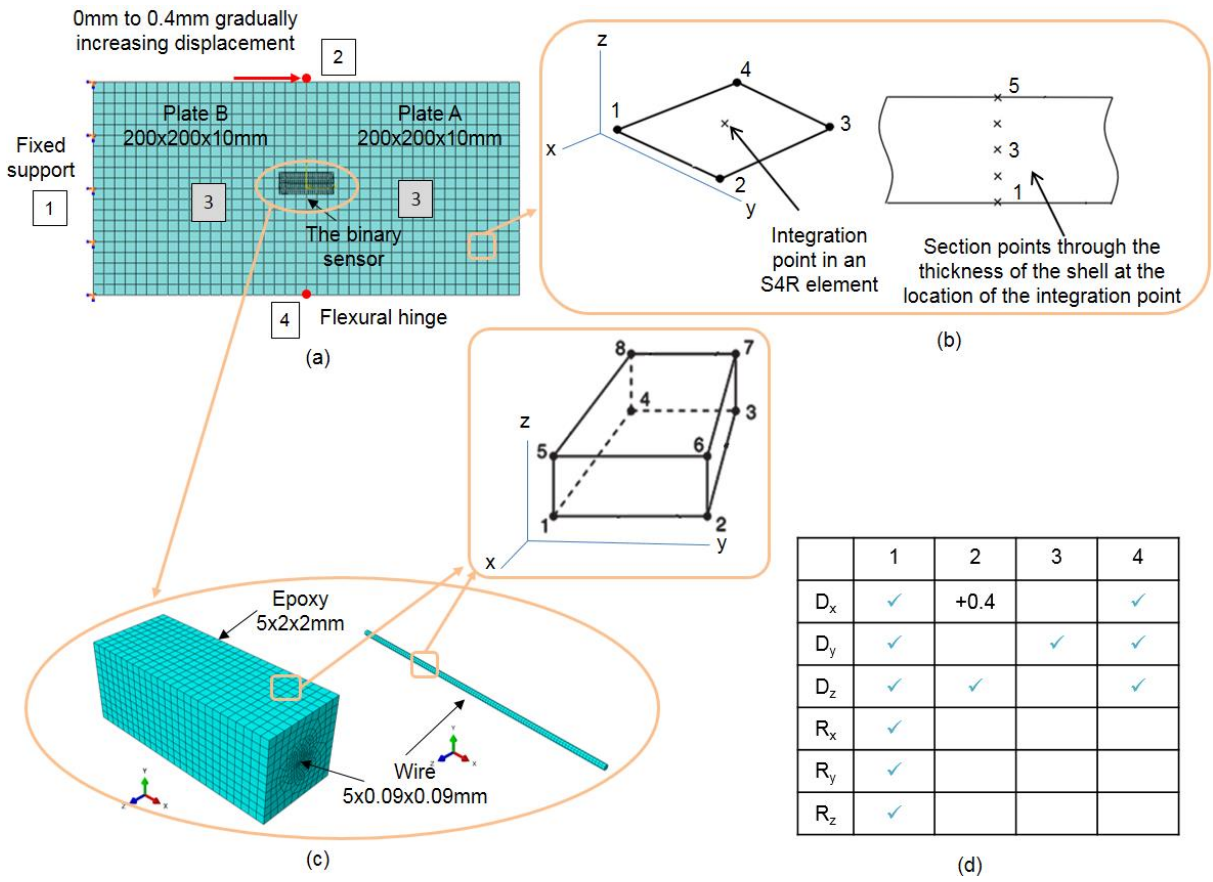

	1	2	3	4
D_x	✓	+0.4		✓
D_y	✓		✓	✓
D_z	✓	✓		✓
R_x	✓			
R_y	✓			
R_z	✓			

Figure 4. 8. Finite Element simulation of the sensor on steel apparatus a) steel plates apparatus were simulated in ABAQUS using a 4-node conventional shell elements, b) An S4 shell element and the integration point on it. 5 section points are considered through the thickness [67], c) the epoxy and the wire were simulated using an 8-node 3-D continuum solid elements, d) the boundary condition of the simulation

Since the binary sensor detects the presence of small cracks with opening of less than 0.2 mm and it will be placed at the middle of apparatus, the maximum displacement that had been assigned to the edge of the steel plate, was 0.4 mm (Figure 4. 8a, d). This amount of displacement was increasing gradually at each step.

4.5.5 Constraints

Connecting different parts of model to each other is the final step to complete the finite element simulation. Steel plates, epoxy and wire should get connected to each other. The bond between steel plates and epoxy should be strong enough to transfer the strains. Therefore, in our experiments and installation parts, any contamination and dirt was removed from the surface of the plates [17]. In the finite element simulation, epoxy was connected to the steel plates using the tie, surface based-constraint in ABAQUS. Other elements to be connected to each other are wire and epoxy. Therefore, the interaction properties in contact region of wire and epoxy are required.

As mentioned before in part 4.3.5, when the forces in the copper wire reaches to approximately 2N the wire breaks. This is before any debonding between wire and adhesive occurs. At this stage, the contact property between wire and epoxy before debonding is elastic and it follows the cohesive behaviour using traction-separation law [56]. The elastic behaviour is written in a form of a stiffness matrix, which relates the separations to the stresses across the interface. It is written as below [68–70]:

$$t = \begin{Bmatrix} t_n \\ t_s \\ t_t \end{Bmatrix} = \begin{bmatrix} k_{nn} & k_{ns} & k_{nt} \\ k_{ns} & k_{ss} & k_{st} \\ k_{nt} & k_{st} & k_{tt} \end{bmatrix} \begin{Bmatrix} \delta_n \\ \delta_s \\ \delta_t \end{Bmatrix} = K\delta \qquad (7)$$

Where t is the nominal traction stress vector, which consists of three components; t_n, t_s, t_t where t_n represents the normal traction and t_s, t_t represent two shear tractions and $\delta_n, \delta_s, \delta_t$ are corresponding separations. For the uncoupled traction-separation behaviour, the terms k_{nn}, k_{ss} and k_{tt} must be defined and other elements in the stiffness matrix (k) will be considered equal to zero [69–71].

In order to define stresses and separations at the interface of wire and adhesive the results of micro-bond test are required. Using equation (7) and calculated data from the microbond test (given in

Table 4.5), the stiffness of the bonding will be calculated as shown in Table 4.5. As it is demonstrated in Table 4. 5 the interaction stiffness varies between 76 MPa/mm to 288 MPa/mm. The wide range of stiffness can be attributed to numerous factors including shape of the cured epoxy beads, position of the knife-edge, coating of the wire at the bonding place, reproducibility of the sample preparation, etc. [56]. The average stiffness calculated and shown in Table 4.5 (76MPa/mm to 288MPa/mm), were used in FEA. Results will be discussed in parts 4.5.8 and 4.5.9.

4.5.6 Numerical analysis

The material and geometric nonlinearity was considered in simulation by applying the incremental step by step analysis. The forces required for opening the crack were applied in increments and at each increment, load iterations were performed until the convergence criteria was satisfied.

4.5.7 Post processing

Three separate sets of analysis were run for wire with different material properties (not pre-strained, pre-strained by 5% and 10%). Each set includes analysis with two groups of interfacial bonding stiffness values; a) the values mentioned in Table 4. 5 (76 MPa/mm to 288 MPa/mm) and b) two more hypothetical values (600MPa/mm and 1000Mpa/mm). The second group of bonding stiffness were considered to prove the accuracy of the measured ones. At the beginning of the analysis, as the opening between two plates starts to widen, both of the epoxy and wire will carry tensile stresses. By increasing the gap between two plates, epoxy will fracture and stop taking more forces. Therefore, all the applied strains will be transferred to the wire. The wire will stretch under available tensile stresses until the strains in the wire reach to the maximum allowable tensile strain. At this point wire will break. Figure 4. 9 demonstrates both experimental results as well as numerical ones for three different wire properties. The graphs show crack opening versus different stiffness of bonding between the wire and the epoxy.

4.5.8 Effect of pre-straining

As mentioned before in part 4.4.1, the experimental results of not pre-strained wires varies in a wide range which can be due to the available kinks on the surface of the wire or errors during the installation procedure. Figure 4. 9(a) demonstrates results of both experiment and FEA of not pre-strained wire. As it is shown in the graph, the minimum crack opening measured in the experimental work is equal to the FEA but the experimental upper limit is higher than the FEA one. Results from FEA prove that the wire is a good candidate for the sensor, since its tensile properties are in a range that will cause the wire to break at the desired crack opening of less than 0.2 mm. It also proves that there were some inaccuracy during installation due to available kinks on the surface of the wire. In order to have more uniform outcomes, the wire was pre-strained by 5% and 10% (Figure 4. 9(b, c)).

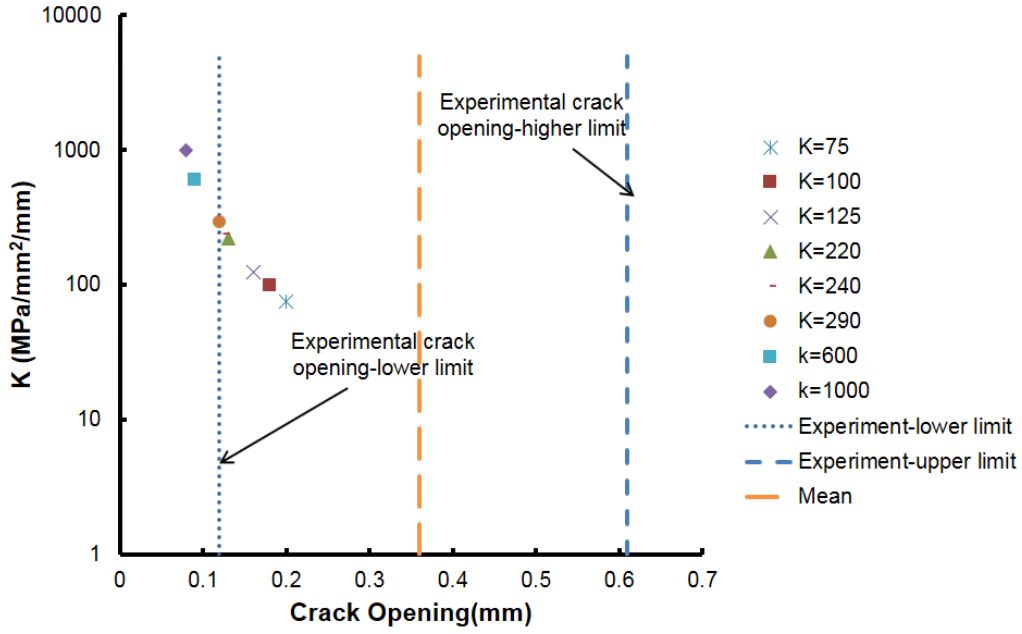

(a)

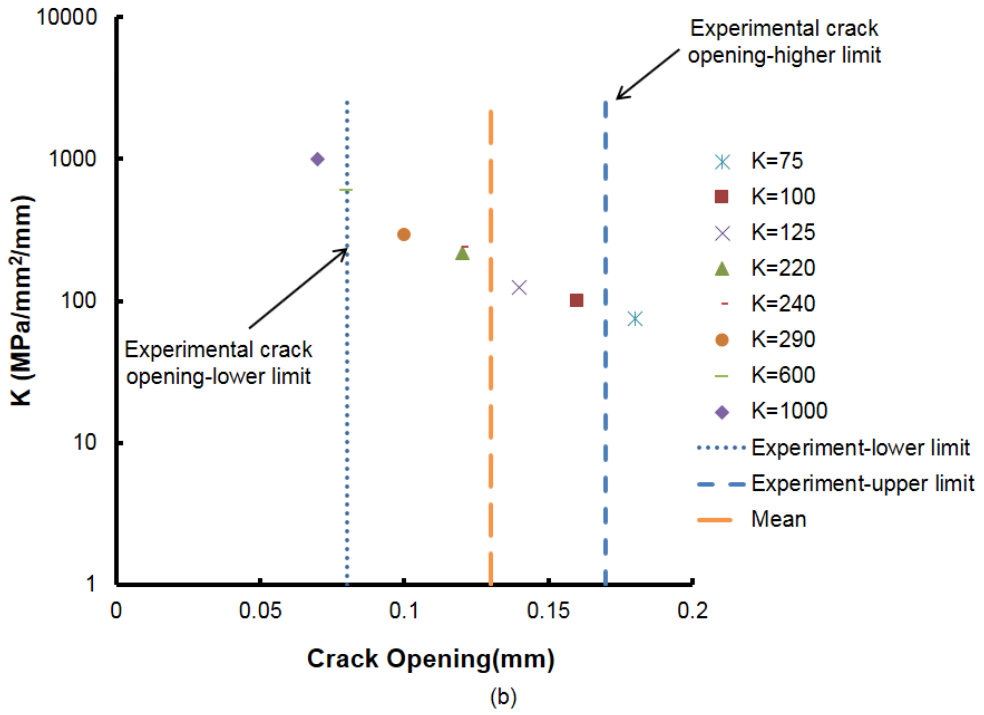

(b)

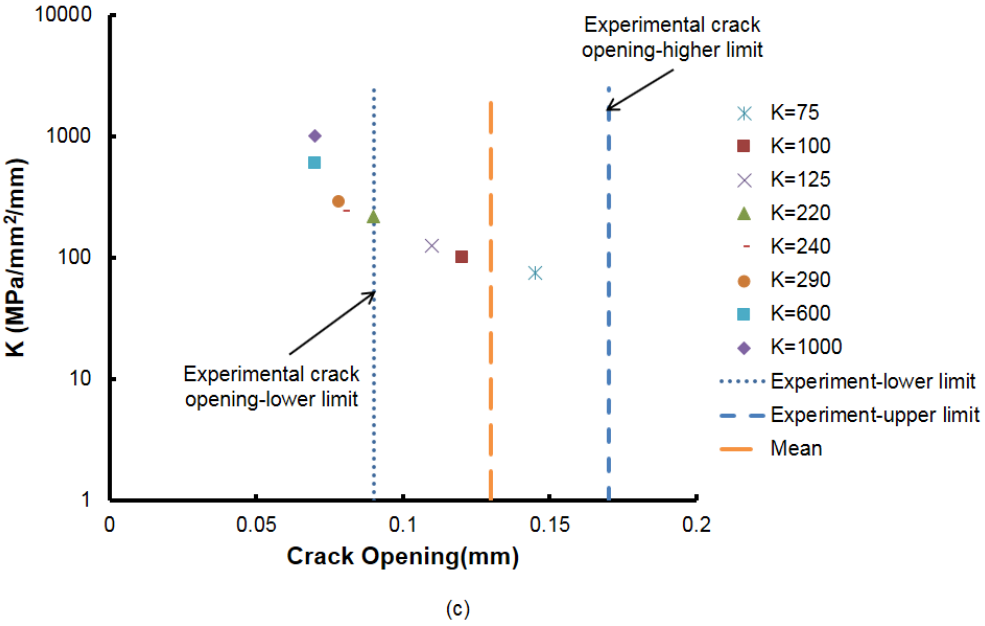

(c)

Figure 4. 9. Results of experiments and Finite Element Analysis of the binary sensor on the apparatus. a)wire is not pre-strained, experimental results are in a wide range and more than the desired crack opening of 0.2 mm but numerical results are in an acceptable range, b) wire is pre-strained by 5%, results are more uniform and less than 0.2mm. Using the interfacial stiffness of

75MPa/mm results in a crack opening out of higher band of experiment c) wire is pre-strained by 10%. Results are uniform and less than 0.2 mm.

4.5.9 Effect of bonding properties

The main purpose of this FE analysis is to find the best choice of the interfacial stiffness between the wire and epoxy for future analysis. Due to different variables in executing the micro bond test such as the position of knife-edge, shape of the cured bead of epoxy, coating of the wire at the bonding place, etc. [56] the measured stiffness varies in a wide range of 75 MPa to 290 MPa. According to the results from finite element analysis shown in Figure 4. 9, using the measured stiffness values (75MPa/mm to 290MPa/mm) in all three cases will result in crack openings which are in a good agreement with the experimental ones. It also proves that using the hypothetical numbers (600MPa/mm and 1000MPa/mm) will have minimal affect on the lower band. In other words, there is always a minimum crack opening required for the sensor to function and increasing the stiffness of the bond will not affect the results.

Looking more closely to all three graphs, results from using the stiffness value of 220 MPa/mm and 240 MPa/mm in finite element analysis are approximately equal to the average of the experimental works. Therefore in future studies of epoxy E-20NS and the copper wire MW79-C, the interfacial bonding stiffness between these two materials will be taken equal to 240 MPa/mm.

4.5.10 Wire radius versus crack opening

The FEM model can be used to better understand the detected crack opening using the ultimate tensile strain of the wire and the bridging length of the wire within the epoxy [72]. The bridging length within the epoxy is the length over which the strain due to the crack formation will be distributed. In order to estimate the bridging length of wire within the epoxy, the reduction of the diameter of wire versus crack opening (change in the length) has been examined using the finite

element model. The interfacial bonding stiffness between wire and epoxy and the ultimate tensile strain of wire was considered to be 240 MPa/mm and 18%. In Figure 4. 10 the diameter of the wire versus distance from the center of the crack opening for openings of 0.075, 0.09 and 0.12 mm has been plotted. As the crack opening increases the diameter of the wire decreases at the center of the crack opening. For example, with a 0.09 mm crack opening, the diameter of wire at the centre of the crack is 0.083 mm. By increasing the crack opening to 0.12 mm the diameter at this point will decrease to 0.08 mm. However, the decrease of the diameter of wire (necking) for all crack openings extends no more than 0.4 mm from the centre of the crack. Therefore, 0.8 mm is bridging length of the wire within the epoxy and is the distance over which the strains will be distributed at the breaking point. The maximum extension of the wire before it breaks can be estimated using the FEM to estimate the bridging length within the epoxy and the ultimate strain.

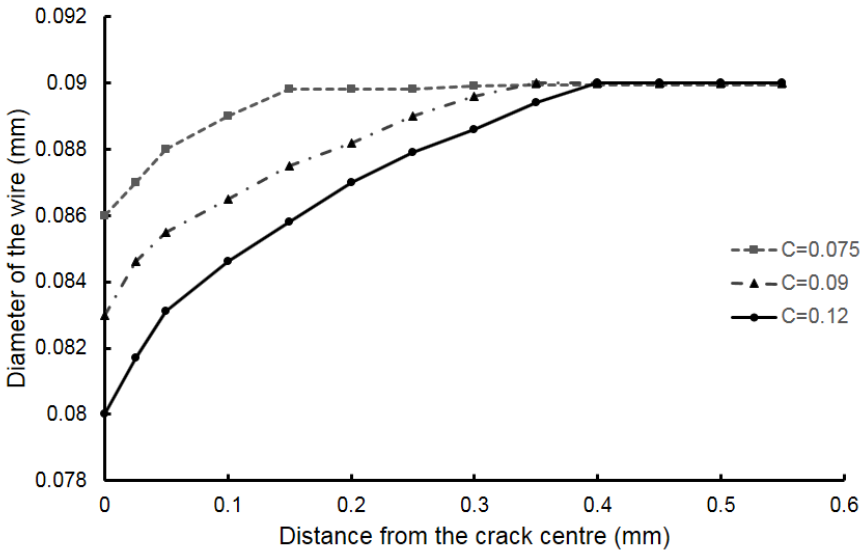

Figure 4. 10. Diameter of wire at distances from the crack centre. By increasing the crack opening, the change in the diameter increases. The entire process of diameter change (Necking of the wire) starts at 0.4mm distance from the centre of the crack for all crack openings.

By using the ultimate strain and the bridging length of the wire within the epoxy then the crack width at which wire breaks can be estimated as follow:

$$Crack\ opening = \varepsilon \times bridging\ length \rightarrow Crack\ opening = 0.18 \times 0.8 = 0.14mm \quad (8)$$

Which is in a good agreement with Figure 4. 9(b) which shows the crack opening of approximately 0.12 mm from finite element simulation results. In addition it also falls in the limits of experimental results which is shown in Figure 4. 9.

4.5.11 Effect of position of wire in the epoxy

Results from analysing the binary sensor in ABAQUS shows that the bonding stiffness between MW79-C wire and E-20NS epoxy can be considered approximately 240MPa/mm. Having all the mechanical properties of materials as well as the interfacial bonding stiffness, the binary sensor was simulated in ABAQUS to study the effect of position of wire in the epoxy (h) on the detected crack opening. Figure 4. 11 shows positioning of the wire in the epoxy on the steel plates.

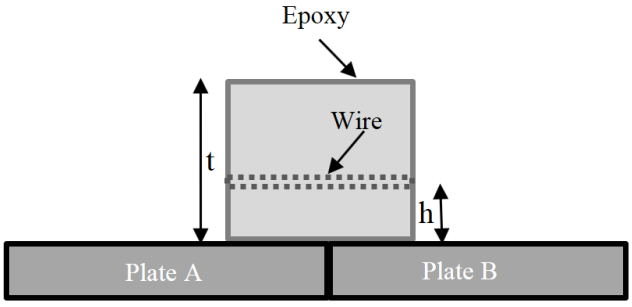

Figure 4. 11. Positioning of the wire in epoxy on steel plates. The wire will be positioned at different depth of the epoxy to study the effect of wire placement on detected crack opening of binary sensor

In this work three different thickness of epoxy was studied (1.0 mm, 2.0 mm and 3.0 mm). At each thickness, the wire was placed at (3/4), (1/2) and (1/4) thickness of epoxy. After completion of

analysis at each step, the crack opening at which the wire was broken, was measured. Results are shown in Table 4. 6. As it is shown in Table 4. 6, the maximum thickness of epoxy which will result in the desired detected crack opening (0.2 mm) is 2.0 mm. At this thickness, placement of wire in the epoxy has minimum effect on the results whereas by increasing the thickness to 3.0 mm, the wire should be placed at less than half of the thickness of the epoxy to be able to detect cracks before they open up to 0.2 mm.

	Position of wire (mm) - h		
Thickness of Epoxy(mm) - t	(3/4)t	(1/2)t	(1/4)t
3.0	0.28	0.22	0.17
2.0	0.17	0.14	0.16
1.0	0.13	0.13	0.12

Table 4. 6. Crack opening width based on different thickness of epoxy and different positions of wire in the epoxy

4.6 CONCLUSION& FUTURE WORKS

North American infrastructure including steel girder bridges are aging and reaching the designed service life. Crack formation and its propagation under service loads may occur in aging girders due to several reasons such as fatigue or deficiency in the welded joints. Structural Health Monitoring systems provide required techniques to monitor bridges and detect cracks before they reach to a critical dimension. Available crack monitoring techniques for monitoring steel girders are either not sufficient or not economical. Numerous bridges will benefit of an economical and easy installed system of monitoring. The new binary crack sensor which was introduced earlier

composed of wire which will be attached to the steel girder using a carefully designed epoxy. When a crack with the opening of approximately 0.2 mm forms in a steel girder, the binary sensor fractures and alarms the monitoring group. Two major parameters, which will affect the design of the binary sensor, are ultimate tensile strain of the wire as well as the bonding properties between wire and epoxy. In this work, the binary sensor using wire MW79-C (gauge 39) was tested on an experimental apparatus. The wire was pre-strained by 5% and 10% to compare the results and investigate the influence of pre-straining on the detected crack opening. A Finite Element Model of the apparatus and the binary sensor was created in a Finite Element software –ABAQUS- and the required bonding properties between wire and adhesive were measured from the microbond testing and was verified with the simulation. Experiments and FEM proved that pre-straining will result in a smoother surface of the wire and will cause the results to be less scattered. It also proved that pre-straining will result in decreasing the ultimate tensile strain of the wire and consequently will result in smaller detected crack widths. The interfacial bonding stiffness between wire MW79-C and epoxy E-20NS was measured to be in a range of 75 to 290 MPa/mm. The results from FEA using this range of bonding stiffness are in good agreement with the experimental results. Therefore in future studies of epoxy E-20NS and wire MW79-C, the interfacial bonding stiffness between these two materials will be taken equal to 240 MPa/mm.

Effect of thickness of the epoxy and position of the wire in the epoxy was studied in the last part of this paper. Results show that the most optimum and feasible thickness of epoxy is 2.0 mm and the position of the wire in the epoxy at this thickness has minimum effect on the results.

The finite element model, which was created in this work, will provide other researchers and practitioners with the means to predict the performance of the binary sensor in other crack detection applications.

In future works, the required steps for installing the binary sensor in the field from very first steps of calculating the best position of the sensor on the girder to the installation procedure and data collected after the installation will be studied.

CHAPTER 5: PLACEMENT OF BINARY CRACK SENSOR ON SIMPLY SUPPORTED I-SHAPED STEEL GIRDERS

5.1. ABSTRACT

Cracks that form in steel girders of bridges have the potential to compromise the integrity of the structure. Therefore, it is critical to detect cracks before they reach an unstable length. In previous work distributed binary crack sensors and distributed fibre optic crack sensors were demonstrated to be capable of detecting cracks with maximum 0.2 mm opening in steel girders. In this work, an FEM of two typical medium-span simply supported steel girder bridge has been simulated (Girder A, 30 m span 1.7 m depth and Girder B, 22 m span 1.2 m depth). The loads used in the simulation were determined using field load test results. Given the detectable crack opening of 0.2 mm, the FEM simulation was used to determine the optimum place to position distributed crack sensors to detect the smallest crack length. Using FEM the crack opening along the length of the crack was estimated for a number of stable crack lengths. The results for distributed sensors were compared with FEM models for an array of discrete strain gauges. It was concluded that approximately 30 sensors would be required for girder A and 24 sensors for girder B. Therefore, an array of

traditional strain gauges is an impractical method for crack monitoring. It was concluded that, the most effective position to install distributed binary sensor and fibre optic crack sensors, is between 15cm to 25cm above the bottom flange for girder A and 15cm to 22cm above the bottom flange for girder B. At this position the sensors will detect cracks once they reach a length of 40 cm.

KEYWORDS: Binary sensor, Crack detection, Steel bridges, Finite Element Analysis

5.2 INTRODUCTION

Many steel girder bridges in North America are approaching the end of their design life [4]. These bridges which were built before mid-1970 are at risk of crack formation in the steel girders [73]. Fatigue cracks may occur as a result of environmental stresses and cyclic truck traffic over a steel girder bridge and it can be categorized as distortion-induced cracks, cracks as a result of large initial defects, cracks related to connection restrained or cracks in welded flange and web gusset plates [6, 27, 74, 75]. Although the cracks may propagate and in some instances it may result in brittle fracture from crack instability [27], in most of the cases, ductility and redundancy of the bridges have prevented the catastrophic failure [73]. Detection of cracks in steel girders is important for public safety, to detect cracks when they can be repaired with minimum loss of service and to prevent the unpredictable loss of service and associated expenses. Visual inspection along with Non Destructive Evaluation (NDE) techniques such as acoustic emission, eddy current and ultrasound testing are one traditional way of detecting damages [10]. However, small cracks might escape detection and grow to lengths that will compromise the structure over the time interval between two sequential inspections. Fracture in a girder of I-95 Highway Bridge over the Brandywine River as well as in Diefenbaker Bridge over North Saskatchewan River in Prince Albert, Canada are two examples of this issue [11, 12]. A number of monitoring techniques are known to be capable of detecting cracks before they grow to an unsafe state [14]. Two general

categories of sensors are available; discrete (such as strain gauges, short gauge or long gauge sensors) and distributed (such as fiber optic sensors, smart film) [13, 16–23]. With the discrete monitoring method, strain sensors are installed at positions so that the strain perturbations due to crack formation can be detected. This requires that enough sensors be installed to ensure that wherever the crack forms a sensor is in close enough proximity to detect the strain perturbation above the background variation and noise [15]. Therefore, for a medium span bridge with multiple girders it might need an impractical number of sensors to be installed. A second way to monitor girders is to use distributed sensors which are installed along the entire length of the girder [15]. In addition, in previous work a distributed binary crack sensor has been demonstrated [14]. It is comprised of an insulated wire bonded to the steel girder using a carefully selected adhesive (Figure 5.1). The binary crack sensor has the potential to detect cracks before they open up to 0.2 mm width which is comparable to what fiber optic sensors can detect [16, 17]. The binary crack sensor will be installed over the entire length of the girder in regions on the web where cracks are expected to form (such as positions on the web where high tensile stresses exists or in the vicinity of those details which will result in fatigue cracking) [6, 17, 27]. When a sufficiently large crack forms under the sensor, the wire breaks and this can be detected by monitoring the continuity of the wire. Extensive testing has been carried out to find materials with proper mechanical properties such as specified tensile strength, ultimate tensile strain and required bonding properties between wire and adhesive. The ultimate tensile strain should be in a range that the wire breaks at openings less than the desired crack opening and the bonding should be strong enough to transfer the strain from the crack on the steel girder to the wire and cause the wire to break. The sensor was tested in the lab in ambient temperature as well as two extreme temperatures (-30ºC and +40 ºC). Results

of these experiments are discussed in previous works [17]. The sensor has also been field tested on a 30 meter span girder of a bridge in Canada [76].

Prior to the installation of the binary crack sensor the position of the sensor should be determined. The optimum placement is the position at which the sensor detects cracks before they grow spontaneously and result in severe damage of the girder and hence the overall structure.

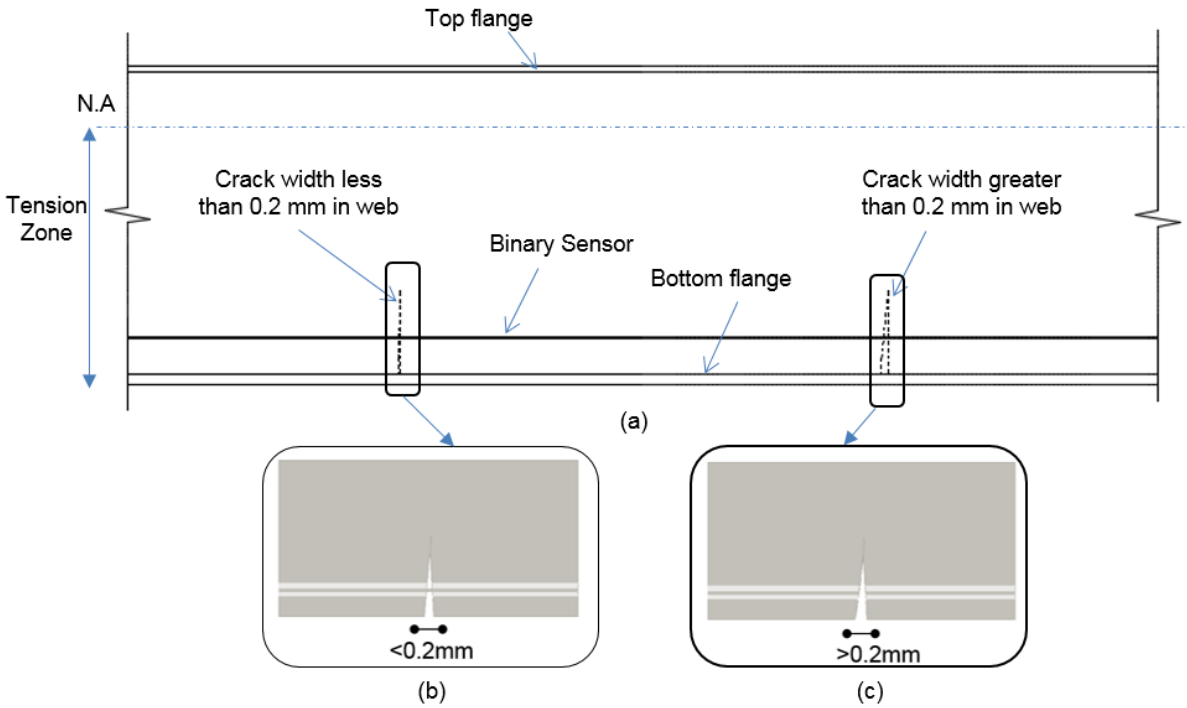

Figure 5. 1. a) The Binary crack sensor will be installed on the entire length of a steel girder and is comprised of wire adhering to the steel girder using an adhesive. By formation of crack in steel girder, strains will be transferred to the epoxy b) crack propagates through the epoxy when crack opening on the girder is less than 0.2 mm but wire remains connected c) over time, under tensile stresses, crack opening increases and causes the wire to break which will result in a change in the resistance of wire [17]

Having the fracture toughness of the steel girder, the behavior of the cracked steel girder under service load at various temperatures can be predicted. Fracture toughness is an indication of the

amount of required stress for propagating a pre-existing flaw. In a steel girder of a bridge -at the point with an existing flaw- the crack will remain stable and will not propagate spontaneously as long as the stress intensity factor (SIF) at the tip of the crack remains less than the fracture toughness. Therefore, it is important to calculate the SIF at the tip of the crack to predict the maximum stable length of it. In this work the behavior of the crack is modelled using the stress intensity factor at the tip of the crack on the girder. Using the critical stress intensity factor, the maximum length the crack can have before it spontaneously propagates can be predicted. The maximum length the crack at which it propagates spontaneously is called the critical length. Using finite element modelling (FEM), the crack opening under load can be calculated at any position on the girder. From this simulation the opening of the crack at any position on the girder, before it reaches the critical length can be predicted. This map can be used to predict where the binary sensor is capable of detecting a crack before it reaches the critical length. In this work, given a minimum crack opening that a crack sensor can detect and using finite element simulations of two typical medium span steel girders the optimum position of crack sensors to detect the minimum crack length has been determined. Also using the finite element simulation, the feasibility of application of distributed crack sensors will be compared to the discrete monitoring using the strain gauges.

5.3 CALCULATION OF THE MAXIMUM STABLE LENGTH OF A CRACK

Cracks may form in the steel girders of bridges as a result of stress concentration in the vicinity of a large initial defect in the material or weld. Cracks will be categorized as distortion-induced cracks, cracks as a result of large initial defects, cracks related to connection restrained or cracks in welded flange and web gusset plates [6, 27, 74, 75]. It is important to detect cracks before they become unstable and propagate spontaneously. This will reduce the rehabilitation costs and

enhance safety. One of the main characteristics of steel which will help to predict its behavior is the fracture toughness. Fracture toughness is an indication of the intensity of stress required for propagating a pre-existing flaw. In a cracked steel girder, if the stress intensity factor at the tip of the crack is less than the fracture toughness, then the crack will remain stable and will not propagate spontaneously. Therefore, it is important to calculate the SIF at the tip of the crack to predict the maximum stable length of the crack. In the following section, the calculation of SIF and critical length of the crack for two typical medium-span girders will be discussed.

5.3.1 Stress Intensity Factor (SIF)

The stress intensity factor can be calculated using the Linear- Elastic Fracture Mechanism (LEFM). LEFM relates the stress magnitude and stress distribution around a crack in a member to the crack size, shape and the crack orientation. In this method, the stress field ahead of a sharp crack in a structural member is called stress intensity factor, which is indicated with parameter K. To better analysis stresses and local deformations at the tip of a crack, three general modes of movement between the two surfaces of cracks have been defined; the opening mode (Mode I), the shear mode (Mode II) and the tearing mode (Mode III). Figure 5. 2 presents the three modes of the crack surface movement [77].

In a steel plate girder under predominantly bending, the fatigue crack propagates in the web plate or tension flange due to the opening mode loading (Mode I) [2, 78]. The stress intensity factor for this case will be calculated using the far-field stresses as shown in Figure 5. 3. When the stress intensity factor at the crack tip reaches the fracture toughness of the steel, then brittle fracture occurs [78].

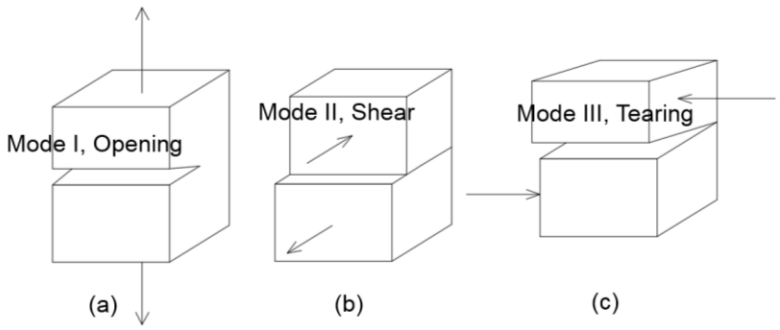

Figure 5. 2. Three basic modes of displacement between two surfaces of crack; a) Mode I, opening, b) Mode II, shear and c) Mode III, tearing

For Mode I loading of a center-cracked tension plate, the stress intensity factor (K_I) can be calculated as:

$$K_I = f(g)\sigma\sqrt{\pi a} \qquad (1)$$

Where σ is the far-field stress, a is half of the length of the crack and $f(g)$ is a correction factor that depends on the crack geometry and the loading geometry [78]. For a girder under bending moments with an edge crack, the stress field around the crack varies linearly. The maximum tensile stress occurs at the end closer to the bottom flange and it is equal to the bending stress within the extreme fibers of the tension flange. The stress field at the other end of the crack can be described using equation (2):

$$\sigma_a = \pm\sigma_f\left(\frac{4a}{d} - 1\right) \qquad (2)$$

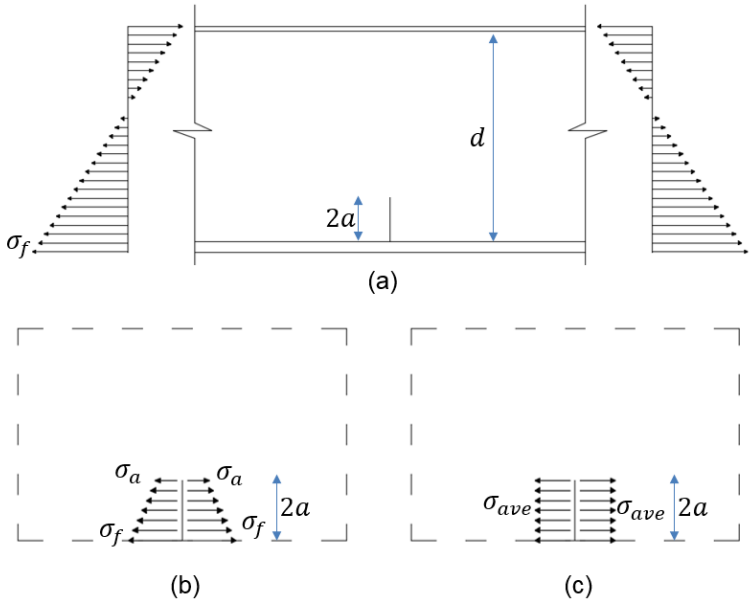

Figure 5. 3. Parameters of calculating the stress intensity factor of a center-cracked tension plate; SIF depends on far-field stress, length and geometry of the crack

According to Mendes [2], for cracks in large web plates, the distribution of tensile stresses around the crack can be approximated as a uniform tensile stress (σ_{ave}). In this work, the average tensile stress around the crack will be calculated according to equation (3):

$$\sigma_{ave} = \pm\sigma_f \left(\frac{2a}{d} - 1\right) \qquad (3)$$

Having the far field stresses around a crack, the stress intensity factor can be calculated using equation (1).

5.3.2 Stress Intensity Factor Calculation for Two Typical Steel Girders

To better understand the propagation of cracks a FEM simulation was used to predict the SIF for two typical steel girders. For a steel girder under bending moments, one of the main crack configurations is the vertical edge-crack extending normal to the tension flange through the web plate (Figure 5. 4b, c). In this work two steel plate girders from two typical medium-span bridges

were selected for SIF calculation. Girder A is typical for a 30-meter span composite bridge and Girder B is typical for a 23-meter span composite bridge. Both girders are simply supported and the thickness of the concrete slab is 200 mm for Girder A and 250 mm for girder B (Figure 4b, c). In both cases cracks are assumed to have initiated at small flaws in connections such as gusset plates positioned at 200 mm above the bottom flange.

Both bridges are assumed to be under service loads with a combination of live and dead load. In order to estimate the maximum stresses at mid-span under the service load, data from monitoring of two bridges of this type have been used. Girder A and B are from multi-girder bridges. Once a truck passes over the bridge, the stresses will be distributed over all girders based on the distribution factors. Results from monitoring of both bridges have been used to calculate the maximum stresses in both girders.

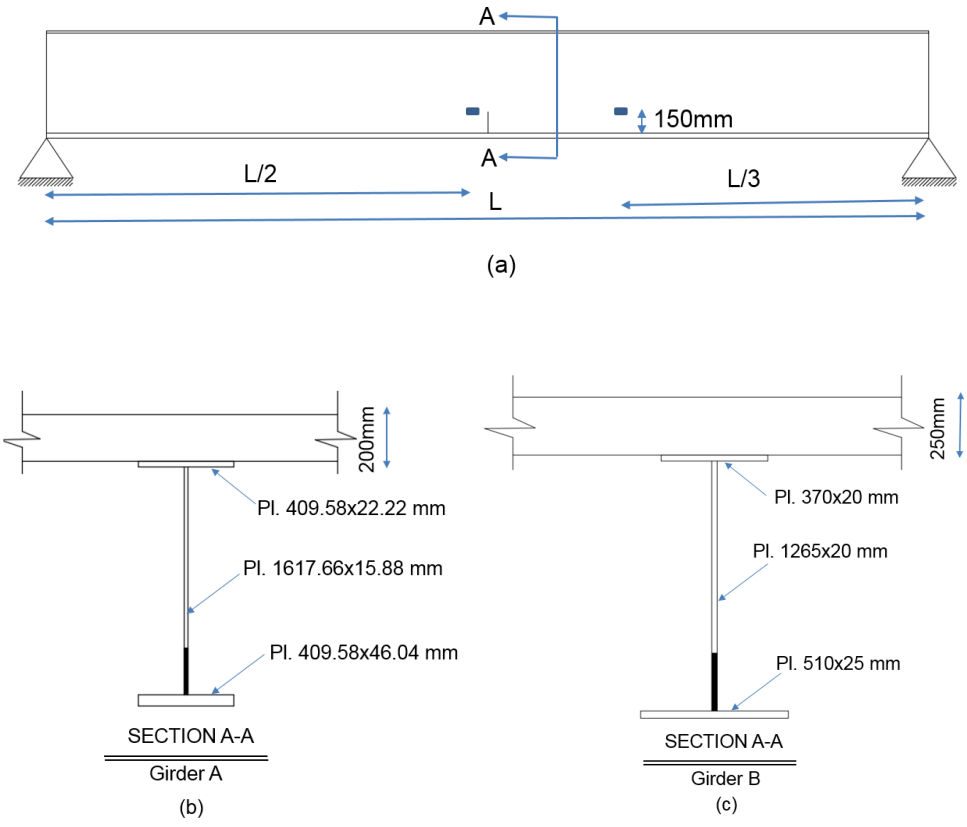

Figure 5. 4. a) Geometry and position of strain gauges on both girders A and B, b) Cross section of girder A, c) cross section of girder B

Girder A is the second girder of an eight-girder bridge. The strain gauges were mounted at one third of the span, 150 mm above the bottom flange. When a test truck weighing approximately the same as the CL-625 truck of the CHBDC passed the bridge over girder A, the strains were distributed over all 8 girder as shown in Figure 5a. The strain at girder A were measured to be 65με. Having the strain, the maximum stress and equivalent loading was calculated (equations 4 to 6).

$$\sigma = E\varepsilon \rightarrow \qquad 200 \times 10^3 \times 65 \times 10^{-6} = 13\ MPa \quad (4)$$

$$M = S\,\sigma \rightarrow \qquad 13 \times 45 \times 10^6 = 549 \times 10^6 N.mm \quad (5)$$

$$\omega = \frac{9M}{l^2} \text{ at L/3} \rightarrow \qquad 549 \times 10^6 \times \frac{9}{30000^2} = 5.49 N/mm \quad (6)$$

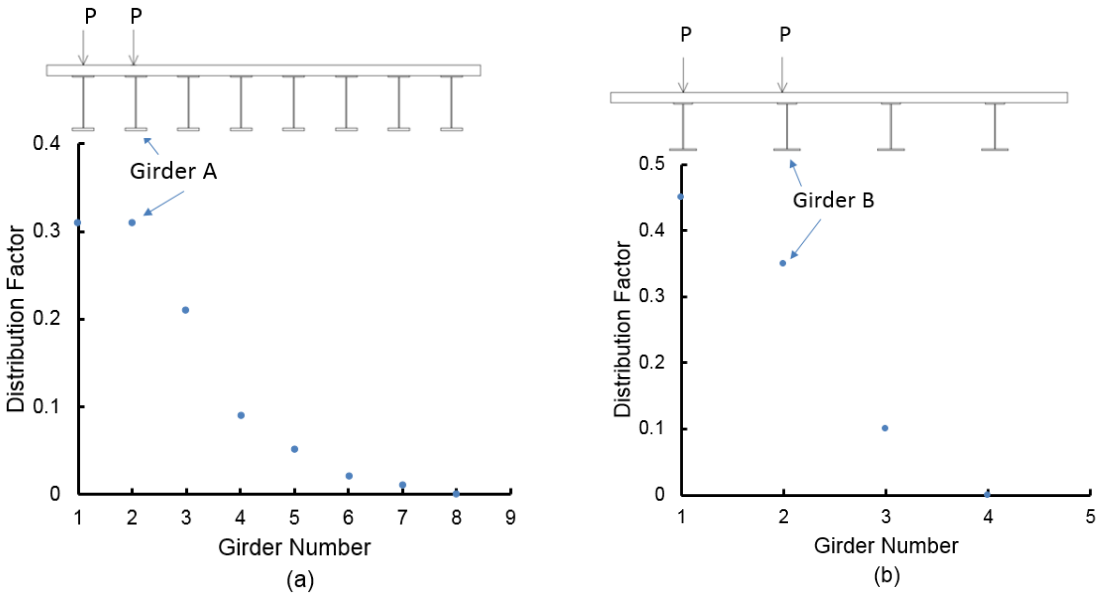

Figure 5. 5. Experimentally measured distribution factors for strains near the bottom flanges of girders due to passing truck over girders of a bridge. a) Truck passing over an 8-girder bridge,

approximately 35% of load is carried by girder A, b) By passing the same truck over a 4-girder bridge at the shown position, girder B carries approximately 38% of the total load.

The same calculations have been done for girder B to estimate the maximum stresses under the service load at mid-span. Girder B is the exterior girder of a four-girder bridge. The strain gauges were mounted at mid-span, 150 mm above the bottom flange. When a test truck (approximately equal to CL-625) passed the bridge over girder B, the strains were distributed over all 4 girders as shown in figure 5b. The strain at girder B were measured to be 65με. Having the strain, the maximum stress due to live loads and its equivalent loading was calculated (equations 7 to 9).

$$\sigma = E\varepsilon \rightarrow \qquad 200 \times 10^3 \times 65 \times 10^{-6} = 13\ MPa \quad (7)$$

$$M = S\,\sigma \rightarrow \qquad 13 \times 29 \times 10^6 = 377 \times 10^6 N.mm \quad (8)$$

$$\omega = \frac{8M}{l^2}\ @\ \mathrm{L}/2 \rightarrow \qquad 377 \times 10^6 \times \frac{8}{22700^2} = 5.85 N/mm \quad (9)$$

The distributed service live load given by equations (6) and (9), in combination with dead load is applied to girder A and B according to the Canadian Highway Bridge Design Code. The stress at mid-span at the extreme tensile fiber for both girders are calculated and used in stress intensity factor calculations (equations 1 to 3).

When a small crack forms at the mid-span at the welding joint of the gusset plate to the web of the girder (200 mm above the bottom flange), the crack will propagate through the web and will be arrested at bottom flange. Therefore, the initial length of the crack will be assumed to be 200 mm. In this work, the stress intensity factor for different length of cracks for both girder A and B has been calculated with the results shown in Table 5.1.

	Girder A							Girder B				
Crack Length (cm)	20	30	40	50	60	70	80	20	30	40	50	60
SIF ($MPa\sqrt{mm}$)	932	1061	1132	1162	1159	1128	1075	895	992	1040	1014	965

Table 5. 1. Stress Intensity Factor (SIF) for girders A and B for different length of the crack

It is assumed that the worst temperature these two bridges will experience during their service life will be between -25 ºC and -50ºC. According to previous studies the fracture toughness of the web of the steel girder at the intermediate loading rate for this temperature will be estimated to be 71 $MPa\sqrt{m}$ (2245 $MPa\sqrt{mm}$) which is within the variation range of the fracture toughness of A36 steel (250MPa) [75]. Comparing the calculated SIF to the critical one, cracks under same conditions as girders A and B with the initial length of 200 mm will not propagate spontaneously. The critical length of the crack before it propagates spontaneously can be calculated as follows:

$$K_I = K_{IC} \tag{10}$$

$$K_I = \sigma\sqrt{\pi a} \rightarrow a = \frac{{K_{IC}}^2}{\sigma^2\pi} \tag{11}$$

According to equation (11) the maximum crack length for girder A and B with SIF equal to 2245 $MPa\sqrt{mm}$ might be more than the depth of the girder. Having the critical length of the crack for both girders, the crack opening along the crack for each length of the crack will be estimated from the finite element simulation. The map showing crack opening versus crack length will be used to predict the critical location of the binary sensor. Therefore, the optimum placement of the binary

sensor on the web of the girder can be predicted. In following part, the finite element simulation of the cracked girder will be discussed.

5.4. FINITE ELEMENT SIMULATION

5.4.1 Introduction

The main purpose of the numerical study is to find the optimal position of the Binary sensor on the steel girder in such a way to detect smallest possible crack length, given a 0.2 mm crack opening detection limit. The Finite element simulation is used to predict the crack opening versus position for different lengths of crack on the steel girder. The results of the simulation can be used to predict the optimum placement of the sensor. The Finite Element Modelling was done using the program ABAQUS.

5.4.2 Simulation

In this work, the steel girder was simulated by using shell elements. Since the thickness of the elements are significantly smaller than the length, shell elements are used for this simulation. Two types of shell elements are available for simulation, conventional and continuum. For thin shell elements, conventional elements are preferred [71]. The FEM was created in the X-Y horizontal plane and was extruded in Z direction (Figure 4. 6a).

In order to simulate the I-shape steel plate girder, a 3-D extruded shell part was used in ABAQUS. Sketch of the web and two flanges was created in part section and then was extruded for 30 meters for girder A and for 22 meters for girder B. The steel was given a modulus of elasticity of 200GPa and the Poisson's ratio of 0.3. The girder was simulated in ABAQUS using the 3-D eight-node reduced integration deformable conventional shell elements (Figure 6b). The thickness of the conventional elements was specified through section properties [71]. For a homogenous section, five integration section points were defined through the thickness of the shell (Figure 6c).

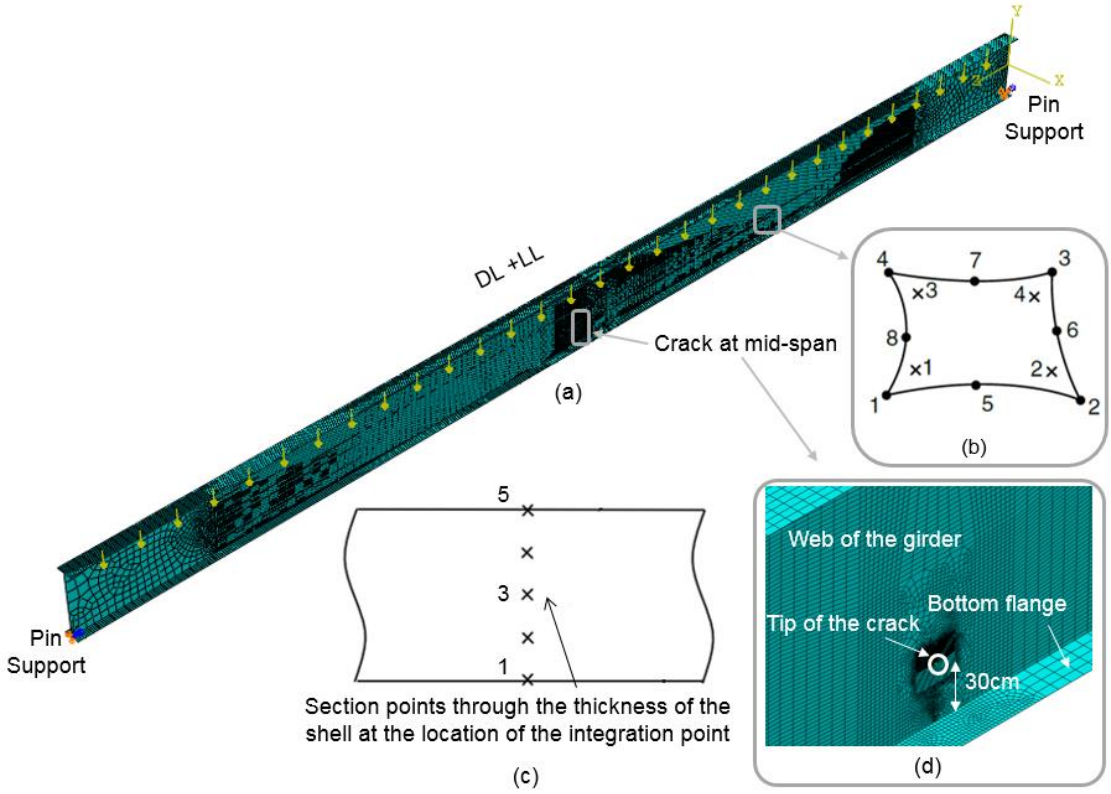

Figure 5. 6. a) Finite element model of the simply supported steel girder under service loads. b) Conventional shell elements, c) five integration section points through the thickness, d) 30cm crack on the web of the steel girder

The finite element simulation assumes a simply supported steel girder. The girder is under the service load which is modelled as a uniform distributed load as described above in the SIF calculation part. A fixed length crack was created at mid-span in the web of the girder. The crack was initiated at the connecting joint of web to bottom flange and propagated into the web. The crack is shown in Figure 6d. After running the simulation the crack opening was measured along the length of the crack. In addition, the stress intensity factor at the tip of the crack was also estimated. This process was carried out for cracks from 20 cm to half the girder depth in 10 cm steps. The 20 cm starting length was chosen to model a crack initiated at a gusset plate located approximately 20 cm above the bottom flange. Cracks have been observed to initiate at gusset

plates due to Constraint Induced Fracture (CIF) [12, 74]. The crack was assumed to propagate first to the bottom flange and then propagated up towards the upper flange. Hence the simulation starts at a 20 cm length and extends upwards towards the upper flange. The stress intensity factor was also calculated manually for each crack length [78].

5.5. RESULTS & DISCUSSION

The main purpose of the FEM in this work is to estimate the gap opening for different crack lengths and then use this information to find the optimum position for a binary sensor to be installed. The stress intensity factor (SIF) was also estimated from the finite element simulation and compared to manual calculations in order to estimate the maximum length of the stable crack.

5.5.1. Stress Intensity Factor Estimation

The stress intensity factor is a function of geometry of the crack and it varies with different lengths of the crack (equation (1)). For the purpose of this paper, different crack lengths for each girder were simulated in ABAQUS in 100 mm steps; 200 mm to 800 mm for girder A and 200 mm to 600 mm for girder B. Evaluating the SIF using the conventional shell methods in ABAQUS depends on the meshing dimensions. The finer the meshes, more accurate the results [70]. In this work, a 1.0 mm mesh was used in the neighborhood of the crack tip. Figure 5. 7(a) and 5. 7(b), plots the stress intensity factors measured and calculated from ABAQUS and manual calculations for both girders A and B versus the crack length. The dotted lines are ±10% bounds above and below the manual calculations.

The simulated and manual calculations are in agreement within this ±10% bound. For smaller lengths of crack, the SIF at the tip of the crack increases with an increase in the length of the crack. As the length of the crack increases and gets closer to the neutral axis of the girder, the average tensile stress remains steady which will cause a small drop in the value of the SIF.

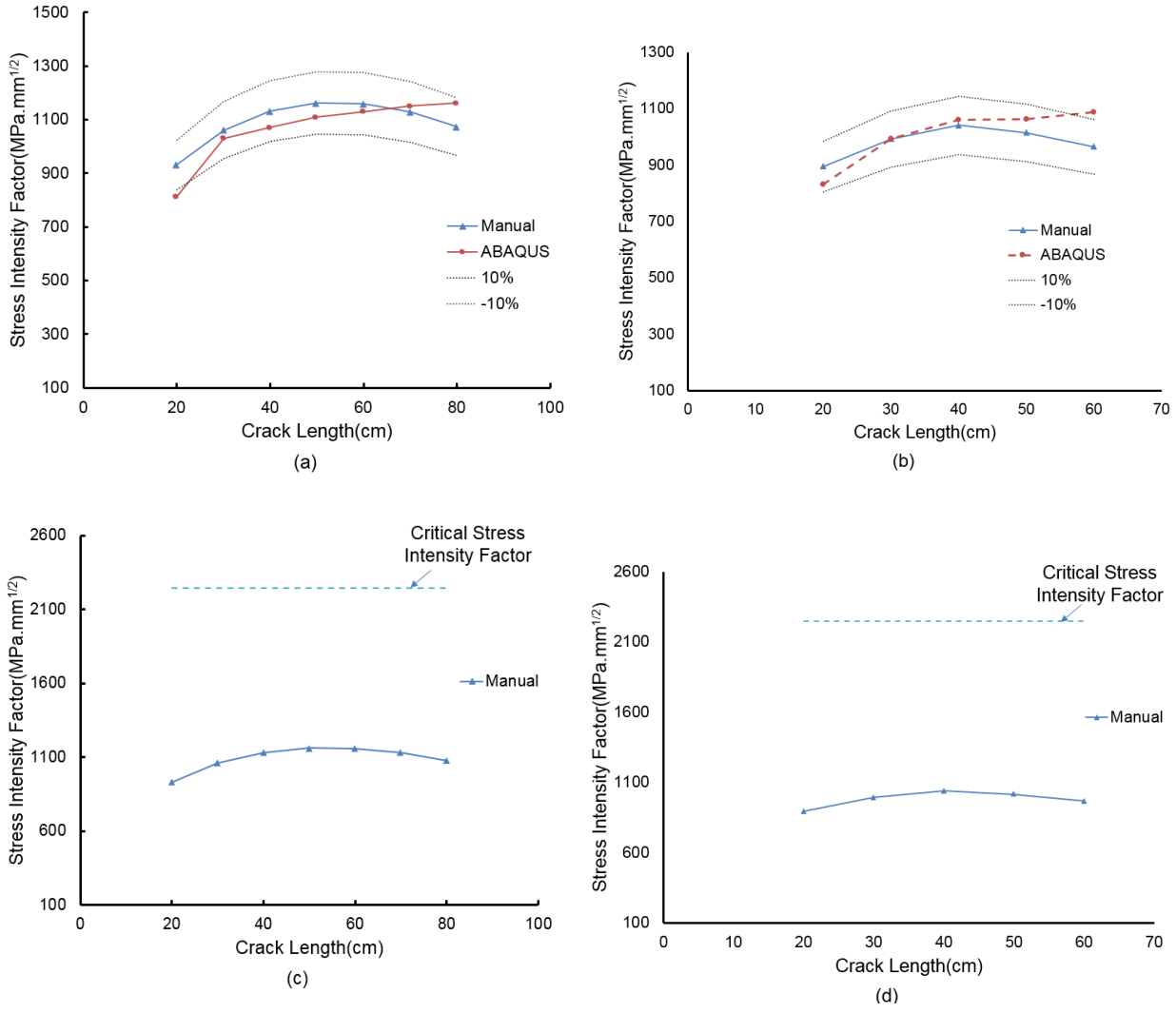

Figure 5. 7. Stress Intensity Factor calculation a) for girder A and b) for girder B. in both cases at smaller crack lengths the FEM results and the manual calculations are in good agreement c) comparing calculated SIF and the critical value for girder A, d) comparing calculated SIF and the critical value for girder B

ABAQUS results which are shown in the graph are in good agreement with manual calculations. The difference between two calculations might be due to the meshing density and dimensions. Figure 5. 7(c) and (d) shows the critical stress intensity factor limit for temperatures between -25 ºC and -50 ºC for girders A and B. The manually calculated values of SIF is shown on the same

graph to make a comparison to the critical limits. Figure 5. 7(c) and 7(d) shows that the critical SIF is much higher than the SIF at the tip of cracks in both girder A and B. Therefore, it is expected that there will be no fracture of the girder under the service load.

5.5.2. Optimum Position for Distributed Crack Sensors

One of the main outcomes of the FEM are estimates of crack opening along the crack. These plots can be used to estimate the optimum point at which to position a crack sensor to detect smallest detectable crack length. The optimum position of the sensor will depend on its characteristics. The binary sensor is capable of detecting cracks with opening of less than 0.2 mm, which is approximately equivalent to what distributed fiber optic sensors are capable of detecting [16]. Therefore, only at positions where the crack opening is wider than 0.2 mm will the binary sensor detect the crack. Different lengths of cracks were simulated in ABAQUS with the service load applied on the girder and the crack opening along the length of the crack was estimated. In Figure 5. 8 the results of finite element simulation are plotted. Different lengths of crack are shown for each girder (20 cm to 80 cm for girder A and 20 cm to 60 cm for girder B). For example, with an 800 mm long crack in girder A, the crack opening at the flange is 0 mm and reaches a maximum value of 0.36 mm at 400 mm above the flange and then reaches 0mm at the crack tip 800 mm above the flange. For the 800 mm long crack in girder A, the maximum crack opening is 0.36 mm. For the 800 mm crack in girder A the crack opening is greater than 0.2 mm from 80 mm above the flange to 690 mm above the flange. Extensive testing was done in the lab for the binary sensor on a small steel girder. Results of testing demonstrate that the binary sensor was able to detect crack openings of 0.13±0.01 mm or greater [17, 79]. In the laboratory the adhesive thickness and the position of the wire within the adhesive can be carefully controlled. However, when the sensor is installed in the field the thickness of adhesive applied and the position of the wire within the

adhesive layer will have greater variability. Using the FEM model the impact of variability in adhesive thickness and wire positioning can be predicted. Using expected variation in adhesive thickness and wire positioning the FEM predicts that the minimum crack opening that can be detected will be 0.2 mm. Therefore, in this work it is assumed that the minimum detectable crack opening for both the binary and fiber optic sensors is assumed to be 0.2 mm. A dashed line has been plotted at 0.2 mm crack opening in Figure 5. 8(a, b). Using the plots in Figure 5. 8a the optimal position for the binary sensor can be predicted. For girders with same specifications as girders A, at approximately 15 cm to 25 cm above the bottom flange the sensor will detect the crack as soon as it reaches a length of 35-40 cm. In addition at 15 cm to 25 cm above the bottom flange, as the crack length grows the crack opening also widens. Whereas by positioning the sensor at 5.0 cm above the bottom flange, the crack would reach 80 cm long before the crack opening reaches the 0.2 mm threshold. Using the crack opening map for girder B, the optimum position for installing the binary sensor is 15 cm to 22 cm above the bottom flange. If the sensor is installed at these positions, when a minimum 35-40cm long crack forms on the web of the girder, the sensor threshold of 0.2 mm opening will be exceeded. In summary, the FEM model predicts the optimum position to install the binary crack sensor is along a line 15 to 25 cm above the flange for girder A and 15 to 22 cm above the flange for girder B.

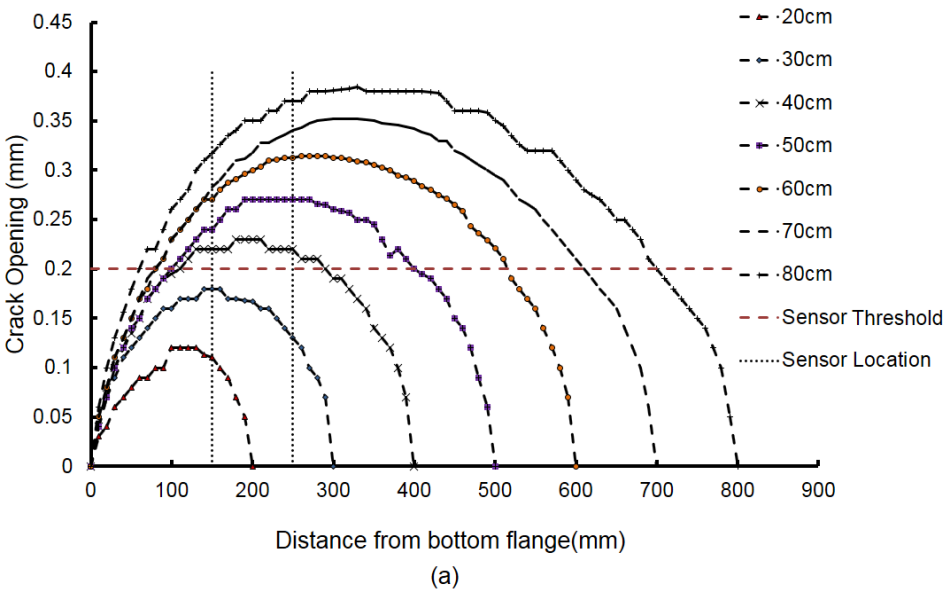

(a)

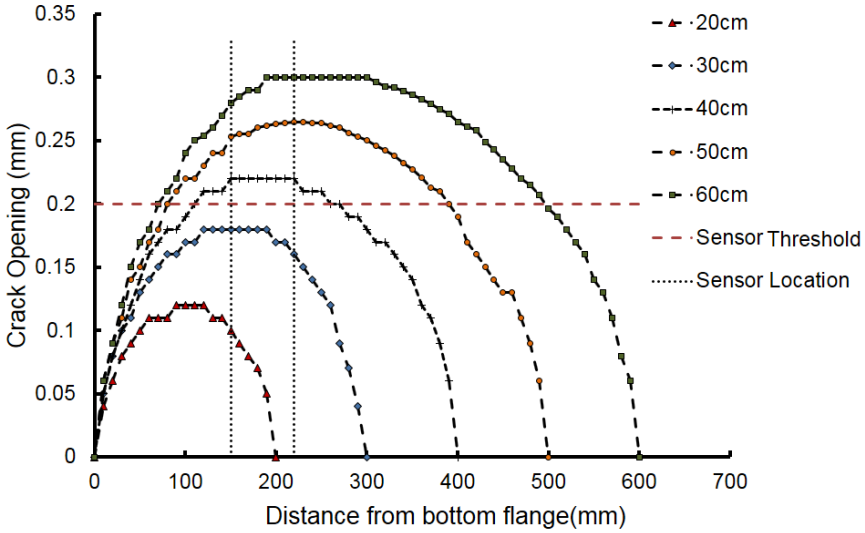

(b)

Figure 5. 8. a) Crack opening vs distance from bottom flange (Girder A) for cracks with different lengths varying from 20 cm to 80 cm. By positioning the binary sensor at 15cm to 25cm above the bottom flange, any crack longer than 40cm can be detected. b) Crack opening vs distance from bottom flange (Girder B) for cracks with different lengths varying from 20 cm to 60 cm. By positioning the binary sensor at 15cm to 22 cm above the bottom flange, any crack longer than 40cm can be detected.

5.5.3. Feasibility Study of Using an Array of Strain Gauges for Crack Detection

Strain gauges are one of the most widely used methods of monitoring the performance of steel girder bridges. When cracks form in steel girders the strain within the girder will be perturbed. The perturbation in the strain field can be used to detect the presence of the crack. For example, for a crack perpendicular to the flange the longitudinal strain near the crack will be reduced. Therefore, a shift in the measured strain can be used to indicate the presence of a crack. The temperature variation of the strain gauge as well as the mounting variations need to be accounted for in any detection scheme. This method has the advantage of simple interpretation of measurements to detect the presence of a crack. However, this method requires a large number of sensors which imposes complex wiring and a large number of data acquisition channels, which makes it unpractical to be used for most bridges [15, 29, 44, 45].

In this work a FEM simulation has been used to determine the minimum number of strain gauges required to detect cracks on girder A and B. In order to measure the shift in the strains in the vicinity of the crack, a finite element model of girders under the service live load was simulated by program ABAQUS. Strain diagrams of the girder with different possible length of cracks were plotted. Figure 5. 9 shows the measured strain at 25cm above the bottom flange (which is the optimum position to install the binary sensor). For an un-cracked girder, the measured strain at mid-span at 25 cm above the bottom flange is approximately 58με. As soon as a crack forms in the girder, there will be a sudden drop in the measured strain in close proximity of the crack.

Assuming that the strain gauge array is capable of detecting a 10με shift in the measured strains, the maximum distance that strain gauges should be installed to detect cracks are shown in Table 5. 2. For example, in order to detect cracks with minimum length of 40cm (which is what binary

crack sensor can detect at 25cm above the flange), the maximum distance between strain gauges should be 101cm. Therefore, approximately 30 strain gauges for girder A are required.

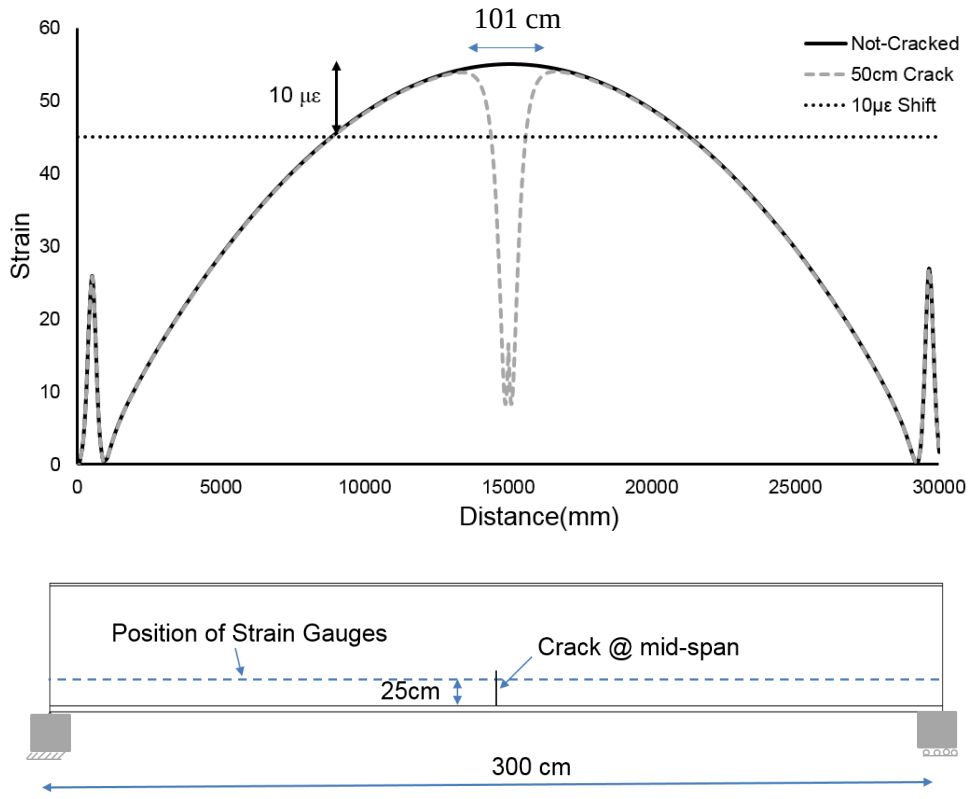

Figure 5. 9. Measured strain at 250 mm above the bottom flange for girders A. The measured strain at mid-span under live load is approximately 58με. As soon as a crack forms in the girder, there will be sudden drop in the measured strain. In order to detect the 10με shift in the strain, strain gauges should be placed at maximum 101 cm from each other to detect cracks longer than 40 cm. Therefore, approximately 30 strain gauges for girder A are required.

Table 5. 3 shows the maximum required distance between strain gauges for girder B. In order to detect cracks longer than 40cm, the maximum distance between strain gauges should be 96cm. Therefore, approximately 24 strain gauges are required.

Crack Length (cm)	Position of Strain Gauges From Bottom Flange (cm)														
	10	15	20	25	30	35	40	45	50	55	60	65	70	75	80
20	52	53	12	21	-	-	-	-	-	-	-	-	-	-	-
30	73	79	81	71	18	29	13	-	-	-	-	-	-	-	-
40	86	**94**	**101**	**101**	83	72	25	37	42	42	-	-	-	-	-
50	94	109	117	125	125	117	109	89	31	43	50	52	34	-	-
60	94	117	125	133	144	145	142	135	119	15	37	50	56	62	63
70	94	117	141	141	156	156	156	156	156	140	40	12	42	56	65
80	94	117	141	141	156	156	180	172	172	172	165	148	36	10	48

Table 5. 2. Numbers in the table are the maximum distance (cm) between strain gauges to detect a 10με shift (due to the presence of crack) in the measured strains. (Girder A)

Crack Length (cm)	Position of Strain Gauges From Bottom Flange (cm)										
	10	15	20	25	30	35	40	45	50	55	60
20	54	53	17	22	-	-	-	-	-	-	-
30	75	81	81	77	18	30	37	36	-	-	-
40	83	**96**	**99**	**99**	91	71	31	40	45	45	-
50	89	109	118	122	124	118	108	87	27	44	52
60	92	110	107	132	134	137	134	126	103	10	41

Table 5. 3. Numbers in the table are the maximum distance (cm) between strain gauges to detect a 10με shift (due to the presence of crack) in the measured strains. (Girder B)

5.5.4. Optimum Position for Placing Fibre Optic Sensors on Girder A, B

Distributed fiber optic sensors based on Brillouin scattering is one way of crack detection [16, 46, 47]. In this method the fiber optic sensor will be installed at specified positions on the girder and

is sensitive at every point along its length. Using the Brillouin based fiber optic sensor, 0.2 mm crack openings can be detected [16]. According to Figure 8, to detect cracks with at least 0.2 mm opening, the distributed sensor should be installed at the same position as binary crack sensor (between 15 cm and 25 cm above the tension flange for girder A and 15 cm to 22 cm above the tension flange for girder B). Therefore the FOS is capable of detecting cracks longer than 40cm at a medium-span simply supported steel girder. A brief comparison between the three types of crack monitoring is shown in Table 5. 4.

Type of crack monitoring	Comments
Distributed strain gauges	A large number of strain gauges are required to detect a 10με shift in the readings. Which will result in complicated wiring system and high cost of installation and interpretation
Fiber optic sensors	Capable of detecting 0.2 mm opening cracks in steel girder of bridges, however high cost of installation and data acquisition systems makes the cost excessive for the majority of bridges
Binary crack sensor	Capable of detecting 0.2 mm opening cracks in steel girder of bridges. It can be installed easily at a fraction of the cost. The binary crack sensor is being field tested on large-scale bridge in Canada and the installation procedure is under consideration for optimization

Table 5. 4. Comparison between three types of crack monitoring using distributed strain gauges, fiber optic sensor and binary crack sensor

5.6. INSTALLATION ON LARGE-SCALE GIRDER OF A BRIDGE

The Binary sensor was installed on a steel girder of a bridge in Canada in August 2017. The main purpose of installing the binary sensor was to evaluate its application under real loading and weather conditions. This includes investigation of the bond between the steel girder and the sensor under cyclic loading, studying the effect of temperature and weather condition on the sensor, optimizing the installation procedure according to real situation on the bridge and testing to see if the sensor can detect cracks if any available. The binary sensor was installed on a 30 meter length of a girder at 150 mm to 200 mm above the bottom flange. The sensor was installed in seven segments with approximately 4 and 5 meter lengths (Figure 5. 10). Each segment has one contiguous sensor terminated to a unique channel on the data acquisition unit. Any crack with opening of at least 0.2 mm can be detected at each segment.

Figure 5. 10. Installation of binary crack sensor on a 30-meter span steel girder of a bridge in 7 segments.

In order to install and place the binary sensor on the steel girder, a frame work (groove) was formed using foam tape. The depth of the groove was 2.0 mm and the width was approximately 250 mm. Then, the wire was mounted on the girder. To hold the wire at its position on the girder, an adhesive

was used at few points (Figure 5. 11a). The ends of wire were connected to a terminal block (Figure 5. 11b). Afterwards, the epoxy was applied on the wire into the groove using an applicator and its surface got leveled using a knife (Figure 5. 11c,d). The required time for the epoxy to cure is 24 hour. After the epoxy was cured, the frame work was removed and the surface of the binary sensor was covered with the use of foil (Figure 5. 11e). The sensor was installed in August 2017 and the Data logger was programmed to synchronize two readings per day on the analytics server based in Structural Monitoring Technology (SMT) office in Vancouver. Readings are available since then and as soon as a crack opens up to approximately 0.2 mm, the change in the continuity of the wire will be monitored.

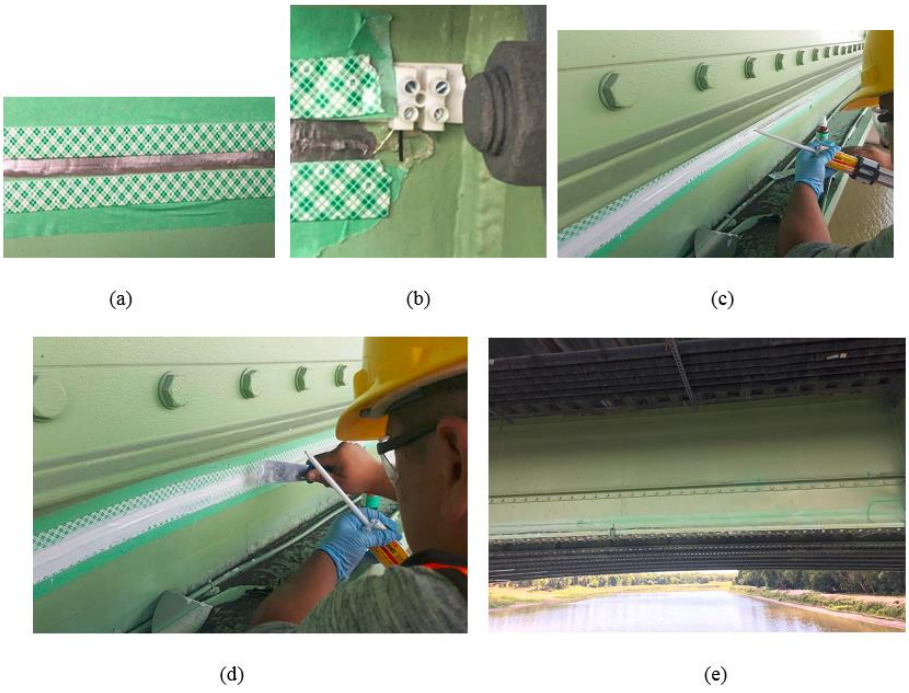

Figure 5. 11. Installation procedure of the binary sensor on girder A.

5.7. CONCLUSION

On steel girder of bridges, cracks may form as a result of cyclic traffic load, deficiency in material or welding or fabrication errors. To detect cracks, a binary crack sensor was developed and

introduced earlier. In this work, the optimal position for installing a binary sensor on typical medium-span simply supported steel girder of two bridges was studied (Girder A; 30m span, 1.7m depth and girder B; 22.7m span and 1.2m depth). The binary sensor is capable of detecting 0.2 mm opening cracks. It is important to install the sensor in a position which detects cracks before they reach an unstable length and fracture. The critical length of the crack was calculated by estimating the stress intensity factor at the tip of the crack. FEM of the steel girders were simulated by program ABAQUS to estimate the crack opening along the crack and finally finding the optimum position for installing a binary sensor. Results from analysis show that in order to detect 0.2 mm width cracks on girders A and B, binary sensor should be installed between 15 cm to 25 cm above flange for girder A and in girder B, it should be installed at 15 cm to 22 cm above the tension flange. Using FEM, the optimum position for discrete strain gauge and fiber optic sensor detection cracks were also considered. Calculations show that in order to detect cracks at the same position as a binary sensor, numerous units of strain gauges are required which will lead to a complicated wiring system. On the other hand, since the Brillouin-based FOS is capable of detecting cracks with 0.2 mm opening, the sensors should be installed at exact positions as a binary sensor. However, high installation cost and monitoring system cost makes the use of FOS impractical for most of the old bridges.

Acknowledgments

The authors wish to express their gratitude and appreciation for the supports received from the following organizations: Natural Science and Engineering Research Council of Canada, Canada Foundation for Innovation, Research Manitoba, Canadian Microelectronic Corporation, Structural Monitoring Technologies

CHAPTER 6: CONCLUSION & FUTURE WORKS

In this project, an innovative distributed binary crack sensor has been developed. The binary crack sensor is composed of thin wire (gauge 39- Diameter = 0.09 mm) which adheres to the steel girders using a carefully selected adhesive. The sensor has the capability to detect 0.2 mm crack openings on the web of steel girders of bridges.

In chapter 3 of this work, the required experimental work for developing the sensor has been explained. In order to select proper material for the binary crack sensor, an experimental apparatus has been designed to simulate the crack opening on the web of steel girders. Different combination of materials has been tested on the experimental apparatus and the best combinations were tested on small scale steel girder in the lab. Results of experiments using copper wire (MW 79C) in combination with Loctite Epoxy E-20NS were consistent and in the desirable range. The binary crack sensor then has been tested in an environmental chamber - at two extreme temperature of (-30ºC) and (+40ºC) - to study the effect of temperature in crack width detection as well as the bonding between materials. Results of this part of the project proved that changes in temperature has minimum effect on the performance of the binary crack sensor.

Chapter 4 of this work discusses the effect of changes in different parameters such as final tensile strain of wire, bonding properties between wire and adhesive and position of wire in the epoxy on the performance of the binary crack sensor. Results of experiments show that by pre-straining the wire, the detected crack opening will decrease. Results were verified using the simulation. In this chapter, a Finite Element Model of the binary crack sensor and the experimental apparatus has been simulated in a finite element software- ABAQUS-. In order to complete the simulation, the mechanical properties of material were required. Experiments were carried out to estimate the tensile properties of the wire, tensile properties of the epoxy and bonding properties between the wire and the epoxy. As a result of simulation, the interfacial bonding stiffness between epoxy and wire is suggested to be 240 MPa/mm^2 /mm. using this stiffness, in order to detect crack openings less than 0.2 mm, the maximum thickness of epoxy is suggested to be 2.0 mm.

The next step in developing the distributed binary crack sensor is to find the optimum position of the sensor on steel girders of bridges. Chapter 5 of this work discusses the optimal placement of the binary sensor on two typical I-shaped steel girders of two medium span bridges. In this chapter, the maximum stable length of the crack on assumed girders has been estimated by estimating the stress intensity factor (SIF) at the tip of the crack. The girders were simulated in ABAQUS and were analysed under service loads. Calculations for simply supported girders of two typical medium span bridges show that a 0.2 mm detected crack opening is sufficient enough to prevent fracture and continuous propagation of the crack into the web of these girders. The crack opening along crack length for different lengths of the crack were estimated and a map of crack length versus crack opening for two typical girders were plotted. Using this map, the optimum placement of the binary crack sensor to detect cracks as soon as possible was suggested.

The sensor is now being field tested on a steel girder of a bridge in Canada for more than a year. The optimization of the installation procedure, behavior of the sensor under cyclic loading, application of the binary crack sensor on other materials and on other applications will be studied in future works.

REFERENCES

1. Barker RM, Puckett JA (2013) *Design of Highway Bridges* (WILEY). 3rd Ed.
2. Mendes S (2014) Elastic Bending Moment and Shear Force Limit States of Steel Bridge Plate Girders Considering Fatigue Crack Growth. Dissertation (University of Rhod Island).
3. Chase SB, Washer G (1997) Nondestructive Evaluation for Bridge Management in The Next Century. *Public Roads* 61(1):16–26.
4. ASCE (2017) *Infrastructure Report Card, A Comprehensive Assessment of America's Infrastructure* (American Society of Civil Engineers, Washington,D.C.).
5. Bisby LA (2004) *ISIS Canada Educational Module5: An Introduction To Structural Health Monitoring*.
6. Ghorbanpoor A, Benish N (2003) *Wisconsin Highway Research Program: Non-Destructive Testing of Wisconsin Highway Bridges* (Wisconsin DOT, Milwaukee).
7. Lamtenzan D, Washer G, Lozev M (2000) *Detection and Sizing of Cracks in Structural Steel Using the Eddy Current Method* (Federal Highway Administration, McLean).
8. Agdas D, Ice JA, Martinez JR, Lasa IR (2015) Comparison of Visual Inspection and Structural-Health Monitoring As Bridge Condition Assessment Methods. *J Perform Constr Facil*:1–10.
9. McKeefry J, Shield C (1999) *Acoustic Emission Monitoring of Fatigue Cracks in Steel Bridge Girders* (Minnesota).
10. Chang PC, Liu SC (2003) Recent Research in Nondestructive Evaluation of Civil Infrastructures. *Mater Civ Eng* 15(June):298–304.
11. Chajes M, Mertz D, Quiel S (2005) Steel Girder Fracture On Delaware's I-95 Bridge Over

The Brandywine River. *Proceedings of the 2005 ASCE Structures Congress* (ASCE, New York).

12. Ellis R, Conner R (2013) Investigation and Repair of the Diefenbaker Bridge Fracture. *Transportation Assosiation of Canada* (Winnipeg).
13. Chang PC, Flatau A, Liu SC (2003) Review Paper : Health Monitoring of Civil Infrastructure. *Struct Heal Monit* 2(3):257–267.
14. Collins J, Mullins G, Lewis C, Winters D (2014) *State of the Practice and Art for Structural Health Monitoring of Bridge Substructures* (FHWA, McLean).
15. Glisic B, Inaudi D (2011) Development of Method For In-Service Crack Detection Based on Distributed Fiber Optic Sensors. *Struct Heal Monit*. doi:10.1177/1475921711414233.
16. Mufti A, Thomson D, Inaudi D, Vogel HM, McMahon D (2011) Crack Detection of Steel Girders Using Brillouin Optical Time Domain Analysis. *J Civ Struct Heal Monit* 1(3–4):61–68.
17. Raeisi F, Mufti A, Mustapha G, Thomson DJ (2017) Crack Detection in Steel Girders of Bridges Using a Broken Wire Electronic Binary Crack. *J Civ Struct Heal Monit* 7:0–23.
18. Sigurdardottir DH, Glisic B (2015) The Neutral Axis Location For Structural Health Monitoring : An Overview. *J Civ Struct Heal Monit* 5(5):703–713.
19. Ni YQ, Xia HW, Ye XW (2012) Neutral-Axis Position Based Damage Detection of Bridge Deck Using Strain Measurement : Numerical and Experimental Verifications. *6th European Workshop on Structural Health Monitoring* (Dresden,Germany).
20. Carden EP, Fanning P (2004) Vibration Based Condition Monitoring : A Review. *Struct Heal Monit* 3(4):355–377.
21. R.Farrar C, Darling TW, Migliori A, Baker WE (1999) Microwave Interferometers For

Non-Contact Vibration Measurments On Large Structures. *Mech Syst Signal Process* 13:241–253.

22. Zhang B, Wang S, Li X, Zhang X, Yang G (2014) Crack Width Monitoring of Concrete Structures Based On Smart Film. *Smart Mater Struct* 23. doi:10.1088/0964-1726/23/4/045031.

23. Zhou Z, Zhang B, Xia K, Li X (2015) Smart Film For Crack Monitoring of Concrete Bridges. *Struct Heal Monit* 10:275–289.

24. Raeisi F, Mufti A, Mustapha G, Thomson DJ, Eden R (2017) Investigation of the Influence of Breaking Strain and Temperature on a Binary Crack Sensor. *8th International Confernece on Structural Health Monitoring of Intelligent Infrastructures* (Brisbane,Australia).

25. Seo J, et al. (2013) Summary Review of Structural Health Monitoring Applications for Highway Bridges. 1–9.

26. FHWA (2018) National bridge inventory (NBI). *Fed Highw Adm*. Available at: https://www.fhwa.dot.gov/bridge/nbi.

27. Fisher JW (1989) *Executive Summary Fatigue Cracking in Steel Bridge Structures*.

28. Fisher JW, Sullivan MD, Pense AW (1974) *Improving Fatigue Strength and Repairing Fatigue Damage*.

29. Yao Y, Tung SE, Glisic B (2014) Crack Detection and Characterization Techniques — An overview. (March):1387–1413.

30. Wipf TJ, Phares B, Doornink JD, Greimann L, Wood DL (2007) Evaluation of Steel Bridges , Volumes I & II.

31. Ryan T, Hartle R, Mann J, Danovich L (2006) Bridge Inspector's Reference Manual. *Rep*

No FHWA NHI 1.

32. Graybeal BA, Phares BM, Rolander DD, Moore M, Washer G (2003) Visual Inspection of Highway Bridges. 21(3).

33. Luther LW, Sundlof SF (2004) National Bridge Inspection Standards Regulations (NBIS). *Fed Regist* 69(239):15–35.

34. Rens K, Wipf T, Klaiber F (1997) Review of Nondestructive Evaluation Techniques of Civil Infrastructure. *J Perform …* (November):152–160.

35. Lee S, Kalos N, Shin DH (2014) Non-Destructive Testing Methods in the U . S . for Bridge Inspection and Maintenance. 18:1322–1331.

36. Bader J (2008) Nondestructive Testing and Evaluation of Steel Bridges. 1–10.

37. Hellier C (2003) *Handbook of Non-Destructive Evaluation* (McGraw-Hill) doi:10.1036/007139947X.

38. Hopwood T, Goff C, Fairchild J, Palle S (2016) *Nondestructive Evaluation of Steel Bridges : Methods and Applications* (Kentucky Transportation Center) doi:https://doi.org/10.13023/KTC.RR.2016.26.

39. Grosse C, Ohtsu M (2008) *Acoustic Emission Testing* (McGraw-Hill).

40. Integrity Diagnostic Introduction to Acoustic Emission. Available at: http://www.idinspections.com/?page_id=126 [Accessed January 1, 2014].

41. Das S, Sasha P, Patro SK (2016) Vibration-Based Damage Detection Techniques Used For Health Monitoring of Structures : A Review. *J Civ Struct Heal Monit*. doi:10.1007/s13349-016-0168-5.

42. Schallhorn C, Rahmatalla S (2015) Crack Detection and Health Monitoring of Highway Steel-Girder Bridges. *Struct Heal Monit* 14:281–299.

43. Farrar CR, et al. (1994) *Dynamic Characterization and Damage Detection in the I-40 Bridge Over the Rio Grande*.

44. Cardini AJ, Dewolf JT (2009) Long-term Structural Health Monitoring of a Multi-girder Steel Composite Bridge Using Strain Data. *Struct Heal Monit* 8(1).

45. Yao Y, Glisic B (2015) Detection of Steel Fatigue Cracks with Strain Sensing Sheets Based on Large Area Electronics. *sensors*:8088–8108.

46. Glisic B (2013) Distributed Fiber Optic Sensing Technologies and Applications – An Overview. *ACI Spec Publ*.

47. Gliši B, Posenato D, Inaudi D (2007) Integrity Monitoring of Old Steel Bridge Using Fiber Optic Distributed Sensors Based on Brillouin Scattering. *Proceedings from the International Society for Optical Engineering Conference* (Vancouver).

48. FHWA (2012) *Feasibility of Nondestructive Crack Detection and Monitoring for Steel Bridges* (FHWA, McLean).

49. Zhang B, et al. (2013) Online Bridge Crack Monitoring with Smart Film. doi:10.1155/2013/303656.

50. VISHAY PRESICION GROUP (2014) Crack Propagation Patterns Special Use Sensors - Crack Propagation Sensors. doi:11521.

51. Plude S (2011) Implementing a Long-Term Bridge Monitoring Strategy for a Composite Steel Girder Bridge. Dissertation (University of Connecticut).

52. Sohn H (2007) Effects of Environmental and Operational Variability on Structural Health Monitoring. *Philos Trans R Soc* (December 2006):539–560.

53. Cruz PJS, Salgado R (2008) Performance of Vibration-Based Damage Detection Methods in Bridges. *Comput Civ Infrastruct Eng* 24:62–79.

54. Mufti A (2001) *Guidelines for Structural Health Monitoring* (ISIS Canada Corporation, Winnipeg).

55. Nishikawa M, Okabe T, Hemmi K, Takeda N (2008) Micromechanical Modeling of The Microbond Test to Quantify The Interfacial Properties of Fiber-Reinforced Composites. *Int J Solids Struct* 45(14–15):4098–4113.

56. Sockalingam S, Nilakantan G (2012) Fiber-Matrix Interface Characterization Through The Microbond Test. *Int J Aeronaut Sp Sci* 13(3):282–295.

57. F.Raeisi, A.Mufti, D.J.Thomson, G.Mustapha (2015) Testing a Binary Crack Sensor Using a Laboratory Model of Cracks in Steel Girders. *The 5th International Conference on Smart Materials and Nanotechnology in Engineering*.

58. F.Raeisi, A.Mufti, B.Saboktakin, D.J.Thomson, G.Mustapha (2015) Crack Detection in Steel Girders of Bridges Using a Binary Sensor. *7th International Conference on Structural Health Monitoring of Intelligent Infrastructure*.

59. Enckell M (2011) Lessons Learned in Structural Health Monitoring of Bridges Using Advanced Sensor Technology. Dissertation (KTH).

60. ASTM Standard C1557 - 14 Standard Test Method for Tensile Strength and Young ' s Modulus of Fibers (2016) (ASTM) doi:10.1520/C1557-14.2.

61. ASTM Standard D638-10 StandardTest Method for Tensile Properties of Plastics (2010) (ASTM) doi:10.1520/D0638-10.

62. Reed RP, Mikesell RP (1967) Low Temperature Mechanical Properties of Copper and Selected Copper Alloys.

63. Technical Data Sheet-Loctite EA E-20NS (2013).

64. H.J.Qi, K.Joyce, M.C.Boyce (2003) Durometer Hardness and The Stress-Strain Behavior

of Elastomeric Materials. *Rubber Chem Technol* 76(2):419–435.

65. DiFrancia C, Ward TC, Claus RO (1996) The Single-Fibre Pull-Out Test. 1: Review and Interpretation. *Compos Part A Appl Sci Manuf* 27(8 PART A):597–612.
66. Singiresu S.Rao (2011) *The Finite Element Method in Engineering* (Elsevier, Florida). fifth.
67. ABAQUS (2014) Getting Started with Abaqus : Interactive Edition.
68. Camanho P, Dvila CG (2002) *Mixed-Mode Decohesion Finite Elements in for the Simulation Composite of Delamination Materials* (NASA).
69. ABAQUS (2014) Abaqus Analysis User Guide. V.
70. User AA (2014) Abaqus 6.14 Analysis User's Guide Volume II:Analysis (Dassault Systèmes Simulia Corp., Providence, RI, USA.).
71. ABAQUS (2014) Abaqus 6.14 Analysis User's Guide Volume IV:Elements (Dassault Systèmes Simulia Corp., Providence, RI, USA.).
72. Khalighi Y (2009) A Study Of Bond Between Fibre Reinforced Polymer And Concrete Under Quasi-Static and Impact Loading. Dissertation (University of British Columbia).
73. Dexter RJ, W.Fisher J (2000) Fatigue and Fracture.
74. Connor RJ, et al. (2007) Prevention and Mitigation Strategies to Address Recent Brittle Fractures in Steel Bridges. *J Bridg Eng* 12(April):164–173.
75. Zhou YE, Biegalski AE (2010) Investigation of Large Web Fractures of Welded Steel Plate Girder Bridge. *J Bridg Eng* 15(4):373–383.
76. Raeisi F, Mufti A, Thomson D, Mustapha G (2018) Binary Crack Sensor for Steel Girder Bridges: Installation Procedure in Field. *10th International Conference on Short and Medium Span Bridges* (CSCE, Quebec City).

77. Rolfe S, Barsom J (1977) *Fracture and Fatigue Control in Structures: Applications of Fracture Mechanics*.

78. Sun C-T, Jin Z (2011) *Fracture Mechanics* (Elsevier).

79. Raeisi F, Mufti A, Thomson D, Mustapha G (2015) Crack Detection in Steel Girders Using a Binary Sensor. *7th International Conference on Structural Health Monitoring of Intelligent Infrastructure*.

Appendix A: Sensing Circuit

Excerpted from supplementary material of "A Finite Element Model and Experimental Investigation of the Influence of Pre-Straining of Wire on the Sensitivity of Binary Crack Sensors", Journal of Civil Structural Health Monitoring, June 2018

The sensing circuit is shown in Figure A.1. Ends of wire are connected to a DAQ in series with a resistor to make a voltage divider sensing circuit. As it is shown in the Figure A. 1 and equations below, when the wire is not broken the voltage of the ends of the wire is expected to be near 0.4mV.

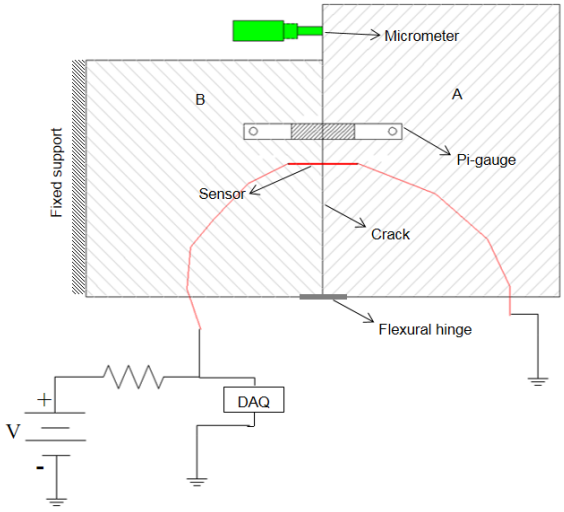

Figure A. 1. Sensing circuit of the binary crack sensor

$$V = RI \quad (1)$$

The input voltage is equal to 5V, the resistance of the wire for 10m length at 0.08Ω/m is 0.8Ω which is in series with a 10KΩ resistor. In the series circuit the voltage electrical current is equal in both resistors and the voltage is divided between the two resistors. By measuring the voltage across the wire it can be determined if the wire is broken or not. Equation (2) shows the voltage across the wire before the break:

$$V_w = R_w \times 5.0 = \frac{0.8}{0.8 + 10^4} \times 5.0 = 0.4mV \quad (2)$$

After the wire breaks, the resistance of the broken wire will be more than 1MΩ. Therefore the voltage across the wire will increase to:

$$V_w = R_w \times 5.0 = \frac{10^6}{10^6 + 10^4} \times 5.0 = 4.95\,V \quad (3)$$

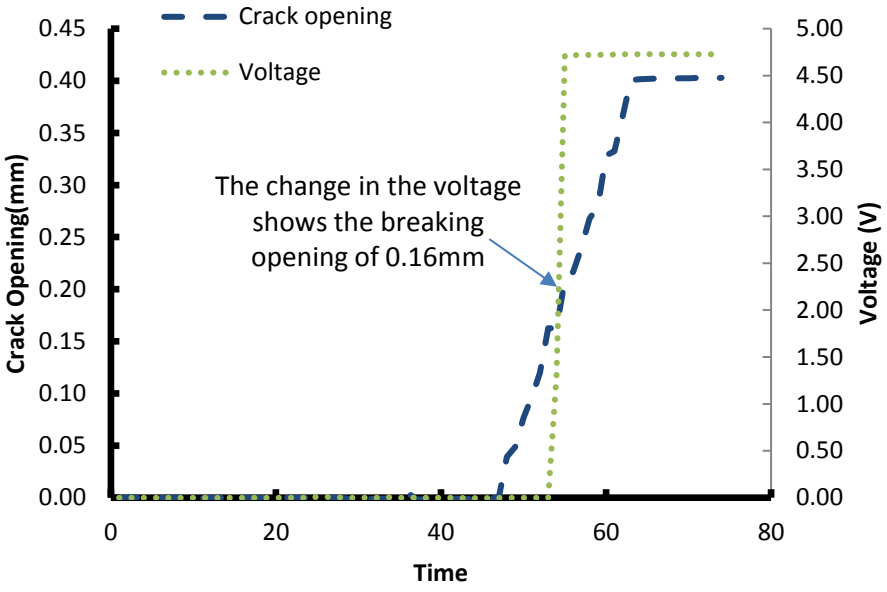

Figure A. 2. Typical output of the binary crack sensor

Appendix B: Experimental Results Using Loctite Quicktite & M-Bond Adhesives

In this work, few adhesives from two categories of cyanoacrylate and epoxy have been tested. The first adhesive tested was Loctite QuickTite which is a gel adhesive and sets in 2 minutes. The crack width at which the binary sensor could detect was about 0.15 mm which is less than the desired crack width; but after curing there were few cracks forming on the surface of the adhesive (Figure B. 1) which made the results unpredictable and therefore not considered any further [58].

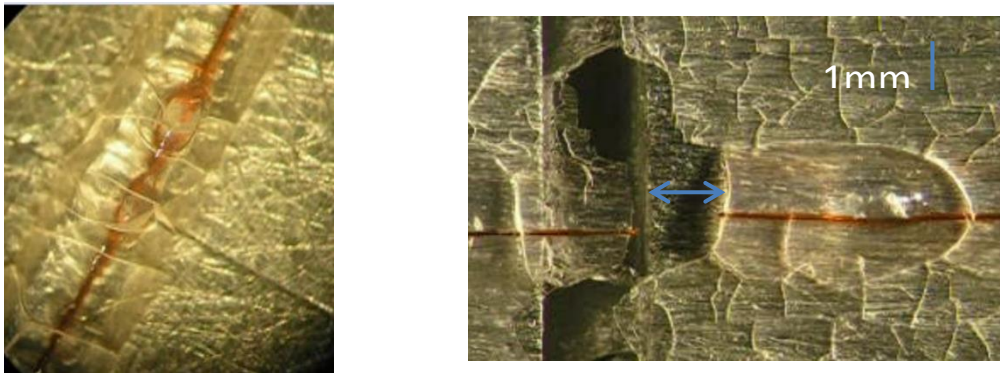

Figure B. 1. Loctite Quicktite was used to install the wire on the steel plates. Micro cracks on the surface of the adhesive after curing caused inconsistency in the detected crack openings.

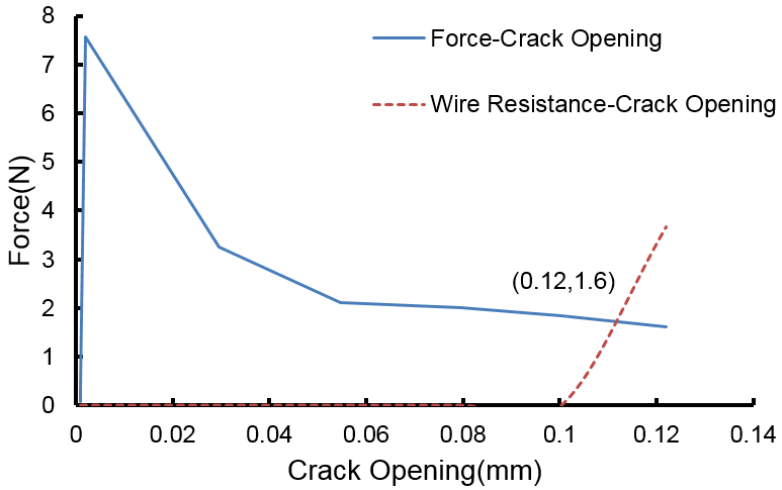

Figure B. 2. Typical detected crack opening. Although the detected crack opening was less than the desired opening, micro cracks on the surface of the adhesive resulted in inconsistent results.

The other cyanoacrylate which was tested was M-Bond 200. This adhesive is commonly used for installing strain gauges on steel beams. Using this adhesive, the binary sensor broke at openings much more than 0.2 mm. There was extensive debonding between wire and adhesive (Figure B. 3), which caused the wire to break at wider than the acceptable crack opening.

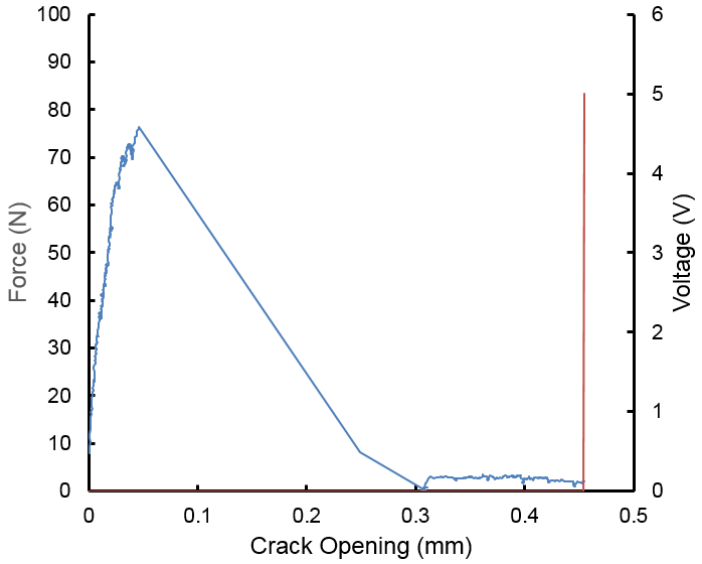

Figure B. 3. Typical force-displacement diagram of binary sensor using M-Bond epoxy.

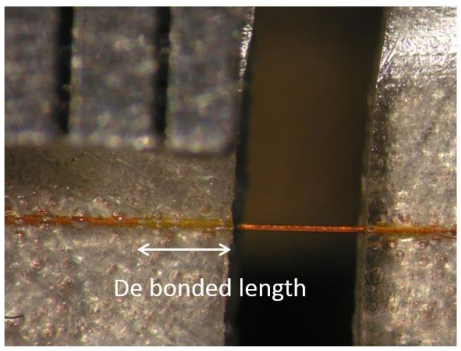

Figure B. 4. M-Bond was used to install the wire on the steel plates. The initial debonding between wire and adhesive resulted in wider effective crack opening. In order for wire to reach the final strain, wider crack opening was required.

Appendix C: Finite Element Simulation to Study Effect of Changes in Mechanical Properties of the Adhesive on the Detected Crack Opening

The main purpose of the simulation of the binary sensor in chapter 4, was to use the model for other combinations of wire and adhesive. In this appendix, different mechanical properties have been assigned to the epoxy to study the effect of changes in adhesive on the detected crack opening. Thickness of the epoxy was assumed to be 1.0 mm and the ultimate tensile strain of the wire was assumed to be 18% (pre-strained by 5%). In the first and second try, the elasticity modulus of the epoxy has changed (increased/decreased) by factor of 2.0 and in the third and fourth try, the maximum tensile stress of epoxy has changed in the same order. The interfacial bonding stiffness between wire and adhesive was assumed to be 240 MPa/mm. Table C. 1 shows the detected crack opening for different mechanical properties of epoxy.

	Elasticity Modulus (GPa)			Maximum Tensile Stress (MPa)			
	(2E)1860	(E)930	(E/2)465	(3S)60	(2S)40	(S)20	(S/2)10
Detected Crack Opening (mm)	0.10	0.11	0.12	0.15	0.11	0.11	0.11

Table C. 1. Effect of change in mechanical properties of epoxy on the detected crack opening

As it is shown in the table, by using an epoxy which is twice stiffer than Loctite E20-NS, smaller widths of crack can be detected. On the other hand, using an epoxy with 3 times higher tensile stress will result in detecting the wider crack openings (0.15 mm crack opening).

Appendix D: Sensitivity analysis of binary sensor

In order to better find the optimal placement of the binary sensor on the web of the girder, the cumulative probability of binary crack sensor detection at different locations on girder A were plotted. To plot the probability function, a normal cumulative distribution of crack width detection with average of 0.2 mm and standard deviation of ± 0.05 mm was used. Then the crack width detection for different lengths of crack (from 20 cm to 80 cm) at different positions along the crack (5 cm to 40 cm above the bottom flange in 5cm increments) was estimated using the FEM. the cumulative distribution curve for each position of the binary sensor were plotted. Results are shown in Figure D. 1. The detected crack width opening is plotted using the dash-dot line. For example if the sensor is being installed at 25cm above the bottom flange (the solid line), the probability to detect cracks with 25 cm long is zero and any crack as long as 40 cm has 60 % chance to be detected. Whereas by positioning the binary crack sensor at 5.0 cm above the bottom flange, cracks as long as 80 cm have less than 40% chance to be detected. Therefore, as mentioned earlier in Figure 5. 8a, the best position to install the binary sensor on girder A is somewhere between 15cm to 25cm above the bottom flange. At this positions, cracks with minimum 40cm length are expected to be detected.

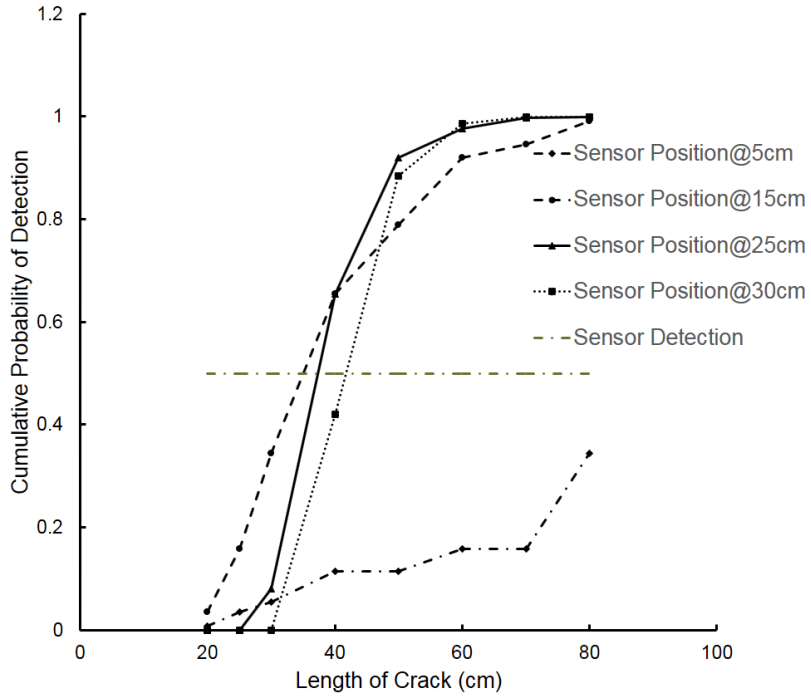

Figure D. 1. Cumulative probability of the detected crack opening at each position of the crack. By placing the sensor at 15 cm to 25 cm above the tension flange in girder A, cracks with minimum 40 cm length can be detected

Appendix E: Placement of Sensor on Girders with Crack Extended Partially into the Bottom Flange

As mentioned in earlier chapters of this work, cracks may start in steel girders of bridges due to initial deficiencies in material or welding of joints. The initial deficiency may grow in size and propagates into the web of the girder and arrested in the tension flange. The crack formed in the steel girder of Quinnipiac river bridge in Connecticut is an example of this kind of cracks [28].

Earlier in chapter 5 of this work, the optimum placement of distributed binary crack sensor on girder A was estimated. In chapter 5, the crack was assumed to propagate into the web of the girder and be arrested before reaching the tension flange. The optimal placement of the distributed binary sensor in this case was estimated to be 15 cm to 25 cm above the tension flange. By positioning the binary crack sensor at these locations, cracks with minimum lengths of 35 cm to 40 cm could have been detected.

In this appendix, the crack is assumed to propagate into the web of the girder and continues into the tension flange as shown in Figure 2. 1 and be arrested in the tension flange. Therefore, a part of the tension flange is assumed to be cracked. Crack opening along the crack for different lengths of the crack has been plotted in Figure E. 1. As it is shown in this figure, the optimal placement of the distributed binary crack sensor will shift towards the tension flange to 10 cm to 15 cm above the bottom flange. By positioning the binary sensor at this positions, cracks with minimum length of 30 cm will be detected.

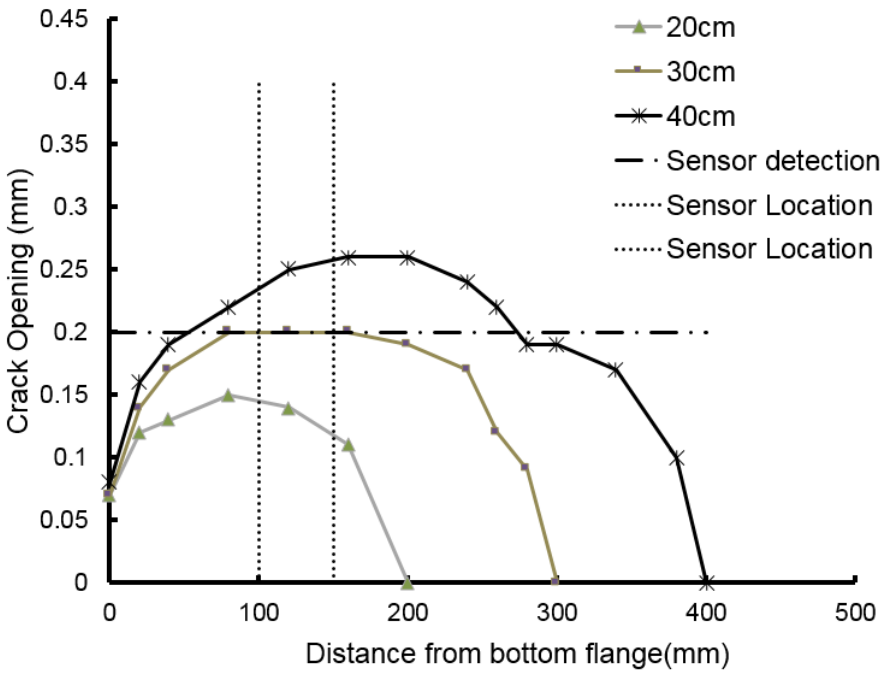

Figure E. 1. Crack opening vs distance from bottom flange for different crack length on girder A. Crack starts at deficiencies on the web of the girder and propagates into the web. Cracks will be arrested in the bottom flange.

Appendix F: Cost Estimation for Three Methods of Distributed Monitoring

Table F.1 shows the breakdown of costs for three different distributed monitoring systems; Fibre optic sensor, Binary sensor and array of strain gauges on a 300 m steel girder of a bridge.

System	Sensor ($/m)	Installation ($/m)	DAQ ($)	Operation (Phone/Internet/Battery) ($/year)	Total for 300 m ($/year)	Total for 300 m ($/5 year)
FOS	20	500	150,000	40,000	346,000	506,000
Binary	5	500	30,000	10,000	191,500	231,500
Strain Gauges	50	500	150,000	40,000	355,000	515,000

Table F. 1. Cost analysis of three methods of distributed monitoring